Xeno-free 3D Culture of Mesenchymal Stromal Cells For Bone Tissue Engineering

Siddharth Shanbhag

UNIVERSITY OF BERGEN

Xeno-free 3D Culture of Mesenchymal Stromal Cells For Bone Tissue Engineering

Siddharth Shanbhag

Thesis for the degree of Philosophiae Doctor (PhD)
at the University of Bergen

Date of defense: 18.12.2020

Year: 2020

Title: Xeno-free 3D Culture of Mesenchymal Stromal Cells For Bone Tissue Engineering

Name: Siddharth Shanbhag

Print: Skipnes Kommunikasjon / University of Bergen

Table of Contents

Scientific environment

The work comprising this thesis was conducted at the Faculty of Medicine, University of Bergen, over the course of four years (2016-2020). The experiments were mainly undertaken at the Department of Clinical Dentistry. The platelet lysate preparation was performed in collaboration with the Bloodbank at Haukeland University Hospital, Bergen. Advanced microscopy and small-animal imaging was performed at the Molecular Imaging Centre (MIC), University of Bergen. All animal experiments were performed at the Laboratory Animal Facility, Department of Clinical Medicine, University of Bergen. The *in situ* hybridization experiments were performed at the Centre for Cancer Biomarkers (CCBIO) and Gade Laboratory for Pathology, Department of Clinical Medicine, University of Bergen.

The chicken embryo experiments were performed at the Department of Physics, Norwegian University of Science and Technology, Trondheim. The spheroid culture (and co-culture) experiments were performed in collaboration with the Department of Periodontology, Faculty of Odontology, Malmø University, Sweden. The non-decalcified histological analysis of *in vivo* samples was performed at the Karl Donath Laboratory for Biomaterial Research at the School of Dentistry, Medical University of Vienna, Austria.

The principle supervisor of the project was Professor Kamal Mustafa. The co-supervisors were Professor Anne Isine Bolstad and Dr. Salwa Suliman. Professor Andreas Stavropoulos from Malmø University served as an external advisor.

Summary

Clinical translation of innovative regenerative approaches using mesenchymal stromal cells (MSCs) is urgently needed for the treatment of challenging bone defects. The overall aim of this thesis, comprising of one systematic review and four original studies, was to optimize a xeno-free three-dimensional (3D) culture system of MSCs, as a clinically relevant strategy for bone tissue engineering (BTE). Secondary aims were to identify a minimally invasive source for MSCs, and to promote angiogenesis within the xeno-free 3D cultures.

Human platelet lysate (HPL) represents a favourable supplement for xeno-free expansion of MSCs (Study I). To standardize HPL production, the storage time of platelet concentrates was optimized in terms of HPL cytokine content and biological efficacy on MSCs. Advantages of HPL culture (vs. bovine serum) were observed in relation to all relevant *in vitro* aspects of MSCs, i.e., growth, immunophenotype and osteogenic differentiation (Studies II and III).

Progenitor cells showing a characteristic MSC-like phenotype and multipotency were isolated from human gingiva (GPCs) and periodontal ligament (PDLCs). Both GPCs and PDLCs demonstrated superior growth and osteogenic differentiation in HPL vs. FBS; a subset of GPCs also showed potent neurogenic differentiation (Study III). Given their relative ease of isolation and minimally invasive tissue harvesting, GPCs were prioritized in subsequent experiments.

To overcome the limitations of traditional monolayer (2D) culture, 3D spheroid cultures were established in HPL. Both GPCs and BMSCs demonstrated significantly increased expression of stemness- and osteogenesis-related genes in spheroids vs. monolayers, confirmed at the protein level by immunocytochemistry. Moreover, the cytokine release profile of GPC and BMSC spheroids was considerably enhanced compared to monolayers. Under osteogenic conditions, GPC spheroids showed *in vitro* mineralization comparable to that of BMSCs (Study III). When implanted *in vivo,* xeno-free GPCs and BMSCs showed ectopic mineralization after 4 and 8 weeks based on micro-CT and histology; implanted human cells were identified at the

mineralization sites via *in situ* hybridization. In the case of BMSCs, significantly greater mineralization was observed in constructs containing spheroids vs. single cells (Study V).

To enhance angiogenesis, a coculture strategy was tested using a xeno-free spheroid coculture model of GPCs and human umbilical vein ECs (HUVECs) embedded in an HPL-hydrogel (HPLG). When cultured as spheroids, HUVECs showed characteristic *in vitro* sprouting angiogenesis in HPLG. A trend for increased *in vitro* HUVEC-sprouting was observed in co-culture with GPCs. Constructs of coculture and HUVEC spheroids in HPLG comparably supported *in vivo* neoangiogenesis in a chorioallantoic membrane (CAM) assay (Study IV).

Clinically relevant BTE constructs were designed combining BMSCs (as spheroids or single cells) encapsulated in HPLG and 3D printed copolymer scaffolds. Viability and osteogenic differentiation of cells within the constructs was confirmed up to 21 days *in vitro*; greater mineralization was observed in constructs containing spheroids vs. single cells. When implanted in rats' calvarial defects, constructs of both spheroids and single cells revealed abundant *in vivo* bone regeneration for up to 12 weeks (Study V).

The results herein suggest clear advantages of xeno-free 3D cultures of MSCs for BTE. GPCs represent a promising alternative to BMSCs with osteogenic and pro-angiogenic potential, and further work is needed to facilitate clinical translation. In particular, the constructs of xeno-free MSCs, HPLG and 3D printed scaffolds developed herein, represent a clinically relevant strategy for BTE.

List of publications

The thesis is based on the following papers and will be referred to according to their Roman numbers:

I. **<u>Shanbhag S</u>**, Stavropoulos A, Suliman S, Hervig T, Mustafa K. Efficacy of humanized mesenchymal stem cell cultures for bone tissue engineering: a systematic review with a focus on platelet-derivatives. Tissue Eng Part B: Rev. 2017; 23:552-569.

II. **<u>Shanbhag S</u>**, Mohamed-Ahmed S, Lunde TH, Suliman S, Bolstad AI, Hervig T, Mustafa K. Influence of platelets storage time on human platelet lysates and platelet lysate-expanded mesenchymal stromal cells for bone tissue engineering. Stem Cell ResTher. 2020; 11:351. doi: 10.1186/s13287-020-01863-9.

III. **<u>Shanbhag S</u>**, Suliman S, Bolstad AI, Stavropoulos A, Mustafa K. Xeno-free spheroids of human gingiva-derived progenitor cells for bone tissue engineering. Front Bioeng Biotechnol. 2020; 8:968. doi: 10.3389/fbioe.2020.00968.

IV. **<u>Shanbhag S</u>**, Rashad A, Suliman S, Osman TA, de Lange Davies C, Stavropoulos A, Bolstad AI, Mustafa K. Xeno-free 3D coculture of human gingiva-derived progenitor cells and endothelial cells to promote angiogenesis. *Manuscript*

V. **<u>Shanbhag S</u>**, Mohamed-Ahmed S, Suliman S, Kampleitner C, Dongre H, Hassan MN, Yassin MA, Costea DE, Tangl S, Bolstad AI, Mustafa K. Xeno-free constructs of mesenchymal stromal cells and 3D printed scaffolds for bone tissue engineering. *Manuscript*

The thesis is supported by the following systematic reviews:

I.   **<u>Shanbhag S</u>**, Pandis N, Nyengaard J, Mustafa K, Stavropoulos A. Alveolar bone tissue engineering in critical-size defects of experimental animal models: a systematic review and meta-analysis. J Tissue Eng Regen Med. 2016; 11:2935-2949.

II.   **<u>Shanbhag S</u>**, Suliman S, Pandis N, Stavropoulos A, Sanz M, Mustafa K. Cell therapy for orofacial bone regeneration: a systematic review and meta-analysis. J Clin Periodontol. 2019; 46 Suppl 21:162-182.

III. **<u>Shanbhag S</u>**, Pandis N, Nyengaard J, Mustafa K, Stavropoulos A. Cell co-transplantation strategies for vascularized craniofacial bone tissue engineering: a systematic review and meta-analysis of pre-clinical in vivo studies. Tissue Eng Part B: Rev. 2017; 23:101-117.

The candidate has also contributed to the following work during the course of the PhD period, not included in this thesis:

I.   Helgeland E, **Shanbhag S**, Mohamed-Ahmed S, Pedersen TO, Rosen A, Mustafa K, Rashad A. 3D printed gelatin-genipin scaffolds for temporomandibular joint cartilage regeneration. J Biomed Mater Res A. *Submitted manuscript*

II.   Gjerde C, **Shanbhag S**, Neppelberg E, Mustafa K, Gjengedal H. Patient experience following iliac crest-derived alveolar bone grafting and implant placement. Int J Implant Dent. 2019; 6:4.

III.   Helgeland E, **Shanbhag S**, Pedersen T, Rosen A, Mustafa K. Scaffold-based TMJ tissue regeneration in experimental animal models: a systematic review. Tissue Eng Part B: Rev. 2018; 24(4):300-316.

IV.   **Shanbhag S**, Pandis N, Nyengaard J, Mustafa K, Stavropoulos A. Bone tissue engineering in peri-implant defects in preclinical in vivo research: a systematic review and meta-analysis. J Tissue Eng Regen Med. 2017; 12:e336-e349.

V.   **Shanbhag S**, Rana N, Suliman S, Mustafa K, Stavropoulos A. Early inflammatory responses of mesenchymal stromal cells on bone substitute materials. *Manuscript.*

Abbreviations

ASC	Adipose-derived stromal cells
ALP	Alkaline phosphatase
ANOVA	Analysis of variance
TSG-6	Anti-inflammatory cytokine stimulated gene/protein 6
AB	Autogenous bone
β-TCP	Beta-tricalcium phosphate
BCP	Biphasic calcium phosphate
BMA	Bone marrow aspirate
BMAC	Bone marrow aspirate concentrate
BMSC	Bone marrow-derived mesenchymal stromal cells
BMP	Bone morphogenetic protein
BTE	Bone tissue engineering
CDM	Chemically-defined media
CAM	Chorioallantoic membrane
Col-GAG	Collagen-glycosaminoglycans
CT	Computed tomography
CM	Conditioned media
CSD	Critical size defects
DPSC	Dental pulp-derived stromal cells
ED	Embryonic day
EC	Endothelial cells
ELISA	Enzyme-linked immunosorbent assay
ECM	Extracellular matrix
EV	Extracellular vesicles
FBS	Fetal bovine serum
FGF2	Fibroblast growth factor 2
GPC	Gingiva-derived progenitor cells
GMP	Good Manufacturing Practices
GF	Growth factors

HGF	Hepatocyte growth factor
HPL	Human platelet lysate
HPLG	Human platelet lysate hydrogel
HPR	Human platelet releasate
HS	Human serum
HUVEC	Human umbilical vein endothelial cells
HA	Hydroxyl-apatite
IHC	Immunohistochemistry
ISH	In situ hybridization
IL	Interleukin
MCC	Mesenchymal cell condensation
MSC	Mesenchymal stromal cells
μCT	Micro-computed tomography
MNC	Mononuclear cell
NANOG	Nanog homeobox factor
OCT4	Octamer-binding transcription factor 4
OMSC	Oral mucosa-derived stromal cells
OCN	Osteocalcin
OPN	Osteopontin
PDLC	Periodontal ligament-derived progenitor cells
PC	Platelet concentrates
PDGF-BB	Platelet-derived growth factor BB
PRP	Platelet-rich plasma
PLLA-TMC	Poly(L-lactic acid) – trimethylene carbonate
PLGA	Polylactic–polyglycolic acid copolymer
qPCR	Quantitative Polymerase chain reaction
PDT	Population doubling time
PGE2	Prostaglandin E2
RUNX2	Runt-related transcription factor 2
SGC	Scaffold-gel constructs
SOX2	Sex determining region Y-box 2

SCGF	Stem cell growth factor
SVF	Stromal vascular fraction
SDF-1	Stromal-derived factor-1
TGF-β	Transforming growth factor-β
TNF	Tumor necrosis factor
VEGF	Vascular endothelial growth factor

List of figures and tables

1. Introduction

1.1. BONE TISSUE ENGINEERING

Bone is a dynamic tissue that is subjected throughout life to continuous *modeling*, as a result of physiological stimuli and biomechanical forces, and *remodeling*, via replacement of old/damaged bone with new bone [1]. Bone also has a unique capacity to regenerate, as in the case of fracture healing, without scar tissue formation [2]. This healing process involves a complex and well-coordinated cascade of interactions between *osteogenic* cells, *osteoinductive* signaling molecules and *osteoconductive* extracellular matrix (ECM) components, in an adequately vascular and mechanically stable environment. However, the capacity for self-repair is limited and bone defects beyond a 'critical-size' cannot completely regenerate via intrinsic mechanisms alone [3]. This is especially true in an ageing population, since the capacity for regeneration reduces with age, and is reflected by the high number of bone transplantation procedures performed in the elderly [4].

The reconstruction of oral and maxillofacial bone deficiencies presents a major clinical challenge. Ridge remodelling following tooth loss is the most common cause for alveolar bone defects [5]. More challenging segmental defects, which include the inferior mandibular border, often result from trauma, tumour resection, or radiation-related osteonecrosis [6]. Further, congenital anomalies are frequently associated with alveolar defects such as orofacial clefts [7]. Current regenerative strategies mainly involve the use of autogenous bone (AB) grafts and/or bone substitute materials. AB is considered the gold standard as it combines all the essential factors required to simulate the physiological healing process via *osteoconduction* (ECM), *osteoinduction* (growth factors), and *osteogenesis* (osteoprogenitor cells) [8].

Although AB transplantation is considered the gold standard treatment, larger defects may require volumes of bone locally unavailable. This creates a need for harvesting bone from a remote site, usually involving general anaesthesia, hospitalization and significantly increased costs [9]. Alternatives have included a range of allogeneic, xenogeneic and alloplastic bone substitutes, but no consensus currently

exists on the effectiveness of one material over the other, in comparison to AB, or for specific clinical indications [10]. Thus, to address this need for an 'optimal' strategy, the bone tissue engineering (BTE) approach aims to combine and deliver the cellular (osteoprogenitor cells), extracellular (ECM/scaffold) and molecular elements (growth factors) involved in the physiological regeneration process, without the need for invasive AB harvesting [11].

BTE involves the harvesting of osteogenic cells from an autologous source, e.g., bone marrow, their 'chair-side' manipulation or *ex vivo* amplification, and combination with an appropriate biomaterial scaffold for *in vivo* implantation. Thus, the 'triad' of osteogenic cells, osteoinductive signals (growth factors released by cells), and osteoconductive scaffolds, aims to replicate the properties of AB (**Figure 1.1**) [11]. The cells can be harvested from various tissues by minimally invasive techniques under local anaesthesia, without the need for hospitalization. Thus, BTE strategies are emerging as promising alternatives to AB and/or biomaterial-based grafting, as demonstrated by several preclinical and clinical studies [12-14].
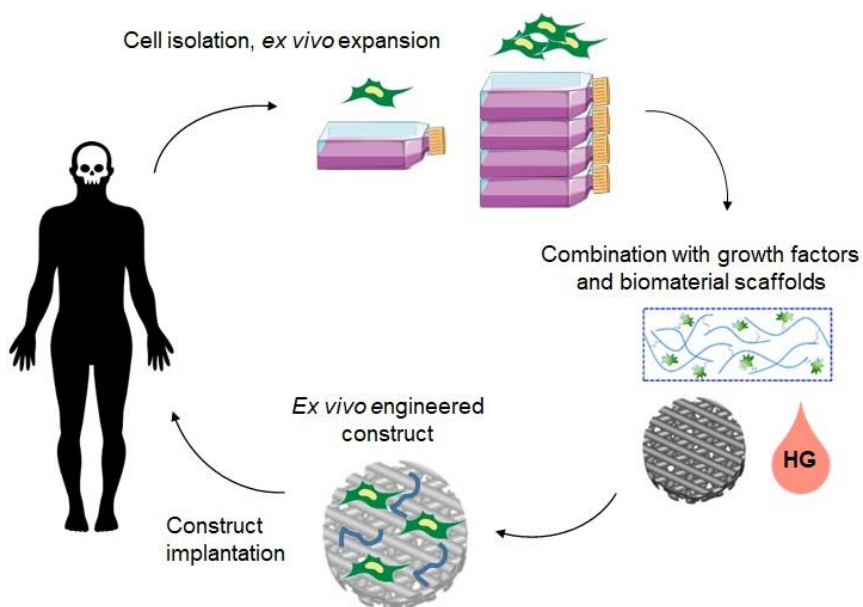
Figure 1.1: The basic concept of BTE represented by the 'triad' of osteogenic cells, osteoinductive growth factors and osteoconductive scaffolds, including hydrogels (HG).

1.1.1. State of the art: preclinical evidence

Preclinical models of bone regeneration typically involve 'critical-size' defects (CSD), i.e., the smallest-size experimental bone defect that will not spontaneously and completely regenerate in a defined time-frame without intervention [15]. To assess the preclinical evidence for orofacial BTE, a systematic literature review and meta-analysis was performed to determine whether implantation of osteogenic cells seeded on biomaterial scaffolds can enhance bone regeneration compared to grafting with only biomaterial scaffolds or AB [12].

After screening, 57 eligible studies in large-animal models [dogs, minipigs and small-ruminants (sheep and goats)] were identified. These studies represented sinus augmentation, ridge augmentation (CSD) and alveolar cleft models. A majority of studies (55%) reported the use of autologous cells, most frequently from bone marrow. Other cell sources included dental pulp, alveolar bone and adipose tissue. A majority of studies (58%) reported the use of mineral-phase alloplastic or xenogeneic scaffolds, used in the block, disc or particulate form. Some studies reported the use of composite scaffolds, composed of a mineral- and non-mineral [(co)polymer] phase. Based on 33 studies, with moderate to high heterogeneity, the meta-analysis revealed significantly greater bone regeneration with BTE vs. scaffolds or AB in sinus augmentation models; significantly greater bone regeneration with BTE vs. scaffolds in CSD models; and no significant differences in bone regeneration between BTE and AB in cleft models.

In summary, BTE was found to be superior to 'cell-free' scaffolds, and comparable to AB, in terms of orofacial bone regeneration in preclinical studies. Thus, the 'direction' of treatment effect was clearly in favour of BTE. Although the preclinical meta-analysis suggested a significant treatment effect in the 'direction' of BTE, only a meta-analyses of clinical studies could yield a reliable estimate or 'size' of such a treatment effect [12].

1.1.2. State of the art: clinical evidence

To assess the clinical evidence for orofacial BTE, a systematic review and meta-analysis was performed to determine the effectiveness of BTE compared to grafting with only biomaterial scaffolds and/or AB [14].

After screening, 47 controlled clinical studies were included, of which 22 were randomized controlled trials, mostly with a low to unclear risk of bias. A majority of the evidence was derived from studies of sinus augmentation studies. Cell therapy approaches were categorized as: (1) *minimally manipulated* whole tissue fractions, usually involving a point-of-care procedure, and (2) *more-than-minimally manipulated* or *ex vivo* culture-expanded cells, further categorized as (a) *uncommitted* stem/progenitor cells, and (b) *committed* bone-derived cells. A majority of included studies reported the use of minimally manipulated fractions, particularly bone marrow; 10 studies reported the use of autologous *ex vivo* expanded cells from bone marrow or adipose tissues, i.e., mesenchymal stromal cells (MSCs). Only one study reported *ex vivo* cell expansion in 'xeno-free' culture. Scaffolds were categorized as (a) ceramics, e.g., hydroxyl-apatite (HA), beta-tricalcium phosphate (β-TCP), (b) (co)polymers, e.g., polylactic–polyglycolic acid copolymer (PLGA), or (c) composites, i.e., combinations of the above. No included studies reported the use of three-dimensional (3D) printed scaffolds.

Based on 24 studies, with moderate to high heterogeneity, the meta-analysis revealed significantly greater bone regeneration with BTE vs. cell-free scaffolds (9 studies), and no significant differences between BTE and AB (3 studies).

In summary, BTE using cells in combination with biomaterial scaffolds results in bone regeneration which is superior to scaffolds alone, and comparable to the gold standard AB, in certain indications. Thus, BTE appears to be a promising alternative to AB grafting. However, it is currently unclear whether implantation of *ex vivo* expanded cells is superior to whole tissue fractions, and whether committed cells, e.g. osteoblasts, are superior to uncommitted cells, e.g., mesenchymal stromal cells (MSCs) [14, 16].

1.2. MESENCHYMAL STROMAL CELLS

Adult MSCs are multipotent cells found in the perivascular niche of a variety of tissues, which possess the capacity to differentiate along multiple mesenchymal lineages. MSCs have a key role in regulating homeostasis, regeneration and repair within their tissues environments [17]. MSCs were originally identified in the bone marrow as non-hematopoietic, plastic adherent, "colony-forming" fibroblast-like cells capable of differentiating into osteoblasts [18, 19]. Since then, cells with similar properties have been isolated from various tissues [20]. To facilitate standardization of MSC-related research, the "minimal criteria" [21] proposed to define MSCs *in vitro* are:

- plastic adherence
- an immunophenotype based on positive expression (>95%) of stromal surface markers (CD73, CD90, CD105) and negative expression (<2%) of haematopoietic markers (CD34, CD45, CD14 or CD11b) and HLA-DR
- the capacity to differentiate into (at least) three different lineages, i.e., osteoblasts (bone), chondrocytes (cartilage) and adipocytes (fat) (**Figure 1.2**).
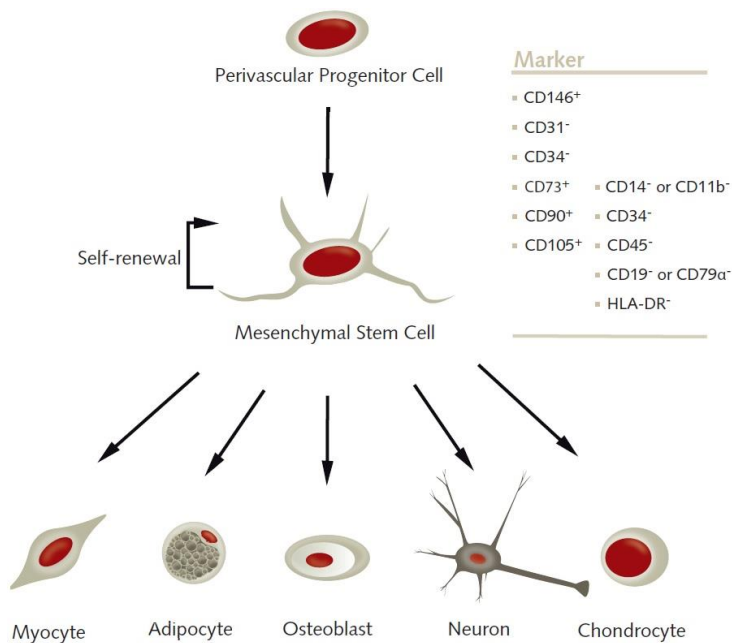
Figure 1.2: Characteristics of MSCs: immunophenotype, self-renewal & multilineage differentiation. Adapted from www.promocell.com/products/mesenchymal-stem-cell-osteogenic-differentiation-medium

1.2.1. Bone marrow MSCs

Based on systematic reviews by us and others, BMSCs are the most frequently used cells in both preclinical and clinical applications of BTE [14, 20]. Bone marrow is a unique organ known to contain a heterogeneous population of progenitor cells including MSCs, haematopoietic stem cells and endothelial progenitor cells [22, 23]. Bone marrow aspirate can be harvested via a relatively non-invasive procedure (vs. AB harvesting), usually from the iliac crest, under local anaesthesia. This BMA may be used either whole (unmanipulated) or following concentration of the mononuclear cell (MNC) fraction (minimally manipulated). Bone marrow concentrate is currently FDA-approved and shown to be efficacious as a point-of-care method of autologous cell delivery [24]. However, BMSCs represent less than 0.01% of the MNC fraction [19] and therefore *ex vivo* expansion strategies have been employed to exponentially amplify BMSCs, to deliver a much higher number of cells, and thereby improve therapeutic efficacy [25]. Although clinical evidence for BTE with *ex vivo* expanded BMSCs is limited [14, 26], preclinical studies have indicated superior outcomes when using expanded (and osteogenically pre-differentiated) BMSCs vs. BMA/MNC [27, 28]. Nevertheless, evidence of age- and other donor-related variations in BMSCs, along with the morbidity of bone marrow harvesting, has led to investigation of 'MSC-like' cells from other, relatively less invasive, tissue sources [29].

1.2.2. MSCs from other tissues

MSCs have also been isolated from other sources such as adipose and dental tissues, among others. In particular, adipose tissue has emerged as a feasible alternative to bone marrow in terms of both minimally manipulated [stromal vascular fraction (SVF)] and culture expanded MSC-like cells (ASCs) [30, 31]. The frequency of MSC-like cells in SVF is reported to be considerably higher than in BMA(C) [32]. Recent studies have revealed ASCs to be comparable to BMSCs in terms of MSC-like properties, with the advantage of less-invasive tissue harvesting [33]. These properties are reported to be further enhanced when ASCs are cultured in xeno- and/or serum-free conditions [34, 35]. However, in the context of BTE, a number of preclinical studies have suggested a lower intrinsic osteogenic potential of ASCs (regardless of xeno-free culture) vs.

BMSCs *in vitro* and *in vivo* [33, 36-39]. A favourable *in vivo* bone-forming capacity of ASCs has been demonstrated when cultured in the presence of additional osteogenic growth factors [40]. This tendency for superior adipogenic differentiation of ASCs and osteogenic differentiation of BMSCs has been termed *"tissue source variability"*, i.e., a propensity for MSCs to differentiate along the lineage of their origin [41]. Osteogenic differentiation is reported to be the default pathway in BMSCs [42, 43]. Whether the tissue of origin affects the *in vivo* regeneration potential of MSCs remains to be determined in comparative clinical studies.

1.2.3. Progenitor cells from dental tissues

The need for harvesting of bone marrow may present a challenge for the clinical translation of BTE strategies [29]. Indeed, MSC-like progenitor cells have been isolated from dental tissues such as dental pulp (DPSCs), periodontal ligament (PDLCs), oral mucosa (OMSCs) and gingiva (GPCs) (**Figure 1.3**) [44]. The existence of such cells has been linked to the neural crest origin of these tissues [45].
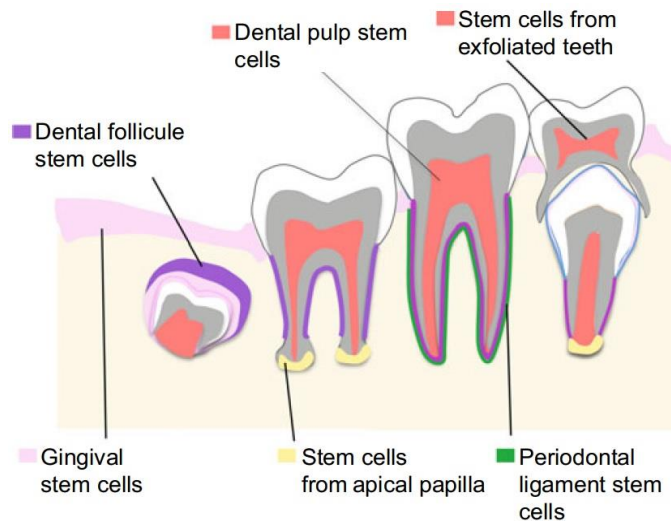
Figure 1.3: Dental tissue-derived MSCs from various intra-oral sources. Adapted from [44]

Gingiva can be harvested with minimal morbidity and rapid scarless healing and contains a subpopulation of progenitor cells (GPCs) with a capacity for osteogenic

differentiation [46, 47]. GPCs have demonstrated comparable, or superior, properties to BMSCs *in vitro*, and the ability to regenerate bone *in vivo* [48-51]. Although GPCs, PDLCs and DPSCs fulfil the "minimal criteria" for MSCs *in vitro*, the existence of 'true' MSC-like populations *in vivo*, may be questioned [52]. While dental pulp and PDL are specialized tissues serving unique functions, gingiva is a connective tissue with a primarily supportive function. Furthermore, all three tissues are known to contain large fibroblast populations. Indeed, fibroblasts from various tissues, including gingiva, are reported to be indistinguishable from MSCs *in vitro*, based on the current "minimal criteria" [53, 54]. However, compared to pulp and PDL, both of which require tooth extraction for harvesting and which undergo age-related degenerative changes, gingiva remains relatively stable in healthy individuals, and thus, represents a more attractive source of cells [55, 56].

Several studies have reported the application of GPCs for *in vivo* bone formation with varying success, as summarized in **Table 1.1**. All studies reported the use of monolayer (2D) GPCs; no studies have reported on spheroid (3D) GPCs. One study reported the use of GPCs in combination with fibrin gel and BCP, but no ectopic bone formation after 8 weeks [40]. Given the large heterogeneity between studies (number of cells, use of osteogenic induction, biomaterials, etc.), the overall reported trend for *in vivo* bone formation by GPCs seems to be highly variable. A number of studies have reported clinical applications of GPCs for mucosal regeneration (summarized in [57]), although none for bone.

Table 1.1: Summary of studies using GPCs for in vivo bone formation

Study	Cells (nos, induction, time)	Methods (material, time, model)	Bone formation (as reported in the studies)
Ectopic			
Fournier et al. 2010 [46]	GMPC, $2x10^6$	HA +/- GF, BMSC 8 w, Nude mice	GMPC = BMSC
Tomar et al. 2010 [58]	GMSC, 10^6, osteo 10d	BCP +/- BMSC 10 w, Scid mice	GMSC = BMSC
Wang et al. 2011 [50]	GMSC, $5x10^6$	Collagen gel 6 w, Nude mice	No bone in GMSC or gel OPN (IHC): GMSC > gel

Ge et al. 2012 [51]	GMSC, healthy or inflamed, 5×10^6 (clones)	BCP + Fibrin gel +/- PDLSC 8 w, Nod-scid mice	PDLSC > GMSC (no bone)
Yang et al. 2013 [48]	GMSC, sheets, osteo 7d+ (+/- TNFα, IL1β)	BS +/- PDLSC 8 w, Id mice	PDLSC > GMSC Unprimed cells > priming
Zorin et al. 2014 [59]	GMSC, 5×10^6	OCP, TCP 3,4,7 w, Nude mice	GMSC = BMSC (IHC markers)
Shi et al. 2019 [60]	GMSC +/- TGFβ-in., 2×10^6	HA 12 w, BALB/c mice	GMSC+TGFβ-in. > GMSC > HA

Orthotopic

Wang et al. 2011 [50]	GMSC-GFP, 1-2×10^6, osteo 10d	Collagen gel 8 w, SD rats MCSD + CCSD	GMSC > gel
Moshaverinia et al. 2014 [61]	GMSC, 4×10^6	Alginate +/- PDLSCs, BMSCs, Nude mice CCSD	BMSC > PDLSC > GMSC
Xu et al. 2014 [62]	GMSC, 10^6	aMEM i.v. injection 1,2,3 w, C57BL/6 mice ACSD	GMSC > empty
Diomede et al. 2018 [63]	GMSC +/- CM	3D-P PLA 6 w, Wis rats CCSD	No bone
Shi et al. 2019 [60]	p-GMSC +/- TGFβ-inh., 2×10^6, osteo	HA, AB 8 w, Minipig ACSD	AB > GMSC+TGFβ-in. > GMSC > HA
Al-Qadhi et al. 2020 [64]	GMSC, 10^6	HA-Si +/- r-BMSCs 2,4,6 w, NZ rabbit TCSD	GMSC = BMSC > HA-Si
Kandalam et al. 2020 [65]	GMSC, 10^6, osteo 7d	Puramatrix +/- BMP2 4,8 w, At-nude rats ACSD	GMSC+BMP2 > GMSC = BMP2 = PM = Empty

GMPC, gingiva-derived progenitor cells; GMSC, gingiva-derived MSCs; PDLSC, PDL-derived MSCs; p-GMSCs, pig GMSCs (terminology used in the original studies); osteo, osteogenic induction; OPN, osteopontin; IHC, immunohistochemistry; TGFβ-in, TGFβ inhibitor; GFP, green fluorescent protein; CM, conditioned medium; BMP2, bone morphogenetic protein 2; HA, hydroxyapatite; OCP, octa-calcium phosphate; BCP, biphasic calcium phosphate; TCP, tri-calcium phosphate; BS, bone substitute; aMEM, culture medium; Si, silica gel; CCSD, calvarial CSD; ACSD, alveolar CSD; TCSD, tibial CSD; d, days; w, weeks.

1.2.4. Clinical translation of MSC therapies

A secondary finding of our preclinical [12] and clinical systematic reviews [14] was a 'gap' in translation of BTE from animal models to patients. Besides the known challenges of translation from animal models, limitations of current BTE strategies were identified. These include, but are not limited to, *ex vivo* factors (xenogeneic culture, suboptimal biomaterials), and *in vivo* factors (insufficient vascularization). *Ex vivo* conditions, i.e., how MSCs are manipulated between isolation and transplantation, can significantly influence their phenotype, bioactivity and *in vivo* performance [66, 67]. Such conditions mainly include the media and supplements used to culture MSCs, and the mode of culture, i.e. 2D or 3D, as discussed in the following chapter.

1.3.   MSC EX VIVO CULTURE CONDITIONS

1.3.1. Xeno-free culture

The use of safe and standardized culture conditions is a critical aspect of current Good Manufacturing Practices (GMP) for *ex vivo* MSC expansion. MSC are cultured using 'basal' media plus supplements to provide growth factors, cytokines, proteins and enzymes to support cell growth [68]. These supplements are broadly categorized as xenogeneic (animal-derived) and xeno-free (human-derived or chemically defined).

Fetal bovine serum (FBS) is the most commonly used (xenogeneic) supplement for MSC expansion, typically at 10-20% concentration; based on recent reports >80% of clinical trials still use FBS-cultured MSCs [69]. FBS has been preferred because the fetal calf milieu is enriched with growth factors (GFs) and poor in antibodies [70]. However, MSCs cultured in FBS may internalize xenogeneic proteins (and infectious agents, e.g. viruses, prions) and carry the risk of infection and immunoreaction [71]. This "xenocontamination" of MSCs via FBS cultures may also lead to hyperimmunogenicity and poor cell engraftment *in vivo* [72, 73]. Additionally, concerns regarding batch-to-batch inconsistency in FBS and animal welfare have been highlighted [74, 75].

Although the use of FBS may be permitted by regulatory agencies in early-phase MSC trials, subsequent studies involving larger patient groups demand the use of 'xeno-free' cultures [76, 77]. Recent European guidelines advocate the use of "non-ruminant" over "ruminant materials" for the manufacture of human medicinal products, which also applies to cell therapies [78, 79]. Accordingly, an increase in the use of xeno-free supplements has recently been reported [80, 81]. Such xeno-free alternatives to FBS broadly include human (blood)-derived supplements, i.e., serum or platelet-derivatives, and chemically-defined media. Since the culture environment can directly influence MSC functions, the choice of supplements should be governed by the intended clinical application. Thus, a systematic review **(Paper I)** was performed to determine the efficacy of xeno-free culture strategies of MSCs for BTE applications.

Three main categories of FBS-substitutes were identified in the review: human serum, human platelet-derivatives and chemically-defined media. Human-blood derivatives are promising alternatives to FBS, due to their high concentrations of physiological GFs and cytokines. A number of studies have reported benefits of human serum for expansion of MSCs, particularly ASCs [35, 82]. Platelet-derivatives are also emerging as attractive FBS-substitutes for clinical-grade MSC production [25, 26]. Finally, given the lot-to-lot variation in blood-derivatives and the theoretical risk of pathogen transmission, fully defined xeno-free and serum-free media formulations are proposed for MSC expansion [34]. A detailed summary of the review findings is presented in chapter 4.1. Based on the review findings, and practical considerations (availability of blood products and ongoing agreements with the local Bloodbank), human platelet derivatives were chosen as the xeno-free supplement herein.

1.3.2. *Human platelet lysate*

HPL is defined as a cell-free, protein- and GF-rich biological material produced from outdated platelet concentrates (PCs) intended for transfusion [83]. PCs are obtained as apheresis products or whole blood-derived buffy coat units, i.e. either as autologous or 'pooled' products [84]. Pooling platelets from multiple donors can provide larger volumes and reduce donor-based variations in terms of platelet counts, GF contents, and effects on MSCs [85]. Concentrations of HPL in culture range from 2-20%; most commonly 5%. Accumulating evidence suggests that HPL can effectively support the clinical-grade expansion of MSCs from different sources [86]. A clinical protocol for HPL-based MSC expansion has been clinically validated by our group [25].

The importance of HPL in GMP-grade MSC production is highlighted by the publication of several recent consensus statements [79, 83, 87, 88]. The most common themes in these reports are the need to scale-up HPL production by blood establishments, and, more urgently, the need for standardization of HPL products. As observed in Paper I, there is currently considerable large variation in the methods used to produce HPL. Standardization has been advised at various levels of the HPL

production process, such as the source material (PCs), the pool sizes (number of PC units pooled), method of platelet lysis, and use of pathogen inactivation strategies [83].

Regarding the storage time of PCs, current recommendations call for blood centres to freeze outdated PCs (within 7 days of collection) for later HPL production, although the maximum duration that PCs can be used after expiry to prepare an efficient HPL is unknown [83]. For many blood centres it may not always be possible to initiate HPL production on the day of (or soon after) PC expiry, it would be of significance to determine the optimal duration and conditions for PC storage. International blood authorities advise a minimum interval of three months between blood donations to allow for repeated viral testing to minimize the risk of disease transmission via platelet products [86]. In the context of HPL, this is especially relevant when pathogen reduction is not applied. Standardizing PC storage would facilitate logistical solutions and encourage more blood establishments to incorporate HPL production into their protocols, and also benefit their economies. Thus, optimizing the storage time of PCs would be a step towards addressing both the standardization and scaling-up of HPL production – as addressed in **Paper II** (**Figure 1.4**).
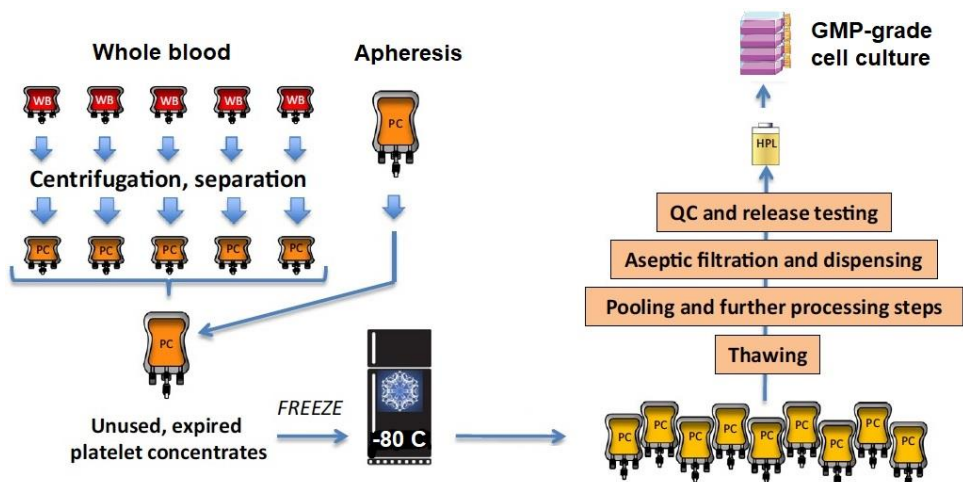
Figure 1.4: The production scheme for HPL involving blood banks, manufacturers and users. Adapted from [83]

In addition to soluble cytokines, HPL also exerts its effects on MSCs via microparticles or extracellular vesicles (EVs), which act as delivery agents for various growth and differentiation molecules. EVs from HPL have demonstrated a significant enrichment of several GFs as compared to whole HPL, in addition to promoting MSC migration, proliferation and osteogenic differentiation [89]. EVs also act as delivery agents for micro-RNAs, which are known to regulate MSC functions including osteogenic differentiation [90, 91]. With the growing interest in 'cell-free' regenerative strategies using MSC-derived EVs, it has been suggested that exogenous EVs from HPL may further enhance the therapeutic effects of HPL-cultured MSC-EVs [92]. Indeed, the therapeutic effects of HPL-cultured MSC-EVs have also been demonstrated in preclinical (ischaemic stroke) [93] and clinical studies (graft-vs.-host disease) [94].

Previous studies have reported enhanced osteogenic differentiation of various MSCs when expanded in HPL [95-99]. Consistently, evidence from preclinical studies suggests enhanced *in vivo* bone regeneration with MSCs cultured in HPL vs. FBS or other supplements (**Paper I**). In a phase-I clinical trial, our group has demonstrated the efficacy of HPL-expanded BMSCs for BTE in the posterior mandible in 11 patients [26]. Interestingly, an additional benefit was observed on soft tissue healing. It was speculated that expansion in HPL may have resulted in osteogenic "pre-conditioning" of the BMSCs, leading to bone formation, and paracrine effects on soft tissues [26]. The xeno-free MSC expansion protocol used in this clinical trial [25] formed the basis for cell culture methods used in this thesis.

1.3.3. 3D culture of MSCs

Bone and bone marrow are 3D structures where the architecture, oxygen tension, mechanical stimuli, cellular cross-talk and paracrine signalling, all influence the functions of resident cells, including MSCs [43]. Traditional strategies for *ex vivo* MSC expansion most commonly employ plastic adherent 2D monolayer cultures, which lack the aforementioned *in vivo* stimuli. Although originally defined as plastic adherent cells, MSC expansion via serial passaging in monolayer cultures is reported to alter their phenotype and diminish their proliferation, differentiation and immunomodulatory potential [100-103]. Since 2D monolayer cultures are not

adequately representative of the *in vivo* microenvironment, this may alter the properties of MSCs and lead to sub-optimal clinical outcomes [104].

To overcome these challenges, 3D expansion of bone marrow MNCs/MSCs directly on biomaterial scaffolds has been proposed as a more biomimetic approach. To further simulate *in vivo* conditions, the cell-scaffold assembly may be cultured in a perfusion bioreactor, where temperature, pH, oxygen tension, etc. may be highly controlled [105, 106]. With regards to BTE, a number of studies have reported superior osteogenic performance of MSCs cultured with this method, as summarized in [43]. An important factor in this assembly is the substrate or scaffold on which MSCs are cultured. Although ceramics represent the most frequently tested biomaterials for BTE, their limited degradation and persistence at defect sites is still a challenge [107]. Synthetic materials, e.g. (co)polymers, with highly tunable macro-/micro-architecture and degradation profiles are emerging. Moreover, recent advances in 3D printing offer new opportunities to produce customised scaffolds for MSCs in BTE [108]. In addition to scaffold-based 3D culture, an alternate approach is to culture MSCs as 3D spheroids.

1.3.4. 3D spheroid culture of MSCs

The self-assembly or spontaneous aggregation of cells into 3D spheroids is mediated by different cell-to-cell and cell-to-ECM interactions, biomechanical cues and signaling pathways as compared to monolayers, which more closely simulate the *in vivo* microenvironment [109]. Spheroid cultures have long been used in relation to embryonic and cancer cells, to study organogenesis and tumour biology, respectively (**Figure 1.5**). Such 3D models have been synonymously referred to as spheres, spheroids, organoids, microtissues, and other tissue-specific terms, such as *neurospheres, mammospheres, cardiospheres, hepatopsheres* and *osteospheres*. In the context of MSCs, spheroid cultures were originally created to investigate the *in vivo* behaviour of MSCs, which spontaneously assembled into spheroids when injected in mice; later studies demonstrated that cell behaviour in spheroids was very similar to that *in vivo* [110, 111]. Spheroid models have since been used in drug discovery, toxicology and engineering of tissues such as liver, nerve, heart and bone [112, 113].
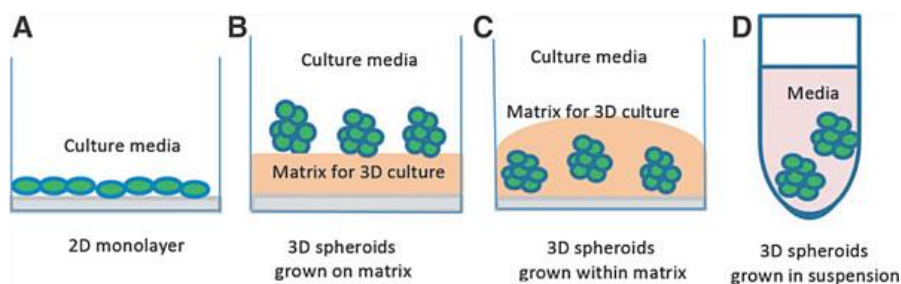
Figure 1.5: Schema of monolayer (A) vs. spheroid (B-D) cultures. Adapted from [113]

Benefits of spheroid culture

Spheroid culture closely simulates their *in vivo* microenvironment of MSCs and has been linked to embryonic events such as mesenchymal cell condensation (MCC) [114-116]. Cytoskeletal changes in MSCs, such as those induced by 3D culture, influence both their stemness and fate determination [117, 118]. Detailed discussions of the benefits of 3D culture, including molecular mechanisms and *in vivo* applications, have been presented in comprehensive review articles [101, 102, 104, 112] – a summary of the reviewed evidence for human MSCs is presented below.

Self-renewal: Stem cell self-renewal is defined as "the process by which a (parent) stem cell divides *symmetrically* or *asymmetrically* to generate at least one daughter cell, which retains a developmental potential that is similar to the mother stem cell." [119] This concept is most often used in the context of *pluripotent* embryonic stem cells (ESCs), which possess *unlimited* self-renewal potential. In ESCs, self-renewal and maintenance of pluripotency are regulated by three main transcription factors – sex determining region Y-box 2 (SOX2), octamer-binding transcription factor 4 (OCT4) and nanog homeobox factor (NANOG) [119, 120]. Ectopic expression of these factors in differentiated somatic cells, e.g., fibroblasts, induces cellular reprogramming back to a pluripotent state, as in induced pluripotent stem cells [121]. However, simply changing the micro-environment from 2D to 3D/spheroid culture is also known to cause a significant upregulation of these pluripotency factors via epigenetic mechanisms [122, 123]. Interestingly, this phenomenon is observed not only in

MSCs/progenitor cells, but also in fibroblasts [124]. Thus, 3D culture is reported to induce cellular "de-differentiation", akin to reprogramming, thereby enhancing the capacity for self-renewal [124].

Multilineage differentiation: The ability to differentiate into at least three different lineages, i.e., bone, cartilage and fat, is a defining feature of MSCs [21]. The cytoskeletal changes induced by 3D culture are reported to influence MSC fate determination [117, 118]. While aggregate cultures have long been used to induce MSC chondrogenic differentiation *in vitro* [125], by simulating cell condensations related to embryonic chondrogenesis and endochondral ossification, osteogenic and adipogenic differentiation have predominantly been performed in monolayer MSCs. However, several studies have also shown the benefits of spheroid/aggregate culture for osteogenic differentiation of MSCs [126-129]. Direct replating of dissociated BMSC and ASC spheroids also showed an increased differentiation potential towards adipogenic and neuronal-like cells, suggesting the use of spheroid culture as a preconditioning strategy to enhance MSC function [130-133]. The benefits of spheroid culture for osteogenesis are discussed in section 1.3.5.

Paracrine activity: In addition to direct differentiation, MSCs are known to exert their regenerative effects via paracrine mechanisms, i.e., secretion of trophic factors to modulate the host response [134]. The results of several recent studies have shown that MSC spheroids are more secretory than their 2D counterparts [102]. For example, increased secretion of anti-inflammatory cytokine stimulated gene/protein 6 (TSG-6), prostaglandin E2 (PGE2; which modulates macrophage responses) and interleukin-24 (IL-24; which reduced the viability of cancer cells) has been reported in BMSC spheroids vs. monolayers [135, 136]. Moreover, MSC spheroids also showed the increased secretion of angiogenic factors, including vascular endothelial growth factor (VEGF), fibroblast growth factor 2 (FGF-2), hepatocyte growth factor (HGF), stromal-derived factor-1 (SDF-1), and angiogenin [137-139]. The increased secretion of endogenous GFs may contribute to the enhanced differentiation potential of MSC spheroids [140].

1.3.5. *Spheroid culture for osteogenesis*

In the context of bone, spheroid culture is especially relevant. Changes in the cytoskeleton induced by 3D culture have been linked to mesenchymal cell condensation (MCC), an important event during skeletal development, which stimulates osteoblastic differentiation, and which can be recapitulated *ex vivo* [114, 115]. MCC have been defined as "the pivotal stage in skeletal development (which) takes place when a previously dispersed population of mesenchymal cells forms an aggregation or condensation, which is the earliest sign of the initiation of a skeletal element or elements" [114]. Aggregates of MSCs/progenitor cells are reported to mimic such condensations *in vitro*, thereby enhancing osteogenic differentiation in comparison to 2D cultures (**Figure 1.6**) [115, 141].

   MCC are mediated by a number of factors, among which are bone morphogenetic proteins (BMPs), particularly BMP2 and BMP4, reported to regulate the size and growth of condensations [114]. BMPs are members of the transforming growth factor-β (TGF-β) superfamily and are among the most potent regulators of osteogenic differentiation and bone formation [142]. Their name is derived from observations that their *in vivo* transplantation in extra-skeletal (ectopic) sites leads to *de novo* bone formation [143]. BMP2 is known to be a key regulator of MSC osteogenic differentiation via downstream regulation of runt-related transcription factor 2 (RUNX2), the 'master' osteogenic transcription factor [142]. In *ex vivo* MSC aggregates, BMP2 is reported to be among the most strongly upregulated genes, regulating their pro-/anti-inflammatory activity, resistance to cytotoxic stimuli and osteogenic differentiation potential *in vitro* [137, 140].
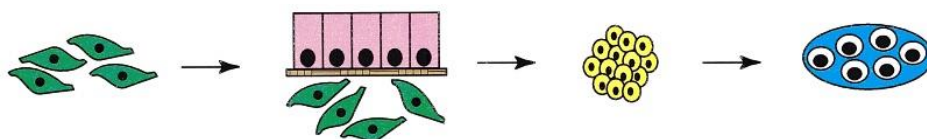
Figure 1.6: Schema of the different phases of skeletal development (from left to right): migration of pre-skeletal cells (green) to the site of future osteogenesis, associated with an epithelium (purple) and epithelial basement membrane (brown); interactions of those cells with epithelial cell products resulting in initiation of a condensation (yellow); and overt differentiation of chondroblasts or osteoblasts (blue). Adapted from [114]

The benefits of MSC spheroid culture for osteogenesis have been validated in a number of *in vivo* studies, summarized in **Table 1.1**. Overall, superior bone formation was observed when using osteogenically induced or 'primed' spheroid vs. dissociated MSCs in ectopic and orthotopic models. However, no studies reported the use of xeno-free cultured MSCs. Thus, the *in vivo* osteogenic potential of xeno-free 3D MSCs, which represents a more clinically relevant strategy for BTE, remains to be tested.

Table 1.2: Summary of in vivo applications of MSC spheroids for BTE

Study	Cells (origin)	3D culture (cell nos., induction, duration)	Scaffold	Model (time)	Bone formation
Ectopic					
Farrell et al. 2011 [144]	Human BMSCs	Pellet (1×10^6; chondrogenic or osteogenic, 28d)	Col-GAG	SC (8 w)	Pellet+scaffold > scaffold alone (chondrogenic) Pellet > pellet+scaffold (chondrogenic)
Chatterjea et al. 2013 [145]; 2017 [146]	Human BMSCs	Microwells (1.5×10^6; osteogenic, 14d)	BCP + PRP	SC (2, 4, 8 w)	3D > 2D MSCs Constructs with PRP > without
Fennema et al. 2017 [38]	Human BMSCs, ASCs/ SVF	Microwells (1.5×10^6; osteogenic, 1d)	BCP + PRP (+/- rhBMP2)	SC (6 w)	3D BMSCs > 3D ASCs 3D BMSCs > SVF + rhBMP2
Ho et al. 2016 [147]	Human BMSCs	Hanging drop (2.4×10^6; osteogenic, 14d)	Alginate gel (+/- RGD)	SC (8 w)	3D > 2D MSCs
Ho et al. 2017 [148]	Human BMSCs	Microwells (2.4×10^6; osteogenic, 14d)	Alginate gel (+/- RGD)	SC (2, 6 w)	Unmod = RGD-mod Alginate (both with 3D BMSCs)
Orthotopic					
Yamaguchi et al. 2014 [149]	Rat BMSCs	Suspension (5×10^4; osteogenic, 7d)	Matrigel	C-CSD (4 w)	3D > 2D MSCs
Suenaga et al. 2015 [127]	Human BMSCs	Rotation (1×10^7; osteogenic, 1d)	BCP	C-CSD (8 w)	3D > 2D MSCs 3D MSCs > 3D MSCs + BCP
Ho et al. 2018 [150]	Human BMSCs	Microwells (2.4×10^6; hypoxic, 3d)	Alginate gel + RGD (+/- BMP2)	Femur CSD (12 w)	3D > 2D MSCs (both hypoxia pre-conditioned) Scaffold + BMP2 > 3D BMSCs

Moritani et al. 2018 [129]	Human PDLCs	Microwells (3×10^4; osteogenic, 14d)	Matrigel	C-CSD (2 w)	3D > 2D MSCs
Iwasaki et al. 2019 [151]	Human PDLCs	Pellet (1×10^5)	Fibrin gel	P-CSD (4 w)	3D MSCs = no treatment
Imamura et al. 2020 [152]	Mouse BMSCs	Suspension (5×10^5; osteogenic or BMP2, 7d)	Col-sponge	C-CSD (2-12 w)	3D > 2D MSCs

Col-GAG, collagen-glycosaminoglycans; BCP, biphasic calcium phosphate; PRP, platelet-rich plasma; mod, modified; rhBMP2, recombinant human BMP2; SC, subcutaneous; C-CSD, calvarial critical size defects; P-CSD, periodontal CSD; d, days; w, weeks.

1.3.6. Spheroid coculture for angiogenesis

In the context of BTE, angiogenesis is an essential component of the wound healing cascade and its inadequacy is a major limiting factor in the clinical translation of cell therapies [153]. The lack of adequate and timely vascularization of implanted cells, which is essential for oxygenation, nutrition, and waste elimination, can result in premature cell death in regions of the construct since diffusion of oxygen and nutrients from the host vasculature is only limited to a distance of 150–200 µm [154, 155]. Moreover, age-related changes in the vasculature of craniofacial bones make the need angiogenesis even more important.

An emerging strategy to overcome this limitation is to *coculture* MSCs with endothelial cells (ECs), to create 'pre-vascularized' constructs, i.e. a primitive network of capillaries that functionally anastomose with host vessels when implanted *in vivo* [156, 157]. When cultured on appropriate ECM, ECs organize into tube-like networks resembling primitive vessels [158]. Coculture with MSCs can enhance this process. The rationale is that since MSCs reside in a perivascular niche they may stabilize EC-networks by adopting a pericyte-like phenotype in cocultures, and enhance EC-mediated angiogenesis [159].

To determine the preclinical evidence for the efficacy of co-culture strategies, a systematic literature review and meta-analysis was performed. The meta-analyses revealed a significant benefit of co-transplantation for bone regeneration in rats'

calvarial defects, although results angiogenesis/vessel regeneration were inconclusive [160]. It should be noted that rodent calvaria are considered as a challenging environment for bone regeneration due to poor blood supply and limited bone marrow. Thus, the role of vascularization in bone graft healing is even more critical in this zone [161]. The review concluded that (a) co-culture of MSCs and ECs under specific conditions *in vitro* can enhance their regenerative potential when co-transplanted *in vivo*; and (b) MSCs and ECs from *human* sources demonstrate synergistic activity when cocultured *in vitro* [160].

All included studies in the review reported the 'monolayer' or 2D coculture of ECs and MSCs. In contrast to monolayers, the 3D spheroid culture of ECs leads to tube formation by closely mimicking *in vivo* sprouting angiogenesis. This pattern of sprouting is considered to be a close representation of the *in vivo* angiogenic cascade. It recapitulates all the key events during which quiescent ECs become activated, degrade their surrounding matrix, migrate towards the angiogenic stimulus, and organize into 3D capillary networks (**Figure 1.7**) [162]. These *in vitro* sprouts have revealed functional lumens and the ability to anastomose with host vessels when implanted *in vivo* [163]. Thus, spheroid culture ECs, preferably with MSCs, represents a promising pre-vascularization strategy to enhance angiogenesis in BTE constructs.
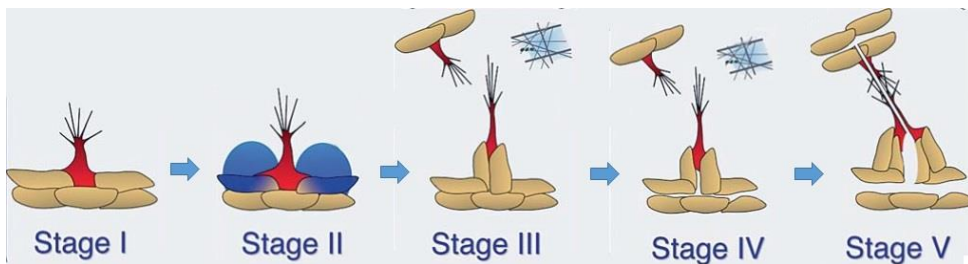
Figure 1.7: Schematic representation of the stages of blood vessel sprouting: Stage I is tip cell specification and sprout initiation; Stage II is sprout elongation and local guidance; Stage III is sprout elongation in response to extrinsic cues; Stage IV is lumen formation; and Stage V is sprout fusion and completion of lumenization. Adapted from [162]

1.4. RATIONALE

In previous work, our research group comprehensively characterized MSCs from bone marrow [39, 164] and dental sources [165, 166], and tested their osteogenic potential *in vitro* and *in vivo*. Monolayer (2D) cocultures of MSCs and ECs have been tested to promote angiogenesis [167-169]. However, most of these studies have been performed in FBS cultures, which limits the translatability of the results.

To facilitate clinical translation, it is important to characterize cells and establish treatment protocols in xeno-free conditions, such as HPL, in addition to simulating *in vivo*-like conditions. Although promising results of BTE have been reported using BMSCs, less invasive cell sources, e.g. GPCs, are sought after, especially for oral-maxillofacial applications. Detailed characterization of the immunophenotype, growth kinetics and differentiation potential of these cells in xeno-free conditions, preferably in comparison to gold-standard BMSCs, is necessary to justify further use and design optimal clinical strategies. Emerging concepts also advocate 3D culture of MSCs to enhance their differentiation and regenerative potential.

Finally, the delivery of clinically optimized cell cultures in 3D scaffolds to regeneration sites is the last step in translational BTE. 3D-printed scaffolds represent a promising approach for delivery of MSCs to advanced bone defects. Such scaffolds have recently been developed, and their printability and *in vitro* biocompatibility has been demonstrated [170]. This favourable *in vitro* performance now warrants *in vivo* validation. Testing these innovative BTE constructs, which combine all aspects of the tissue engineering 'triad', in appropriate *in vivo* models would bring us closer towards the treatment of challenging bone defects.

2. Aims

The overall aim of this work was to optimize a xeno-free 3D culture system of MSCs as a clinically relevant strategy to enhance osteogenic differentiation for BTE. Secondary aims were to identify a less invasive source of MSCs, comparable to BMSCs, and to promote angiogenesis within xeno-free 3D constructs.

The specific objectives related to each of the studies were as follows:

		Paper
1.	To identify the optimal xeno-free supplement for human MSC culture in the context of BTE via a systematic literature review.	**I**
2.	To optimize the production of HPL and test its cytokine content and biological efficacy for MSCs, specifically osteogenic differentiation.	**II**
3.	To characterize xeno-free BMSCs and GPCs as 3D spheroids and to test their osteogenic differentiation potential.	**III**
4.	To coculture xeno-free GPCs with ECs as 3D spheroids and test their angiogenic potential.	**IV**
5.	To test *in vivo* bone formation with constructs of 3D spheroids of GPCs and/or BMSCs, hydrogels and 3D-printed scaffolds in ectopic and orthotopic models.	**V**

3. Methods

3.1. CHOICE OF METHODS AND STUDY DESIGN

The clinical translation of novel BTE approaches can only be achieved through rigorous preclinical testing. A variety of *in vitro* and *in vivo* methods were used in this thesis to achieve the objectives in each study – the central focus being *clinical relevance and feasibility of translation*.

To ease translation of the findings, all cell culture experiments were performed using human cells – BMSCs, ASCs, GPCs, PDLCs and HUVECs. 3D spheroid culture was tested as an approach to further mimic the *in vivo* microenvironment and cellular niche. Cells were cultured and characterized in HPL, which is emerging as the clinical standard for cell manufacturing. An HPL-based hydrogel, a modification of PRP, was also tested as a cell carrier, especially for spheroids. The combination of hydrogels and 3D printed scaffolds was also tested as a potential cell-delivery strategy.

The choice of *in vitro* methods was evidence-based, following commonly reported practices. Different methods were often used to confirm findings in a single experiment. For example, qPCR was extensively used to quantitatively assess gene expression of early molecular events in cell cultures. However, since gene expression is only a 'surrogate' indicator of events, this was further confirmed at the protein level, e.g., via immunocytochemistry and 3D confocal imaging, since *"seeing is believing"*.

For the *in vivo* studies, immunocompromised animal models were used to test the efficacy of constructs containing human cells. For angiogenesis, the CAM assay in chicken embryos is well-established given the lack of an immune system and quick responses to angiogenic stimuli. For BTE, athymic nude rat/mouse models lacking T cell-function are well-established for human MSC-transplantation. While ectopic (subcutaneous) models provide a starting point for proof-of-principle studies, orthotopic models (calvarial defects) aim to test BTE strategies in more clinically relevant settings.

Summary of study design

Study	Design	Methods
I	Systematic review	Literature search
II		A: HPL characterization • Cytokine assay B: BMSC characterization (vs. FBS) • Growth • Osteogenesis • Ectopic bone assay*
III		A: 2D GPC characterization (vs. FBS) B: 3D GPC / BMSC characterization Stemness • Stemness • Osteogenesis
IV		GPC+EC 3D coculture • In vitro sprouting • Chicken embryo CAM assay
V		2D/3D BMSC + gel + 3D printed scaffold constructs • Ectopic, subcutaneous [T] • Calvarial defect regeneration

In the figure, column headers A and B appear above studies II and III; "In vitro" and mouse icons (marked *) appear in II; "In vitro" in III; "In vitro" and CAM assay in IV; "Ectopic" and "Calvarial" in V.

Key: PPC, HPL, 2D BMSC, 2D GPC, 3D BMSC, 3D GPC, HUVEC, 3D Coculture, 3D-P Scaffold, HPL gel

* ectopic bone formation data was not included in the manuscript (Paper II)

[T] experiments also performed with GPC and will be reported separately

3.2.   ETHICAL APPROVALS

Ethical approvals for using human tissues were obtained from the Regional Committees for Medical and Health Research Ethics (REK) in Norway: 2013-1248/REK sør-øst C (bone marrow and adipose tissue) and 2016-1266/REK nord (gingiva and PDL). Tissues were harvested after informed patient consent. HPL was prepared from outdated PCs considered biological waste, therefore no ethical approval was needed. Animal experiments were approved by the Norwegian Animal Research Authority *(Mattilsynet)*: FOTS 18738 and 17443. All experiments were performed following the ARRIVE guidelines [171].

3.3.   SYSTEMATIC REVIEW (Paper I)

The primary aim of this systematic review was to answer the focused question: do MSCs expanded in xeno-free media possess superior osteogenic potential compared with MSCs expanded in FBS-supplemented media? A secondary aim was to compare different platelet-derivatives in terms of their GF contents and efficacy for cell expansion. A review protocol was developed based on the Preferred Reporting Items for Systematic reviews and Meta-Analyses (PRISMA) guidelines [172]. Electronic databases and additional resources were searched for relevant literature based on a search strategy. Risk of bias in the selected studies was assessed using the *SY*stematic *R*eview *C*entre for *L*aboratory animal *Ex*perimentation (SYRCLE) RoB tool [173].

3.4.   HPL PRODUCTION (Paper II)

3.4.1. *PC preparation and storage*

The HPL herein (Bergenlys®, Norway) was prepared from outdated pooled PCs. Briefly, the PCs were prepared at the Haukeland University Hospital Bloodbank, by manually pooling five interim platelet units (IPUs) in 30% plasma and 70% platelet additive solution and subsequently leukocyte-filtered (Terumo BCT, USA). Pooled PCs containing $>2 \times 10^{11}$ platelets (and $<1 \times 10^6$ leukocytes) were X-ray irradiated at a dose of 25 Gy and stored at 22°C $\pm$ 2°C under agitation for no longer than 7 d for use

as transfusion units. All unused 7 day-old PCs were frozen at –80°C within 24 hours for subsequent HPL production.

3.4.2. HPL production and EVs isolation

Unused 7 day-old PCs were used for HPL production via the freeze/thaw lysis method. PCs (corresponding to 20 donors) were exposed to multiple freezing (–80°C) and thawing cycles (+37°C) to ensure platelet lysis before pooling (**Figure 3.1**). Pooled PCs were then centrifuged to remove platelet fragments and aliquoted as the final HPL product. No fibrinogen depletion step was performed. HPL aliquots were stored at –80°C and thawed overnight at 4°C for subsequent use in experiments.

Figure 3.1: The HPL production process showing (A) outdated PC; (B) PC freezing; (C) PC thawing; and (D) pooled HPL after centrifugation.

EVs from HPL were isolated via ultracentrifugation [174] and size-exclusion chromatography [175]. EV size was measured via dynamic light scattering (Zetasiser, UK) and were visualized via transmission electron microscopy (TEM; JEM-1230 microscope, USA). The total protein in EVs relative to HPL was quantified using the bicinchoninic acid (BCA) assay (Thermo Fisher). Cytokine concentrations were measured using a multiplex assay (BioRad, USA) as described in **Paper II**.

3.5. CELL CULTURE (All Papers)

3.5.1. Primary human BMSCs and ASCs

Donor-matched BMSCs and ASCs were isolated and expanded following established protocols [33]. For each donor, BMSCs and ASCs were isolated in 5% HPL and 10% FBS (GE Healthcare, USA) supplemented growth media as described in Paper II. In HPL-supplemented media, 1 IU/mL of heparin was added to prevent gelation. Cells were sub-cultured and expanded with a seeding density of 4000 cells/cm^2; passage 2–4 cells from at least three different donors were used in experiments.

3.5.2. Primary human GPCs and PDLCs

GPCs and PDLCs were isolated and expanded according to established protocols [46]. Extracted teeth were obtained from healthy donors aged 18-31 years. From each donor, primary connective tissue-explant cultures of GPCs and PDLCs were established in 5% HPL and 10% FBS supplemented growth media.

3.5.3. Primary human umbilical vein endothelial cells

Pooled passage one human umbilical vein endothelial cells (HUVECs) (Lonza, USA) were cultured in EGM-2 growth medium (Lonza) supplemented with 2% FBS according to manufacturer's instructions, or alternatively with 5% HPL; all other media components were maintained. Cells were sub-cultured and expanded under humidified 5% CO2 at 37°C; passage 2-4 cells were used in experiments. For all cell cultures, cell number and viability were assessed using Trypan blue stain and an automated cell counter (Invitrogen).

3.5.4. 3D spheroid culture

Formation of cell spheroids was assessed via two methods: mesenspheres [176] and aggregates [177]. Briefly, dissociated passage 1-2 monolayer cells in HPL media were seeded (1000 cells/cm^2) in low-attachment dishes (Corning, USA) for 7 days to obtain mesenspheres, or in microwell plates (Sphericalplate®, Kugelmeiers, CH) for 24 hours to obtain aggregates of 1000-2000 cells. Mesenphere formation occurs via self-renewal

of primary MSCs seeded in low-density suspension cultures, and is reported to propogate 'true' stem cell fractions [176, 178]. Athough BMSCs predictably formed mensenspheres, only a small fraction of GPCs and PDLCs herein demonstrated this capacity in HPL media (**Figure 3.2**). Since this method relies on self-renewal of individual cells, the size and shape of mesenspheres varied considerably and the overall frequency of sphere formation was low.

Sphere formation via aggregation is achieved either via self-assembly or forced aggregation [135, 177]. Aggregate spheroids herein were generated via 'guided' self-assembly in novel microwell-patterned tissue culture plates. Highly consistent spheroids of GPCs and BMSCs could be produced with this method (~1000 cells/spheroid, ⌀ 100-300 μm; **Paper III**). High cell viability within the spheroids was confirmed via live/dead staining up to 7 days in culture. Since aggregate spheroids could be formed more predictably than mesenspheres, only the former were used in subsequent experiments. The terms 2D or monolayer and 3D or spheroid culture are interchangeably used throughout the thesis.
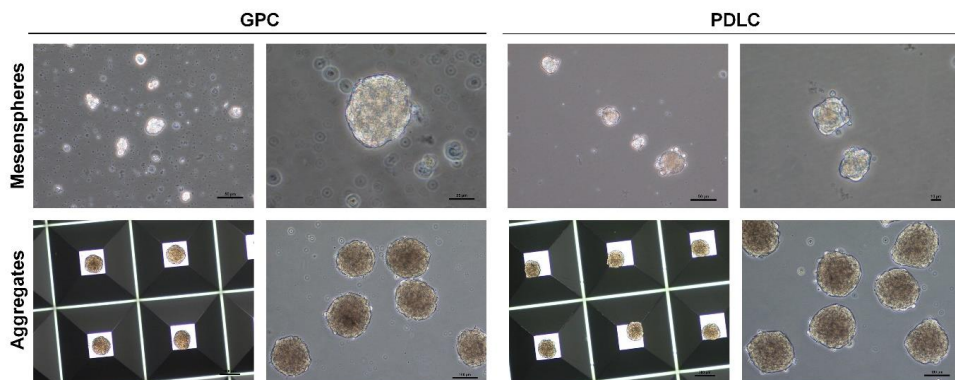
Figure 3.2: Spheroid formation of GPCs and PDLCs as mesenspheres or aggregates.

3.6. IN VITRO METHODS (All Papers)

3.6.1. *Summary of in vitro methods*

The experimental methods used in this thesis are described in detail in the included manuscripts. This chapter contains a summary, with a focus on selected methods of particular importance.

Table 3.1: Summary of methods used in the thesis.

Method	Purpose	Paper
HPL production		
HPL gel	Cell delivery, ECM	IV, V
Rheometry	Gel characterization	IV
Ultracentrifugation	Exosome isolation	-
Size exclusion chromatography	Exosome isolation	-
Dynamic light scattering	Exosome quantification	-
Cell culture		
Primary cells – isolation + culture	2D cell culture	*All*
Spheroid culture	3D cell culture	III, IV, V
Flow cytometry	Cell immunophenotyping	II, III, V
Fluorescence associated cell sorting	Cell sorting	III
Trypan blue assay	Cell viability	*All*
Live dead assay	Cell viability	III, IV, V
CFU-F assay	Colony formation	II, III
Population doubling	Cell growth kinetics	II, V
Alamar blue assay	Cell metabolic activity	III
DNA assay	Cell DNA quantification	II, III, V
Senescence associated β-galactosidase assay	Cell senescence	II
MSC differentiation assays	Cell characterization	*All*
Alkaline phosphatase assay	Osteogenic differentiation	II, V
MSC conditioned medium	Secretome analysis	III, V
Wound healing assay	Secretome efficacy	V

Molecular biology		
qPCR (incl. RNA extraction/ quantification, cDNA preparation)	Gene expression	All
Bicinchoninic acid assay	Protein estimation	II, III, V
Enzyme-linked immuno assay	Protein estimation	II
Multiplex assay (+ STRING analysis)	Multiple cytokines estimation	II, III, V
Western blotting	Protein estimation	II
Immunofluorescence	Protein identification	III, IV, V
Microscopy		
Transmission electron microscope (TEM)	Exosome imaging	-
Scanning electron microscope (SEM)	Scaffold (+cell) imaging	III, V
Stereomicroscope	Scaffold/specimen imaging	IV, V
Confocal laser scanning microscope (CLSM)	Immunofluorescence	III, IV, V
Digital virtual scanning microscope	Histology	V
3D printing		
Poly-LTMC scaffolds	Scaffold production	V
In vivo methods		
Chick embryo CAM assay	Angiogenesis	IV
Subcutaneous implantation	Ectopic bone formation	V
Calvarial defect model	Orthotopic bone regeneration	V
CT scanning (in vivo)	Hard tissue imaging	V
Micro-CT (μCT) scanning	Hard tissue imaging	V
Standard (paraffin) histology	Histology	IV, V
Non-decalcified histology	Bone histology	V
Immunohistochemistry (IHC)	Protein identification	IV
In-situ hybridization (ISH)	RNA identification	V

CFU-F, colony forming unit-fibroblast; qPCR, quantitative polymerase chain reaction

qPCR was extensively used in this thesis to quantify gene expression in cell cultures. A summary of the gene assays is presented below.

Table 3.2: TaqMan® real-time PCR assays used in gene expression experiments

Gene name	ID	Assay ID	Amp
Housekeeping gene (Papers II, III, V)			
Glyceraldehyde 3-phosphate dehydrogenase	GAPDH	Hs 02758991_g1	93
Stemness-related (Papers III, V)			
Sex determining region Y-box 2	SOX2	Hs01053049_s1	91
Octamer-binding transcription factor 4	OCT4	Hs00999632_g1	77
Homeobox transcription factor nanog	NANOG	Hs02387400_g1	109
Adipogenesis-related (Papers II, V)			
Peroxisome proliferator activated receptor gamma	PPARG	Hs01115513_m1	90
Lipoprotein lipase	LPL	Hs00173425_m1	103
Chondrogenesis-related (Paper V)			
Sex determining region Y-box 9	SOX9	Hs00165814_m1	102
Osteogenesis-related (Papers II, III, V)			
Runt-related transcription factor 2	RUNX2	Hs01047973_m1	86
Bone morphogenetic protein 2	BMP2	Hs00154192_m1	60
Alkaline phosphatase	ALPL	Hs01029144_m1	79
Collagen type 1	COL1A2	Hs00164099_m1	68
Osteopontin	OPN/SPP1	Hs00959010_m1	84
Osteocalcin	OCN/BGLAP	Hs01587814_g1	138
Bone sialoprotein	IBSP	Hs00913377_m1	87

Amp, Amplicon length

In **Papers III and V**, conditioned media (CM) from 2D and 3D BMSCs were collected after 48 hours culture in HPL-free medium and the concentrations of several cytokines were measured using a custom multiplex assay. Although the initial number of cells seeded in 2D and 3D cultures was the same, to account for differences in the rates of cell proliferation between the conditions, cytokine concentrations (pg/mL) were normalized to the corresponding total DNA (ng/mL).

Multiplex cytokine assays were used to determine the concentrations of several growth factors, chemokines and cytokines in HPL and CM. The list of cytokines used is reported in the Supplementary data files of **Papers II and III**.

Immunofluorescence staining was also extensively used to correlate gene and protein expression, especially in 3D spheroids. Considerable optimization of the staining methods were performed and repeated to confirm positive staining and reduce non-specific background. A summary of the antibodies tested is presented below.

Table 3.3: Primary antibodies used in immunostaining experiments

Antibody	Dilution	Manufacturer
Mouse monoclonal anti-TUJ1	1:100	Abcam
Chicken monoclonal anti-GFAP	1:100	Abcam
Rabbit polyclonal anti-SOX2	1:1000	Abcam
Rabbit polyclonal anti-OCN	1:100	Abcam
Mouse monoclonal anti-BMP2	1:200	Bio-Techne

TUJ1, β-III Tubulin; GFAP, glial fibrillary acidic protein.

3.6.2. HPL hydrogels

Traditional cell delivery methods involve direct seeding of cells on scaffolds prior to *in vivo* transplantation. However, this method may not be optimal for 3D spheroids – the 3D structure, which is important to maximize *in vivo* effects, is lost by direct seeding. In contrast, the encapsulation of spheroids in hydrogels may be an effective *in vivo* delivery system [139, 147]. In some cases, the hydrogels may also provide additional stimulatory effects to the cells and/or local environment [179].

To extend the application of HPL to xeno-free cell-carriers, HPL hydrogels were produced by addition of thrombin and $CaCl_2$ (both from Sigma-Aldrich), as described in **Paper IV**. The resulting hydrogel was referred to as 'unmodified' HPLG. To improve the hydrogel properties, HPL was supplemented with fibrinogen (Sigma-Aldrich) in different concentrations (1.25-25 mg/mL) prior to gelation. These hydrogels were referred to as 'modified' HPLG (**Figure 3.3**).
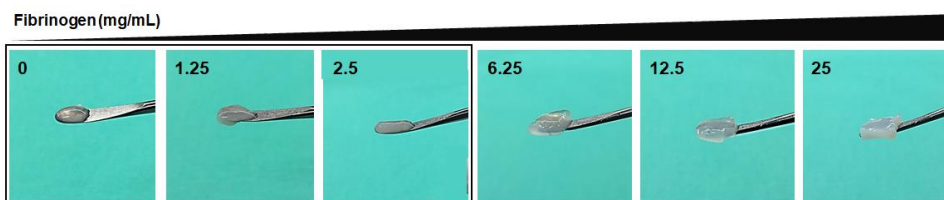
Figure 3.3: Appearance of HPLG at different fibrin concentrations, 0-25 mg/mL.

In **Paper IV**, sprouting angiogenesis was assessed in HUVEC spheroids encapsulated in unmodified and modified HPLG. Since favourable sprouting and viability were only observed in HPLG with <2.5 mg/mL fibrinogen (**Figure 3.3**, box), only these gels were used in subsequent experiments. Rheology was used to test their storage and loss modulus using a Physica MCR 301 rheometer (Anton Paar, UK).

In **Paper V**, the concentration of fibrinogen in HPLG was determined based on a survey of previous studies reporting optimal growth and osteogenic differentiation of MSCs in fibrin gels (**Table 3.4**).

Table 3.4: Selected studies reporting on MSCs in fibrin gels

Study	Conc. (mg/mL)	Model	Results
Abiraman et al. 2002 [180]	In vivo mSC: 2.5, 5	HA +/- BG	Bone: HA-BG+F > HA-BG (no bone) at 4 w; high F (5) > low F (2.5)
Bensaid et al. 2003 [181]	In vitro: 1.8 – 90 In vivo mSC: 18	BMSC BMSC + BCP	Proliferation: max. in 18 (+ 100UT) High viability up to 14 d
Catelas et al. 2005 [182]	In vitro: 5 – 50	BMSC	Proliferation: low (5) > high (34) ALP: high (50, 34) > low (5) Mineralization: high (34) > low (5)
Ho et al. 2006 [183]	In vitro: 5 – 50	BMSC	Proliferation: max. in 34 (+ 1UT)
Trombi et al. 2008 [184]	In vitro: 15, 30, 60	BMSC	Proliferation: low (15, 30) > high (60) Mineralization confirmed in 30
Kim et al. 2014 [185]	In vitro: 5-40 In vivo rCSD: 20	BMSC + a-Coll a-Coll	Proliferation: 5-20 > 40 Bone: F+Col > F > empty at 8 w
Linsley et al. 2016 [186]	In vitro: 5, 10, 25	BMSC +/- BCP	Proliferation: max. in 5 (- BCP); max. in 25 (+ BCP)

Conc.,fibrinogen concentration; F, fibrin; HA, hydroxy-apatite; BG, bioglass; BCP, biphasic calcium phosphate; a-Coll, atelo-collagen; UT, units thrombin; mSC, mouse subcutaneous; rCSD, rabbit CSD; d, days; w, weeks.

In general, while lower concentrations favoured MSC proliferation, concentrations >10 mg/mL favoured osteogenic differentiation. Several studies have reported optimal outcomes when using 20 mg/mL fibrin gels in combination with MSCs and/or biomaterials [139, 187-190]. Thus, HPLG with 20 mg/mL fibrinogen were prepared for the *in vivo* experiments in **Paper V**. Viability of BMSCs in HPLG up to 21 days was confirmed via live/dead staining (**Figure 3.4**). To prepare the scaffold-gel constructs (SGC), the HPL and thrombin solutions were mixed, seeded on pre-wetted scaffolds, and incubated at 37°C for 15 min for polymerization.
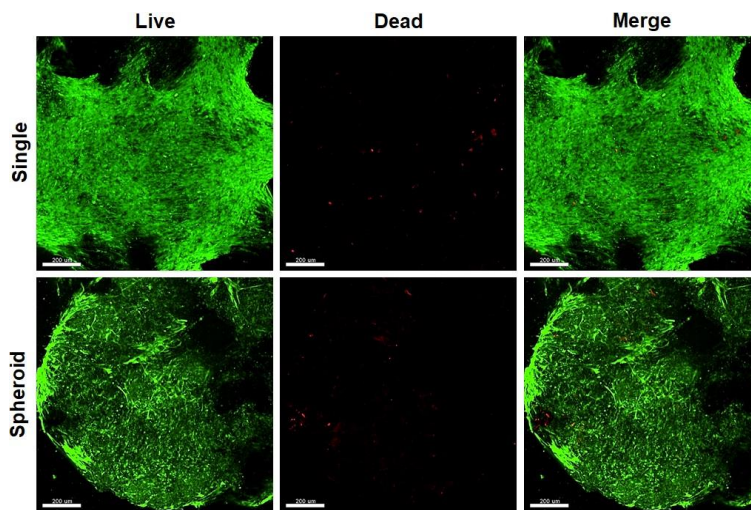
Figure 3.4: Cell viability in HPLG after 21 days, scale bars 200 μm.

3.6.3. *3D printed copolymer scaffolds*

3D printing allows the fabrication of customized bone scaffolds with controlled macro- and micro-architecture [108]. Although synthetic (co)polymers, e.g. PLGA, are most frequently used for 3D printing bone scaffolds, a major disadvantage is the local acidosis caused by their degradation, which may be detrimental to cell growth and function [108]. An alternative copolymer of poly(L-lactic acid) and trimethylene carbonate (PLA-TMC) has recently been developed [170]. TMC shows a superior degradation profile with non-acidic/non-toxic by products and high printability.

Recent studies in our group have characterized PLLA-TMC scaffolds, in terms of MSC attachment, growth and differentiation, for BTE applications [191]. Medical grade copolymer containing 40 mol% TMC (Evonik, Germany) was printed using a 3D-Bioplotter (EnvisionTEC, Germany). PLA-TMC sheets composed of 3-4 layers were printed and disc-shaped scaffolds (5 mm x 1.2 mm) were punched out. Prior to use in experiments, the scaffolds were sterilized via a combination of ethanol and UV light.

3.6.4. Preparation of BTE constructs

BMSCs as dissociated single cells or spheroids, were suspended in HPLG and, following addition of thrombin, were seeded on the scaffolds and incubated for 15 min. This resulted in SGC containing BMSCs as single cells or spheroids encapsulated in HPLG (**Figure 3.5**). Cell viability and osteogenic differentiation in SGC up to 21 days were assessed. For *in vivo* experiments, SGC containing single or spheroid BMSCs were cultured *in vitro* for 7 d in osteogenic media (ectopic implantation) or for 24 h in standard growth media (calvaria implantation) prior to transplantation.
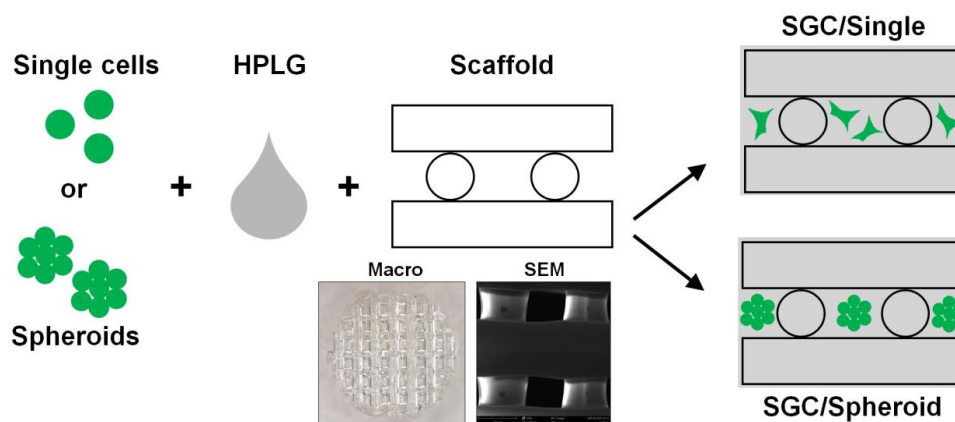
Figure 3.5: Schematic representation of SGC used in the study and macroscopic and SEM images (scale bar 300 μm) of the 3D printed PLLA-TMC scaffolds.

3.7.   IN VIVO METHODS (Papers IV & V)

For all *in vivo* experiments, animals were housed in stable conditions (22 ± 2 °C) with a 12 hours dark/light cycle, *ad libitum* access to food and water and allowed to acclimatize for one week prior to experiments. Animals were regularly monitored for signs of pain/infection, food intake and activity during the experimental period.

3.7.1. Ectopic subcutaneous implantation

For these experiments, 25 female athymic nude **mice** (Rj:ATHYM-Foxn1nu/nu, Janvier Labs) were used. The animals were anesthetized with a mixture of sevoflurane (Abbott, UK) and O_2 using a custom-made mask. The surgical site was disinfected before making two 1 cm incisions in the midline of the dorsum of the mouse. Four subcutaneous pouches were created using blunt dissection, followed by random implantation of cell-seeded implants or cell-free controls, as described in sections 4.1.3 and 4.4.2 (**Figure 3.6**). The skin was sutured (Vicryl, Ethicon, USA). Animals were injected subcutaneously with buprenorphine (0.03 mg/kg) after surgery, and 2 days postoperatively. Animals were euthanized 4 or 8 weeks later.
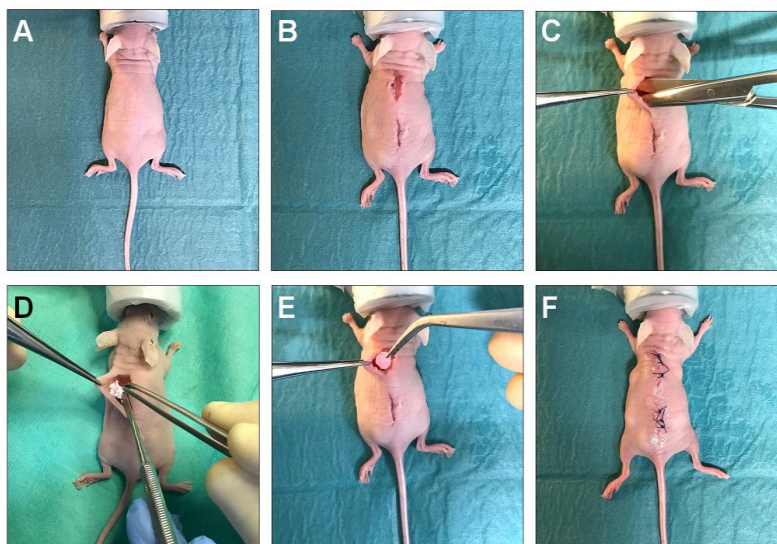
Figure 3.6: Subcutaneous implantation model in nude mice showing (A) anaethesia; (B) incisions; (C) blunt dissection; (D) implantation of granules or (E) scaffolds; and (F) suturing.

3.7.2. *Orthotopic calvarial defect model*

Eleven male athymic nude **rats** (LOU/MRj-Foxn1rnu/rnu, Janvier Labs) were used. Following anesthesia and disinfection, a 2 cm sagittal incision was made in the midline to reflect the periosteum. In each animal, two circular 5 mm defects were created on either side of the parietal bone using a trephine bur (Meisinger, Germany) (**Figure 3.7**). SGC containing $3x10^6$ BMSCs as single cells (n=8) or spheroids (n=8) were randomly implanted in the defects; SGC without BMSCs (n=6) served as controls. The periosteum and skin were sutured (Vicryl) and animals were injected subcutaneously with buprenorphine (0.03 mg/kg) after surgery and for 2 days postoperatively. Animals were euthanized 12 weeks later.
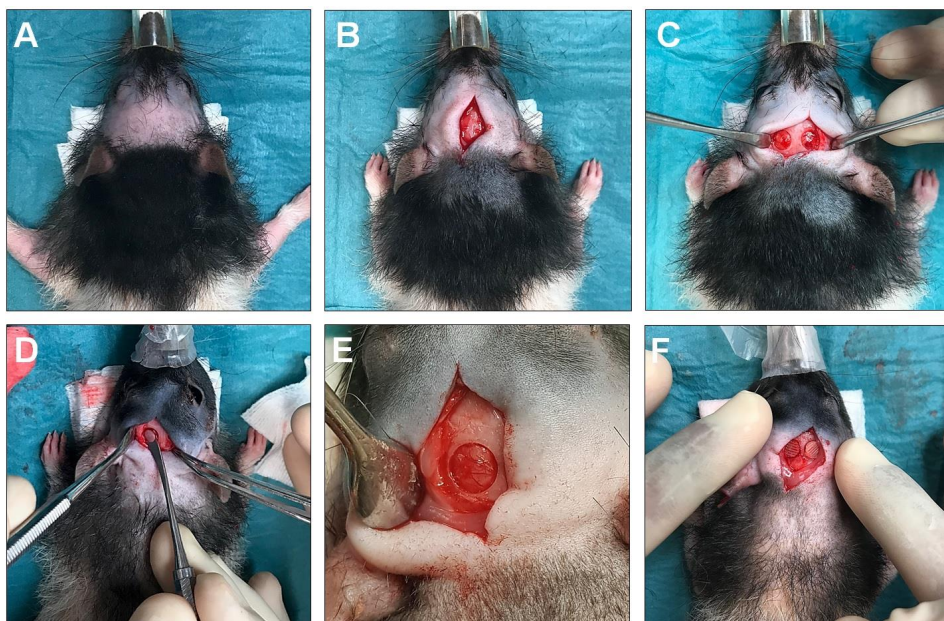
Figure 3.7: Calvaria CSD implantation model in nude rats showing (A) anaethesia; (B) incisions; (C) defect preparation; (D) bone elevation; (E) prepared defect; and (F) construct implantation.

3.7.3. Chick embryo Chorioallantoic Membrane (CAM) assay

The angiogenic potential of 3D HUVEC and coculture spheroids was tested in an *ex ovo* CAM assay [192]. Briefly, fertilized chicken eggs were incubated for 72 hours. On embryonic day 3 (ED 3), the eggs were carefully opened, their contents transferred into petri dishes and incubated for another 4 days. On ED 7, HUVEC or HUVEC-GPC coculture spheroids encapsulated in HPLG were implanted on the CAMs – gels were contained within silicone 'O-rings' on the CAM surface (**Figure 3.8**). On ED 14, the O-rings were photographed using a stereomicroscope, and the embryos were sacrificed. Images were analysed for angiogenesis-related parameters using an automated software (Wimasis, Spain) and the tissues were processed for paraffin histology.
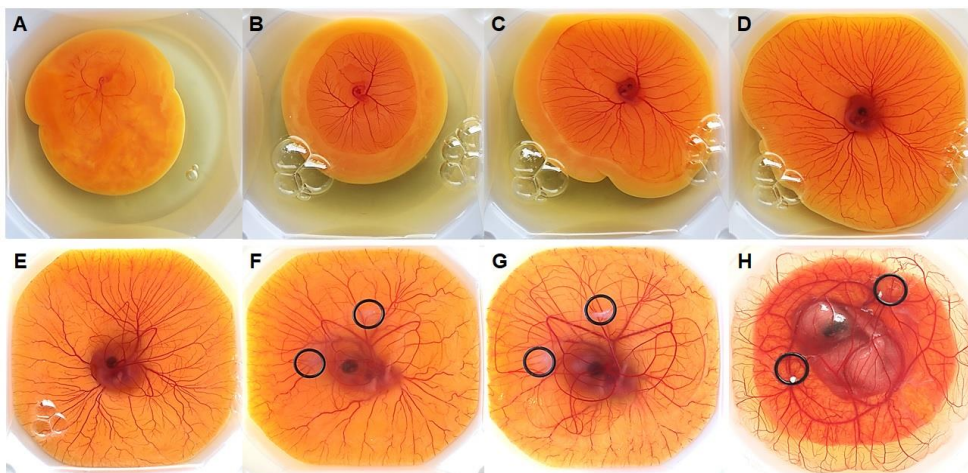
Figure 3.8: The *ex ovo* CAM assay in the developing chick embryo, showing (A-E) embryonic development during the first 7 days; (F) placement of the O-rings and cells on ED 7; and (G-H) development of the CAM vasculature up to day 14.

3.8.   ANALYSIS OF IN VIVO STUDIES (Papers IV & V)

3.8.1. *In vivo computed tomography*

To track calvarial bone regeneration, the rats were scanned 4, 6, 8 and 12 weeks after surgery using a small-animal computed tomography (CT) scanner (nanoScan, Hungary). Using pMOD software (PMOD, Switzerland), a standard volume of interest was set for each defect and a ratio of volume of regenerated bone/total defect volume (BV/TV) was calculated.

3.8.2. *Micro-CT*

The ectopic and calvaria specimens were scanned using either a SkyScan 1172 (Bruker, Berlgium) or SCANCO 50 micro-CT (µCT) scanner (SCANCO, Switzerland). Scans of calvarial defects were reconstructed using Amira software (Thermo Fisher) so that the drill direction was oriented along the Z-axis with the defect in the approximate center of the image. BV/TV was calculated for each sample/defect.

3.8.3. *Histology*

All CAM tissues were processed via paraffin-embedded histology. The subcutaneous transplants were processed for either paraffin- or resin-embedded (non-decalcified) histology. All calvaria transplants were processed via resin-embedded histology.

Paraffin-embedded histology: Tissues were fixed in 4% PFA/10% buffered formalin, dehydrated in ascending alcohol grades and embedded in paraffin using standard protocols. Sections (3-5 µm) were cut using a tissue microtome (Leica), and stained with hematoxylin and eosin (H&E), Alizarin red (ARS) or Masson's trichrome (MT).

Resin-embedded (undecalcified) histology: A µCT-guided technique for undecalcified resin-embedded histology using the technique of Donath and Breuner [193], was applied. A virtual slice was positioned in 3D through the centre of each defect parallel to the sagittal suture (**Figure 3.9**) and manually transferred to the specimen-blocks. Further processing of the blocks was performed using EXAKT cutting and grinding

equipment (Exakt, Germany). Standardized thin-ground sections were obtained and stained with Levi-Laczko dye. Histomorphometric analysis was performed using the Definiens v.2.0.0 (Definiens, Germany) and Adobe Photoshop software (Adobe, USA). The percentages of newly formed bone tissue (NBF) and the blood vessels were calculated for each specimen.
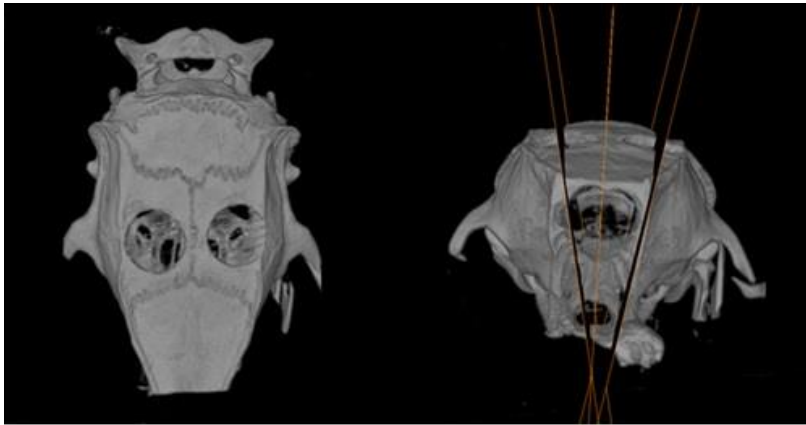
Figure 3.9: Micro-CT planning of standardized central histological sections in calvarial defects

3.8.4. Immunohistochemistry

Detection of human endothelial marker CD31 was performed in the CAM tissues. Following antigen retrieval, mouse monoclonal anti-human CD31 (M0823, Clone JC70A; Dako) diluted 1:50 was applied ON at 4°C, followed by an HRP-conjugated secondary antibody and counterstained with hematoxylin (all from Dako).

3.8.5. In situ hybridization

Identification of human cells in ectopic implants was performed using the human-specific repetitive *Alu* sequence, which comprises approximately 5% of the total human genome. The RNAscope® 2.5 High Definition Brown Assay and Hs-Alu-Rp-Sxj probe (Advanced Cell Diagnostics, UK) were used. This is a novel method for detection of RNA within cells, designed to amplify target-specific signals and minimize background noise. The hybridized probes were visualized using a diaminobenzidine (DAB) substrate and counterstained with haematoxylin (Dako).

3.9. STATISTICAL ANALYSES

Statistical analyses were performed using GraphPad Prism v 8.0 (GraphPad, USA). Data are presented as means ($\pm$ SD), unless specified. Analyses of qPCR data are based on delta-CT values and results are presented as relative (log) fold changes using scatter plots. Multiplex proteomic data are presented on a logarithmic (log10) scale. All other linear data are presented as bar graphs. Normality testing was performed via the Shapiro-Wilk test. The student *t* test, Mann-Whitney U test and/or One-way Analysis of Variance (ANOVA), followed by a post-hoc Tukey's test for multiple comparisons, were applied as appropriate, and $p < 0.05$ was considered statistically significant.

4. Main results and general discussion

This chapter includes the results considered of particular importance, and additional upublished supporting data. Detailed results from each of the studies are reported in the respective papers/manuscripts.

4.1. XENO-FREE CULTURE IN HPL (Papers I, II & III)

To identify the optimal FBS-substitute for MSC expansion, a sysmetatic review was performed (**Paper I**). As mentioned, three main categories of FBS-substitutes were identified: human serum, human platelet-derivatives and chemically-defined media.

Human serum

A majority of studies in this review investigated human serum (HS), most frequently at 10% concentration. Concentrations >10% significantly increase the amount of blood needed [194]. Use of both autologous and pooled HS was reported; autologous HS was superior in terms of MSC survival and proliferation [195]. However, the amount of autologous serum needed for large-scale MSC expansion is a potential limiting factor. Considering a 2- to 3-week expansion period at 10% concentration, 200 mL of serum would require at least one 500 mL blood donation [196]. However, the lack of availability of HS from blood establishments also limits its large-scale use as an allogeneic product [197]. Nevertheless, the benefits of allogeneic HS vs. FBS for expansion and osteogenic differentiation of MSCs, particularly ASCs, has been documented [34, 35].

Chemically-defined media

To avoid the risk of pathogen transmission and the difficulty of standardizing blood-derivatives, chemically-defined media (CDM) have been developed. These contain recombinant human GFs, although the exact contents of commercial products are rarely disclosed [197]. Although relatively fewer studies have reported the use of CDM for MSC expansion, superior *in vitro* proliferation and/or *in vivo* osteogenesis has been reported in CDM vs. FBS [198-200]. Advantages of commercial CDM over HS and

FBS have been reported in terms of expansion and osteogenic differentiation of ASCs [34, 35]. However, the feasibility of using CDM for large-scale MSC expansion is debated, given (a) the inherent variability and specificity of MSC cultures, (b) the need for specific combinations of GFs for MSCs from different sources, and thus (c) the need approval of several GF-combinations from regulatory authorities [197]. The current cost of CDM is also a limiting factor.

A recent study from our group compared the effect of pooled HS supplemented with fibroblast growth factor-2 (FGF-2), i.e. a combination of HS and CDM, vs. pooled HPL for MSC osteogenic differentiation [201]. FGF-2 is a known promoter of MSC proliferation and differentiation. While both *in vitro* osteogenic differentiation and *in vivo* bone formation were enhanced in BMSCs cultured in HS + FGF-2, MSCs in HPL seemed to retain a more undifferentiated phenotype with delayed differentiation [201]. Although encouraging, the translation of these results may be limited by the need for GF-supplementation of HS, contrary to the use of unsupplemented HPL, which is generally approved by regulatory agencies.

Human platelet-derivatives

Three types of HPDs were identified: (a) platelet-rich plasma (PRP), (b) platelet *releasates* (HPR), produced by *chemical* activation of platelets in PRP via addition of thrombin and/or calcium, and (c) platelet *lysates* (HPL), produced by *mechanical* disruption of platelets in PRP via repeated freezing and thawing cycles. While HPL contains the entire intracellular contents released from platelets, activation with thrombin/calcium in HPR mimics the physiological platelet activation and GF release during wound healing [74]. Both HPR and HPL contain high concentrations of GFs and equally support MSC proliferation and differentiation; an overall trend for higher GF concentrations in HPL was observed.

To extract growth factors from platelets, two methods were compared in preliminary experiments: *chemical* activation (releasates) and *physical* lysis (lysates). Activation was acieved via treating PCs with thrombin (1-10 IU/mL) and/or $CaCl_2$ while lysis was achieved via repeated freezing and thawing cycles. Based on ELISA,

the concentrations of selected growth factors were found to be comparable or higher in lysates vs. releasates. Cell proliferation of MSCs based on Alamar-blue assay was also found to be superior in lysates vs. releasates (at 5% and 10% concentrations), and in both cases, superior than FBS (**Figure 4.1**). Given the relative ease of production, without the need for exogenous reagents (thrombin), HPL was selected as the optimal supplement for GMP-grade expansion of MSCs for BTE.
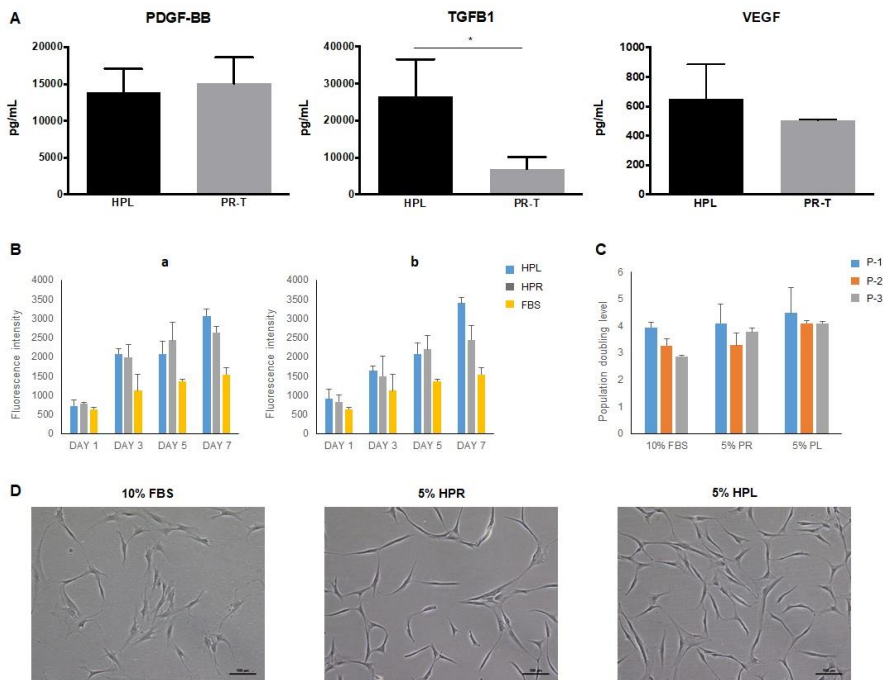
Figure 4.1: Comparison of platelet lysates and releasates. (A) Concentrations of selected growth factors measured via ELISA in HPL and thrombin-activated platelet releasate (PR-T); * $p < 0.05$. (B) Cell metabolic activity measured via alamar blue in media supplemented with HPL or platelet releasate (HPR) at 5% (a) or 10% (b) concentrations in comparison to 10% FBS. (C) Population doubling rate of MSCs cultured in 10% FBS, 5% HPR or 5% HPL over three serial passages (P1-3). (D) Morphology of MSCs cultured in 10% FBS, 5% HPR or 5% HPL; scale bar 100 μm.

Recent international guidelines are in agreement with the benefits of HPL [83, 88] and there is now a growing need for HPL to support xeno-free MSC expansion. There is also an increased need for standardization and scaling-up of HPL production. Among various aspects which require standardization, is the storage time of the source material, i.e. PCs produced by blood establishments. Thus, the next steps were to characterize HPL in terms of its cytokine content and efficacy for MSC expansion (vs. FBS), and to investigate the effect of PC-storage time on the cytokine content and efficacy of HPL in terms of MSC proliferation and osteogenic differentiation.

4.1.1. HPL contains several cytokines and EVs

Platelets are known to release a multitude of growth factors, cytokines and chemokines which influence MSC growth and differentiation [202]. A multiplex immunoassay was performed using HPLs produced from frozen PCs stored for 1–9 months; 30 of the 48 cytokines tested, including various GFs, chemokines and inflammatory mediators, were detected in all tested HPLs. Interactions between the cytokines were visualized via STRING network analysis (**Paper II**).

Stem cell growth factor (SCGF) – a cytokine not previously identified in HPL, was detected herein. SCGF is a protein encoded by the CLEC11A gene, and is associated with the growth of hematopoietic stem cells [203]. SCGF/CLEC11A was also found to be expressed in bone marrow stromal cells, and was recently shown to promote the osteogenic differentiation of murine BMSCs and *in vivo* healing in a fracture model [203]. Thus, in addition to platelet-derived growth factor BB (PDGF-BB) and TGF-β1, SCGF/CLEC11A signaling may be involved in the regulation of MSC osteogenic differentiation; further investigation of this GF is warranted.

In addition to soluble cytokines, HPL also exerts its effects on MSCs via microparticles or EVs which act as delivery agents for various growth and differentiation molecules [89]. EVs with a characteristic rounded cup-shaped morphology were isolated from HPL (**Figure 4.2**). The average particle size of EVs isolated by ultracentrifugation was 205.02 $\pm$ 2.25 nm. Using size exclusion chromatography, the EV population was further purified into exosomes (~100 nm).

Although total protein concentrations were ~16-fold lower in EVs as compared to HPL, multiplex assay revealed a significant enrichment of several GFs (relative to total protein) in EVs (**Figure 4.2**). It has been shown that HPL-EVs can be internalized by MSCs and enhance osteogenic differentiation [89]. Further studies are needed to understand how EVs may modulate MSC activity in HPL cultures.
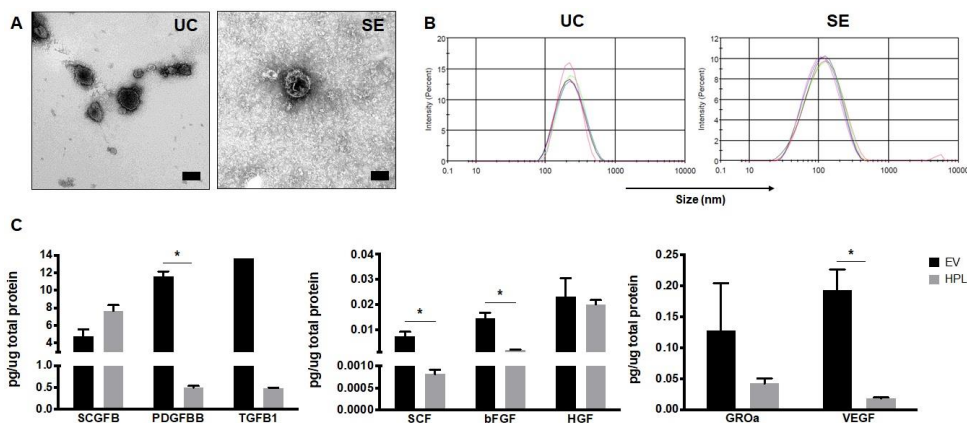
Figure 4.2: Characterization of HPL-EVs. (A) TEM images of EVs isolated by ultracentrifugation (UC) or size-exclusion (SE); scale bar 100 nm. (B) Particle size estimation via DLS of UC- and SE-derived EVs. (C) Concentrations of selected cytokines (normalized to total protein) in HPL and EVs via multiplex assay; * $p < 0.05$.

4.1.2. PC storage time influences HPL cytokine content

To determine whether the duration of frozen storage of PCs affects the cytokine content of HPL, the storage times were divided into two categories: storage <4 months and >4 months, as explained in **Paper II**. The concentrations of 27 of 30 tested cytokines were significantly reduced in the >4 months group. Several key growth factors considered necessary for MSC proliferation [204], such as FGF2, PDGF-BB, hepatocyte growth factor (HGF) and VEGF were elevated in the <4 months group. Interestingly, all inflammatory mediators [various interleukins (IL), tumor necrosis factor-α (TNF-α) and TNF-β] were present in relatively lower concentrations.

To determine if a more specific threshold for PC storage time could be identified, a second multiplex assay was performed using PCs stored for 0-4 months. For this purpose, HPL batches were specially produced from PCs frozen for controlled durations of 1, 2, 3 and 4 months. However, no significant differences were observed between the different storage times for any of the tested cytokines, and no definitive threshold below 4 months could be identified.

With regards to biological efficacy, the growth kinetics and osteogenic differentiation of BMSCs was tested in HPLs produced from the different PC storage times; BMSCs from multiple donors were used to test account for donor-related variations. PC storage time up to 4 months did not seem to affect the biological performance of HPL. No significant differences were observed with regards to proliferation kinetics [population doubling time (PDT)] between the different PC storage times. Similarly, no significant differences in ALP activity or mineralization of BMSCs were observed between the different PC storage times; considerable variation was observed between different BMSC donors in all groups. These observations are consistent with those of a recent study from our group on MSCs from a similar cohort – healthy young patients, which also reported large inter-donor variations in MSC properties [164]. While it is well-known that several biological, and other, factors may influence MSC proliferation and osteogenic differentiation [205], it must be acknowledged that the observed donor variation may have confounded the detection of significant differences between PC storage times in the present study.

4.1.3. *MSC osteogenic differentiation is enhanced in HPL*

In **Paper II**, donor-matched BMSCs and ASCs demonstrating characteristic plastic adherence and fibroblastic morphology were cultured in both HPL- and FBS-media. Similarly, GPCs (**Paper III**) and PDLCs demonstrating similar properties were isolated from dental tissue explants (**Figure 4.3**). A strength herein was the comparison of donor-matched cells from different tissue sources, to evaluate HPL efficacy**.** MSCs in both HPL and FBS, demonstrated the characteristic immunophenotype, i.e., >95% of the cells were positive for CD73, CD90 and CD105, while <5% of the cells

expressed HLA-DR or the hematopoietic markers CD34 and CD45. It must be noted that in GPCs from some donors, expression of HLA-DR was higher in HPL cultures. However, cells in HPL showed a more compact morphology vs. FBS cultures, which allowed higher cell proliferation in each passage.
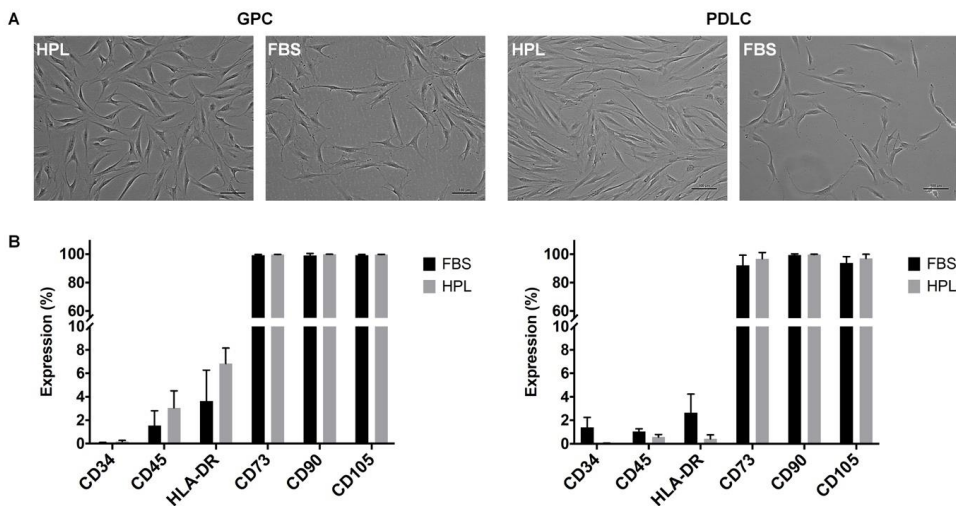
Figure 4.3: Characterization of GPCs and PDLCs in HPL. Morphology (A) and immunophenotype (B) of GPCs and PDLCs in HPL and FBS (n=3 donors); scale bars 100 μm.

Multipotency is a defining feature of MSCs. All cells herein – BMSCs, ASCs, GPCs and PDLCs, in both HPL and FBS, demonstrated the capacity to differentiate into adipocytes and osteoblasts. Additionally, the CD271+ fraction of GPCs in HPL also showed a capacity for neurogenic differentiation (**Paper III**). Interestingly, significantly greater *in vitro* mineralization was observed in HPL- vs. FBS-cultured cells in all MSCs, indicating enhanced osteogenic potential. It may be hypothesized that this is related to growth factors in HPL, which may stimulate MSCs' osteogenic differentiation (**Paper I**). To test an alternate, dentally relevant source of MSC-like cells, GPCs and PDLCs were cultured in HPL and FBS. While previous studies have characterized xeno-free PDLCs [206], ours was the first to characterize GPCs in HPL (**Paper III**). Both GPCs and PDLCs demonstrated characteristic MSC-like properties and enhanced osteogenic differentiation in HPL (**Figure 4.4**).
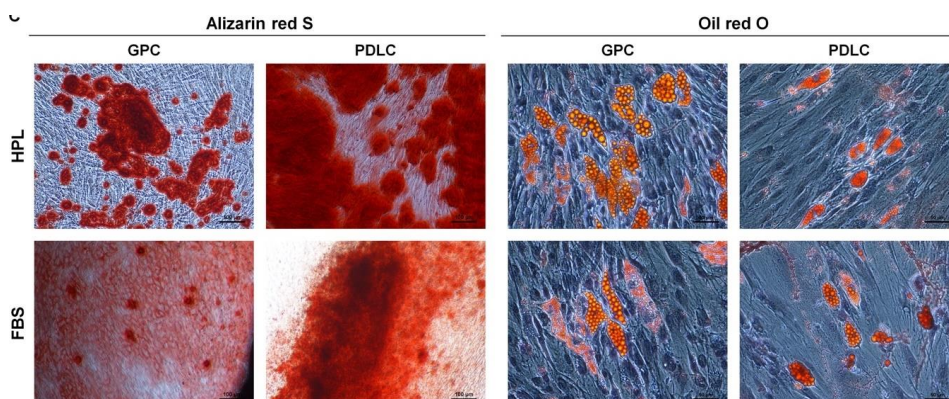
Figure 4.4: Differentiation of GPCs and PDLCs in HPL. Osteogenic (Alizarin red) and adipogenic differentiation (Oil red) of GPCs and PDLCs in HPL and FBS; scale bars 100 μm.

The ectopic bone formation assay is commonly used to test MSC potency *in vivo* [207, 208]. To determine whether osteogenic induction of HPL-cultured MSCs is necessary to induce *in vivo* bone formation, passage 3 BMSCs ($2x10^6$ cells) seeded on commercially available BCP granules (Biomatlante, France) were implanted subcutaneously in nude mice (see chapter 4.5). Constructs were cultured in osteogenic or standard HPL medium for one week; cell-free granules served as controls. After 8 weeks, histology revealed dense collagenous ECM in constructs with BMSCS; a trend for more 'osteoid-like' tissue was observed in BCP with induced cells (**Figure 4.5**). As previously reported [209], a strong inflammatory reaction was observed in all transplants, despite the animals' immunodeficient status. While some less-organised ECM was also observed in cell-free constructs, a trend for higher inflammatory reaction was observed herein, suggesting that this response was more towards the granules than transplanted cells. Consistent with previous reports [27, 208], the results herein suggest a benefit of osteogenic induction in HPL-cultured BMSCs.
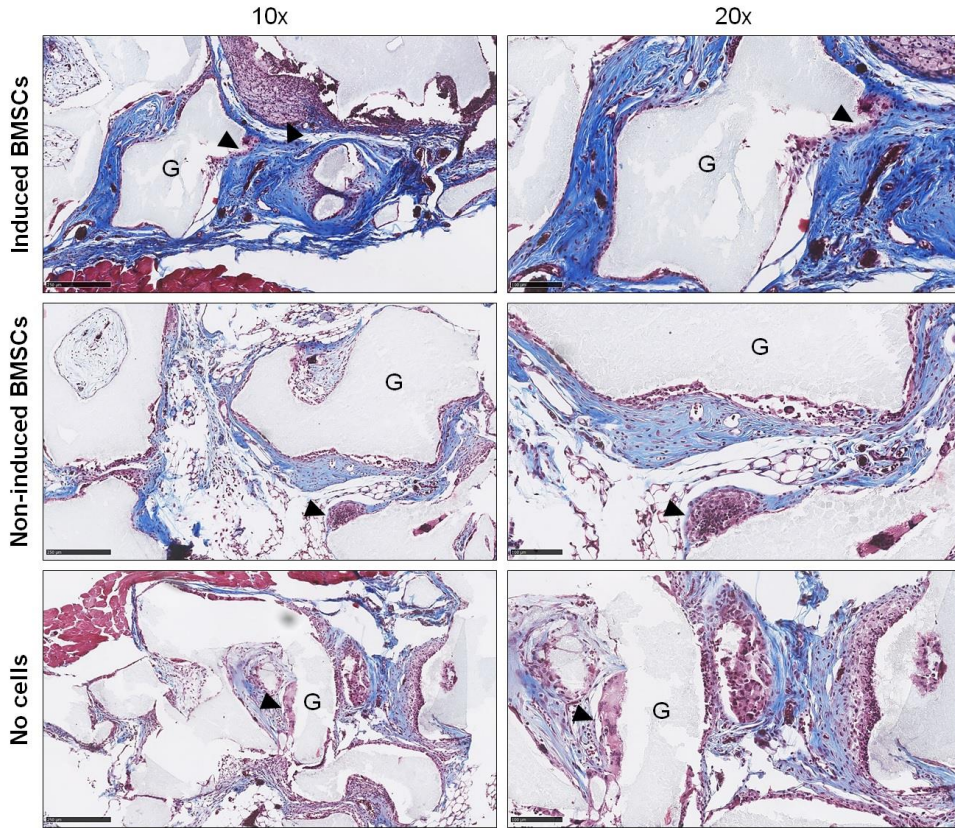
Figure 4.5: Ectopic transplantation of HPL-BMSCs. Histological tissue formation in BCP granules seeded with induced or non-induced BMSCs and cell-free controls (Masson's trichrome, collagen stained blue); black arrows, inflammatory cells; G, granules; scale bars: 250 µm (left), 100 µm (right).

4.2. SPHEROID CULTURE: STEMNESS & OSTEOGENESIS (Paper III)

The objectives in **Paper III** were to establish xeno-free spheroid cultures of BMSCs and GPCs in HPL, and to test their osteogenic potential *in vitro*. Preliminary experiments also included PDLCs, as reported below.

4.2.1. Aggregate spheroids are more feasible than mesenpheres

As described in section 3.5.4, aggregate spheroids could be formed more predictably than mesenspheres and therefore only the former were used in subsequent experiments. Indeed, aggregate cultures are routinely used to induce chondrogenic differentiation of MSCs *in vitro*, and often show signs of 'hypertrophy' suggestive of endochondral ossification [125]. Even in osteogenically differentiated monolayer MSCs *in vitro*, mineral deposition is observed most prominently in regions of high cellular 'confluence' or condensation [210]. Spheroid culture of MSCs may mimic such condensations and recapitulate embryonic events (MCC) linked to endochondral ossification [141].

4.2.2. Pluripotency and osteogenesis genes are upregulated in 3D spheroids

A significant upregulation of pluripotency factors SOX2, OCT4 and NANOG was observed in 3D vs. 2D cells after 7 days of culture. A relatively higher degree of gene upregulation was observed in spheroids of GPCs as compared to BMSCs. Expression of SOX2 in 3D GPCs and BMSCs was confirmed via IF staining. Interestingly, in preliminary experiments, similar gene upregulation was observed in PDLCs (**Figure 4.6**), as recently reported by others [129]. However, donor variation was particularly high in PDLC spheroids, and this was also why GPCs were selected for subsequent experiments. In context, no additional benefit of PDLCs to bone substitutes was found in recent clinical trials of periodontal regeneration [211, 212].

In addition to pluripotency markers, a higher expression of early (RUNX2, BMP2) and late markers of osteogenesis (OPN, OCN) was observed in 3D GPCs and BMSCs as compared to monolayers. Interestingly, this upregulation was independent of osteogenic induction. Protein expression of BMP2 and OCN after 14 days was

confirmed via IF staining, and mineral deposition after 21 days of osteogenic induction was confirmed via Alizarin red staining. Indeed, previous studies have reported superior *in vivo* bone regeneration by osteogenically induced spheroids of human BMSCs vs. monolayers (Table 1.1). Thus, it appears that spheroid culture may intrinsically 'prime' MSCs towards osteoblastic commitment, although additional signals/supplements may be required for terminal differentiation and mineralization [115, 116]. Moreover, the simultaneous upregulation of pluripotency and osteogenesis-related genes in 3D spheroids may provide further evidence for an *in vivo*-like microenvironment. The co-existence of self-renewing stem cells and more-committed progenitor cells is a characteristic feature of the stem cell-niche [119, 120], which appears to be recapitulated in 3D spheroids.
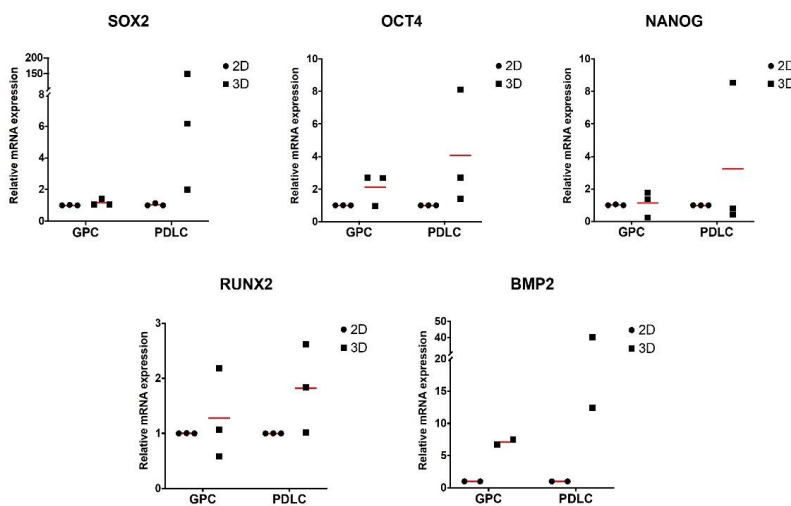
Figure 4.6: Gene expression in GPC and PDLC spheroids vs. monolayers. Data represent means of donor-matched GPCs and PDLCs; each symbol represents a single donor.

4.2.3. *The secretome of MSCs is enhanced in 3D spheroids*

Emerging concepts in BTE highlight paracrine- and immune-modulation as primary mechanisms for MSC-mediated bone regeneration [20]. The concentrations of various growth factors, chemokines and inflammatory cytokines were measured in the 48 h CM of spheroid and monolayer GPCs and BMSCs. Several growth factors and chemokines

were elevated in spheroid cultures (**Figure 4.7**). Notably, both spheroid and monolayer GPCs and BMSCs produced high concentrations of SCGF-β. Interestingly, several pro-inflammatory cytokines were downregulated in the CM of GPC and BMSC spheroids, while IL-8 was markedly elevated, especially in BMSCs. The anti-inflammatory IL-10 was upregulated in monolayers in both GPCs and BMSCs. However, no differences in wound closure were observed between 2D and 3D-CM in an *in vitro* wound healing assay [213] of rat BMSCs after 24 and 48 hours (**Paper V**).
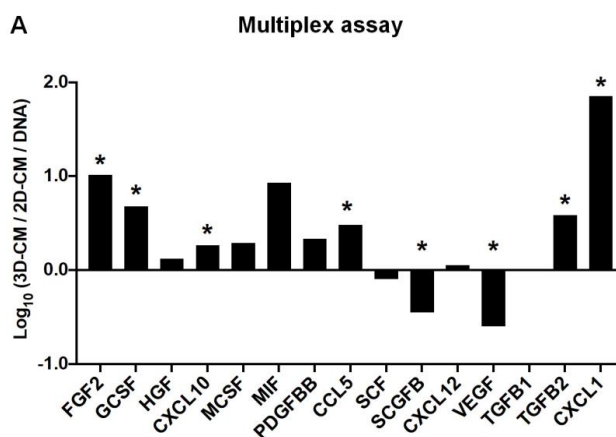
Figure 4.7: Secretome of 2D and 3D MSCs. Normalized cytokine concentrations in CM of 2D and 3D BMSCs; data are presented as the logarithm (log10) of the ratio between 3D-/2D-CM, * $p < 0.05$.

This enhanced paracrine activity could, at least partly, explain the observed *in vivo* benefits of spheroid MSCs [214, 215]. Moreover, the enrichment of several cytokines implicated in MSC recruitment and osteogenic differentiation, suggests that transplantation of HPL-cultured 3D MSCs, or their CM, may induce a favourable *in vivo* host-response. However, it must be ultimately determined *in vivo* whether the combination of HPL supplementation and 3D culture enhances the bone regeneration capacity of GPCs and BMSCs.

4.3. SPHEROID COCULTURE: ANGIOGENESIS (Paper IV)

The objective of **Paper IV** was to investigate whether GPCs could support sprouting angiogenesis of ECs in a xeno-free 3D coculture system.

4.3.1. 3D coculture enhances sprouting angiogenesis in vitro

Cocultures of GPCs and HUVECs were established to test whether (a) GPCs promoted EC sprouting, and (b) if so, whether this was via paracrine mechanisms, or direct cell-cell contact. No significant effect of indirect coculture was observed on HUVECs. In direct cocultures a combination of sprout formation (by HUVECs) and spreading (by GPCs) was observed. HUVEC-sprouting and GPC-spreading were differentiated by cell labelling and confocal imaging. GPCs appeared to be organized along HUVEC sprouts and provided a substrate for HUVEC migration (**Figure 4.8** and **Paper IV**).
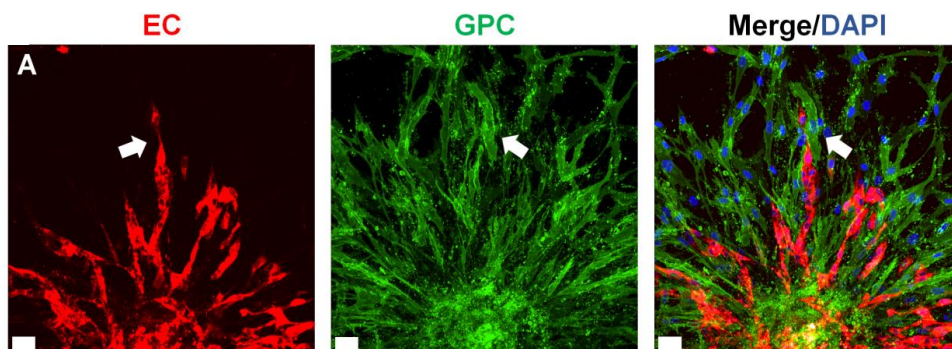
Figure 4.8: Sprouting angiogenesis in 3D cocultures. HUVEC-spouting in direct coculture with GPCs. Differential cell-labelling showing HUVEC (EC) sprouting and GPC spreading; scale bars 100 µm.

The influence of co-culture ratios was also tested herein. A 1:1 ratio of MSC:HUVEC is most frequently reported. However, previous studies have suggested that a higher fraction of ECs may promote angiogenesis in cocultures. In our studies, coculture with GPCs at both low (5:1) and high (1:1) ratios comparably enhanced HUVEC sprouting (**Paper IV**).

4.3.2. *Hydrogel properties infuence sprouting in 3D cocultures*

With regards to 'modified' HPLG, the addition of fibrinogen >2.5 mg/mL significantly reduced the viability and sprouting of encapsulated HUVECs. Sprouting in 0F and 1.25F HPLG was significantly greater than that in 2.5F gels after 72 hours. Overall, a trend for superior sprouting was observed in the 5:1 cocultures and 1.25F HPLG and this combination considered the most optimal (**Paper IV**).

4.3.3. *3D coculture stimulates angiogenesis in a CAM assay*

The angiogenic potential of HPLG-encapsulated HUVEC and coculture spheroids (5:1) was tested on chick embryo CAMs. After implantation for 7 days, angiogenesis was observed in both groups with formation of new vessels and dense vascular netwroks. No significant differences were detected in any of the angiogenesis-related parameters between HUVEC and coculture spheroids. The presence of CD31-positive human cells was not detectable in the CAM tissues via IHC.

Although no significant additional benefit of co-culture was observed in terms of short-term EC-mediated angiogenesis, two potential arguments for co-culture may still be made. Firstly, in the absence of supporting cells such as MSCs, *in vitro* EC networks are reported to be stable for shorter durations [216]. These networks must be stable for long enough when implanted *in vivo*, to anastomose with the host vessels. The addition of GPCs may help to stabilize EC networks in more advanced *in vivo* applications [217]. Secondly, in the context of BTE, it is hypothesized that in co-culture systems, MSCs (or in this case GPCs) would serve dual functions of supporting angiogenesis and promoting osteogenesis, via direct differentiation into osteoblasts and/or paracrine stimulation of native MSCs [159]. However, it remains to be verified whether the transplanted MSCs adopt a more pericytic or ostoblastic phenotype *in vivo* when co-cultured with ECs.

4.4. IN VIVO BONE TISSUE ENGINEERING (Paper V)

The delivery of osteogenic cells encapsulated in a growth factor-rich hydrogel and contained in a space-maintaining scaffold represents a clinically relevant strategy, combining all aspects of the BTE 'triad'. Thus, cell-scaffold-gel constructs (SGC) of BMSCs, HPLG and 3D printed PLA-TMC scaffolds were tested *in vitro* and *in vivo*.

4.4.1. In vitro mineralization is enhanced in spheroid BMSCs

SGC containing single or spheroid BMSCs were prepared and cell viability was confirmed up to 21 days *in vitro*. Initially, the cells appeared rounded and mainly suspended within the matrix, but as the gels degraded, they attached and spread on the scaffold surface. Spheroids retained their 3D structure after 21 days. Moreover, significantly greater mineralization (following osteogenic induction) was observed in SGC with spheroid BMSCs. Some mineralization was also observed in non-induced constructs, albeit lower than in induced counterparts. These results are consistent with previous reports of gel-encapsulated MSC spheroids [147, 188]

4.4.2. Ectopic mineralization is enhanced by spheroid BMSCs

The *in vivo* bone forming capacity of xeno-free spheroids vs. single cells was tested in a subcutaneous model using BMSCs and GPCs in two separate experiments. An important consideration for subcutaneous bone formation is the absence of any local endogenous osteogenic progenitor cells within the intradermal environment, which, at least theoretically, ensures that any newly formed bone is predominantly of exogenous origin [218]. SGC containing passage-3 BMSCs or GPCs ($2x10^6$ cells) as spheroids or single cells were cultured in osteogenic induction medium for one week before implantation; cell-free constructs (scaffolds+gel) served as controls. After 4 and 8 weeks, μCT analysis revealed mineralization in all implants. Significantly greater mineralization was observed in spheroid vs. single BMSCs (**Paper V**). Mineralization in GPCs was generally lower than in BMSCs, with no significant differences between spheroids and single cells (**Figure 4.9 A**).
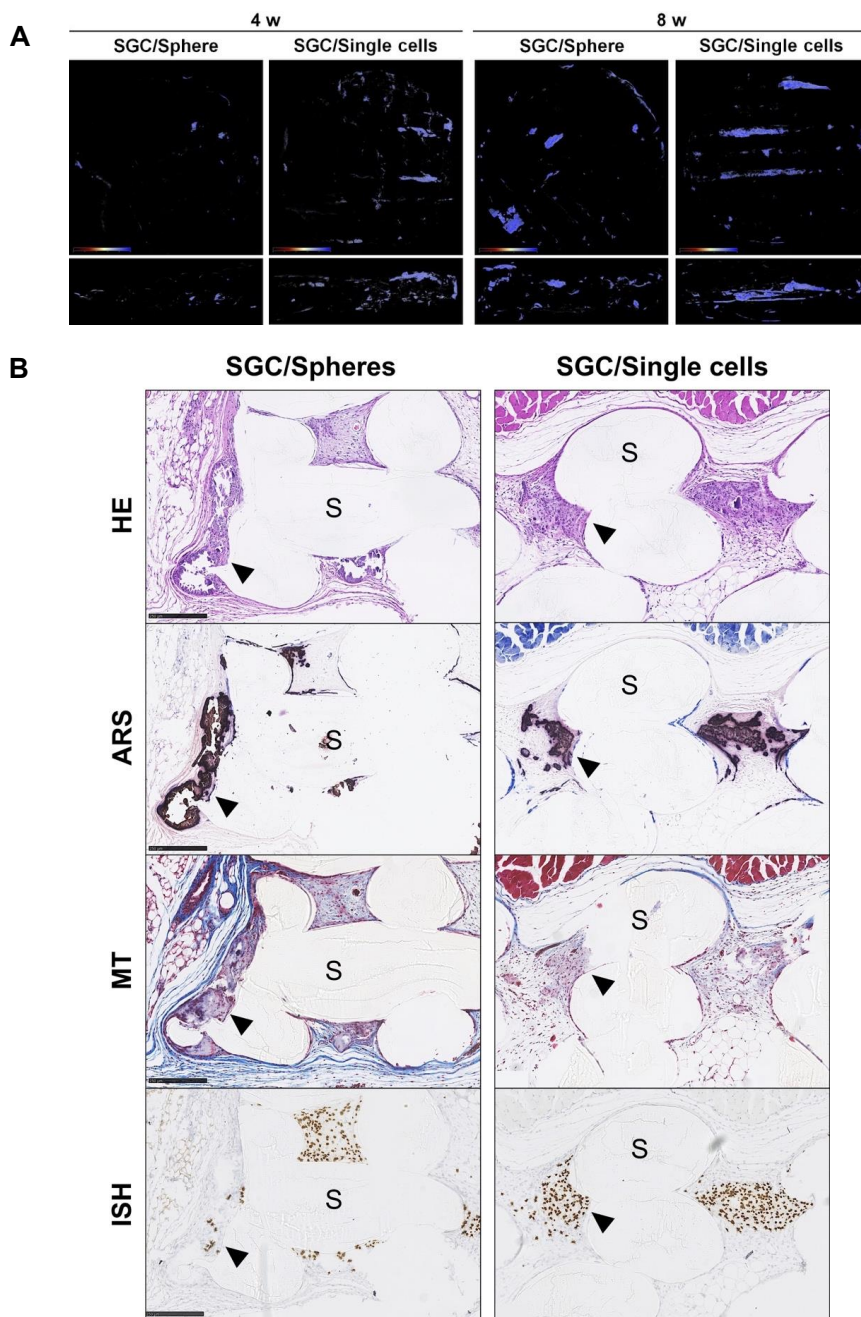
Figure 4.9: Ectopic mineralization by GPCs. (A) Reconstructed μCT images (frontal and lateral) of SGC+spheroid or single GPCs; only mineralized tissue in the 'high density' (blue) range is shown. (B) Histological images of mineralized areas (black arrows) stained with H&E, Alizarin Red (ARS) and Masson's trichrome (MT). ISH for human *Alu* gene shows surviving GPCs (black arrows). S, scaffold; scale bars 250μm. Note: Imperfect sectioning of mineralized tissue is the result of non-decalcification*.

Histologically, after 8 weeks, dense tissue formation was seen around the scaffold margins in cell-loaded SGC (HE staining), and correlated with aggregations of *Alu*-positive cells in serial ISH sections. MT and ARS staining subsequently confirmed the presence of collagen and calcium, respectively, in these tissues (**Figure 4.9 B**). The localization of *Alu*-positive cells to these sites suggests the participation of implanted GPCs/BMSCs in the mineralization process. In addition to mineralized areas of organized and cellular woven bone, some disorganized acellular mineral deposition was observed (**Paper V**). This pattern of mineralization has previously been reported; although the exact mechanism is unknown, a 'cell-independent' theory has been proposed [219]. Most interestingly, the structure of GPC/BMSC spheroids appeared to be retained in several SGC, and mineralization was seen to occur within the spheroids. This observation lends support to our hypothesis, based on our own *in vitro* data and reports from others [115, 116], that mineralizing spheroids may act as 'foci' for initiating *in vivo* bone formation.

A relatively high number of implanted cells, both GPCs and BMSCs, were detected in the implants even after 8 weeks (**Paper V**). The survival of implanted MSCs *in vivo* is debated; while some studies have reported that BMSCs do not survive ectopically for longer than 2 weeks when seeded on BCP [220], recent studies from our group [201] and others [146, 221, 222] have detected BMSCs in ectopic transplants at later time-points via ISH. It can be hypothesized that the encapsulation of cells in HPLG may have contributed to their enhanced survival in the present study. Indeed, several studies have reported superior ectopic bone formation when BMSCs, either single cells [223-226] or spheroids [38, 146], were encapsulated in PRP gel than when combined only with a bone substitute. Thus, the encapsulation of MSCs in HPLG seems to be a feasible strategy for *in vivo* mineralization.

* Technical note: The ectopic tissue samples were processed via undecalcified paraffin histology. In a pilot experiment, some of the samples were decalcified via a "fast" protocol [227]. However, ISH did not work in these samples and therefore, given the time and COVID19-related limitations, an undecalcified protocol was used. A limitation of this method was the imperfect sectioning of the mineralized tissues.

4.4.3. Orthotopic bone regeneration is comparable in spheroid and single BMSCs

The bone regeneration potential of SGC contructs containing BMSCs as single cells or spheroids was tested in rats' calvarial CSD. A CSD is the smallest size experimental defect in an animal that will not spontaneously regenerate with bone within a defined time frame without intervention [15]. Rodent calvaria are considered as a challenging environment for bone regeneration due to poor blood supply and limited bone marrow [161].

Since superior ectopic mineralization was observed with BMSCs vs. GPCs, only these cells were used in the calvarial model. All defects showed some degree of bone regeneration, which progressively increased from 4 to 12 weeks (**Paper V**). Bone formation started from the margins of the defect and followed the scaffold architecture (**Figure 4.10**). These findings were verified by µCT analysis after 12 weeks. No significant differences in bone volume (CT or µCT) were observed between the groups. However, the volume of new bone in the form of 'islands' not connected to the host bone, was significantly greater in spheroid SGC ($p < 0.05$).

Undecalcified histology of calvaria explants revealed new bone originating from the endocranial margins of the defect. This bone showed a mature phenotype, similar to the native bone, with embedded osteocytes (**Figure 4.10**). In the central part of the defect, the newly formed bone tissue presented as a mixture of mature lamellar bone and less-mature plexiform bone, i.e., woven and parallel-fibered bone, formed in the early healing stages. Areas of new bone were associated with several blood vessels. Despite the relatively robust bone formation, the scaffold material was always lined with a layer of fibrous tissue, i.e., bone did not form directly on the scaffold surface (**Figure 4.10**). This observation is reported to be a function of the immunodeficient animal model [228]. No significant differences were observed between the groups in terms of histomorphometric new bone formation. This is in contrast to our observations in the ectopic model and previous reports, which demonstrated superior performance of human MSC spheroids in rodent calvaria [127, 129]. As discussed in **Paper V**, an additional 'osteopromotive' effect of the HPLG used herein, along with local stimuli from a 'native' bone environment, may have masked differences between the groups.
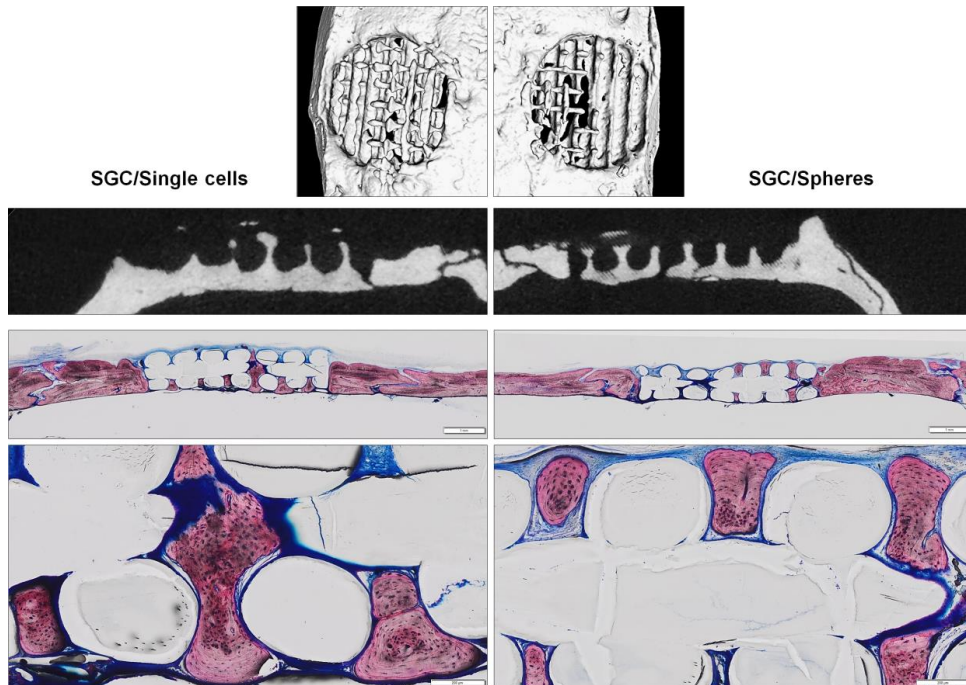
Figure 4.10: Calvarial bone regeneration by BMSCs. μCT images and corresponding central undecalcified sections showing low (scale bar 1 mm) and high magnification (scale bar 200 μm) images of bone after12 weeks in SGC with single (left) and spheroid BMSCs (right). Note the radiographic bone 'bridging', histological mature lamellar bone (pink) with embedded osteocytes and the fibrous capsule (blue) aroumd the scaffold.

An interesting observation, was the abundant mineralization in cell-free SGC, not only in the calvaria, but also in ectopic sites (where local osteogenic cells/signals are lacking). In another study within our group, implantation of similar cell-free (and gel-free) PLA-TMC scaffolds did not result in any ectopic mineralization in immunocompetent rats, although considerable bone formation occured when rat MSCs were added (unpublished data). Variation in animals notwithstanding [228], this suggests that the observed mineralization may be induced by HPLG. Indeed, previous studies have reported benefits of HPL 'coating' of scaffolds for MSC attachment and ectopic bone formation [28, 229]. Others have reported superior ectopic bone formation when using PRP in combination with MSCs, than MSCs alone [146, 223, 225, 230]. In our study, even after 4 weeks, comparable ectopic mineralization was observed in cell-

free and cell-loaded constructs; the trend continued at 8 weeks (**Paper V**). However, some differences in the quality of ectopic mineralized tissue were observed between cell-free and cell-loaded implants. As mentioned before, ectopic 'bone' formation in this study presented as a mixture of well-organized osteoid-like tissue (with embedded cells) and less-organized (acellular) mineralization. Although the mechanism of such mineralization is not fully understood, a trend for higher frequency of atypical mineralization was observed in cell-free implants (**Paper V**).

Based on our findings, and in the context of the state-of-the-art, xeno-free culture in HPL enhances the osteogenic differentiation potential of BMSCs and GPCs. Gene expression patterns suggest that culturing these cells as 3D spheroid aggregates vs. 2D monolayers recapitulates *in vivo*-like conditions, and further 'primes' the cells, particularly BMSCs, towards osteogenic differentiation [115, 141]. Hydrogels represent a favourable delivery system for spheroids while maintaining their 3D structure and activity. When encapsulated in HPLG, single and, particularly spheroid BMSCs, showed a high capacity for *in vitro* osteogenic differentiation. Implantation in nude mice revealed greater ectopic mineralization in encapsulated spheroids vs. single BMSCs. Spheroids retained their 3D structure *in vivo* and even showed signs of mineralization, suggesting their role as 'foci' for initiation of bone formation. Encapsulated GPCs produced less ectopic mineralization than BMSCs, and showed a reverse (non-significant) trend, i.e. superior mineralization in single cells vs. spheroids. Since BMSCs performed significantly better than GPCs, these cells were further tested in a calvarial defect model. Here, considerable bone regeneration was observed in defects treated with constructs of PLA-TMC scaffolds, HPLG and BMSCs, regardless of spheroid culture. However, the frequency of bony 'island' formation was enhanced in the presence of spheroids. This further supports the role of MSC spheroids as potential foci of osteogenesis. Overall, the xeno-free constructs of BMSCs, HPLG and PLA-TMC scaffolds developed herein represent a promising strategy for BTE and now warrant testing in a large-animal model to facilitate clinical translation.

5. Conclusions

Based on the findings herein, the main conclusions of this thesis are as follows:

1. HPL is a favourable supplement for xeno-free MSC expansion, particularly for BTE applications. The osteogenic differentiation of MSCs from different sources is enhanced in HPL. Outdated PCs stored frozen for 4 months or less are preferred for HPL production, in terms of cytokine content and ability to support MSCs' growth and osteogenic differentiation.

2. GPCs with a characteristic stromal immunophenotype and superior multi-lineage differentiation potential can be isolated in HPL (vs. FBS). Xeno-free GPCs demonstrate osteogenic differentiation potential *in vitro* and ectopic bone formation *in vivo*.

3. When cultured as xeno-free 3D spheroids, BMSCs and GPCs demonstrate superior expression of stemness- and osteogenesis-related genes and an enhanced cytokine profile, as compared to 2D monolayers. Both BMSC and GPC spheroids demonstrate ectopic bone formation *in vivo*; in the case of BMSCs, this is significantly greater in spheroids vs. single cells.

4. When cocultured as xeno-free 3D spheroids with HUVECs in an HPL hydrogel, GPCs enhance sprouting angiogenesis *in vitro* and support HUVEC-mediated neoangiogenesis *in vivo* in chicken embryo CAMs.

5. Constructs of 3D printed PLA-TMC scaffolds combined with HPLG adequately support BMSC growth and osteogenic differentiation *in vitro*. These constructs, with BMSCs either as spheroids or single cells, also demonstrate robust *in vivo* bone regeneration in rats' calvarial defects, thus representing a promising strategy for clinical BTE.

6.   Future perspectives

Development and testing of xeno-free approaches to enhance MSC-mediated osteogenesis is critical for the clinical translation of novel BTE strategies. It is increasingly evident that HPL represents the optimal serum-substitute for xeno-free *ex vivo* MSC expansion, with particular advantages for BTE. As observed herein, HPL culture (vs. FBS) seemed to enhance the osteogenic differentiation potential of MSCs from different tissue sources. However, the HPL herein was also found to contain a complex mixture of cytokines and exactly which components contribute to promoting osteogenesis remains to be investigated. Future work should also aim to scale up HPL production by increasing pool sizes, while ensuring safety by incorporating pathogen reduction strategies.

To facilitate the clinical translation of cell therapy in regenerative dentistry, human gingiva and PDL were explored as a potential sources of MSC-like cells. Indeed, both GPCs and PDLCs seemed to comprise of a heterogenous population, of which a subset showed characteristic MSC-like properties and robust osteogenic differentiation potential, comparable to that of BMSCs, *in vitro*. However, the *in vivo* identity and function of these cells is relatively poorly understood and therefore, based on the work herein, we cannot label these cells as 'MSCs' with any degree of certainty. It would be of interest to further investigate the *in vivo* identity and function of these cells and to simultaneously identify methods to 'purify' or 'sort' the multipotent cell fractions *ex vivo*, e.g., via identification of specific surface markers. In the context of regenerative dentistry, further work is needed to determine the clinical efficacy of these cells for bone and periodontal tissue regeneration [212].

Spheroid culture of MSCs was tested herein to simulate *in vivo* conditions. Interestingly, simulatenoeus upregulation of plutipotency- and osteogenesis-related genes was observed in xeno-free 3D spheroids, suggesting recapitulation of the 'stem cell niche'. This phenomenon has been linked to MCC-like events during embryonic development and endochondral ossification. Indeed, chondrogeneic pre-induction of MSCs, to induce endochondral bone formation, is an emerging strategy in BTE [231].

Whether this strategy can be further enhanced and translated using xeno-free MSC spheroids, i.e. via chondrogenic differentiation, hypertrophy and ossification, in combination with biomaterials, e.g. hydrogels, warrants further investigation.

The hydrogel (HPLG) used herein was found to be especially 'osteo-promotive', i.e. encapsulation of MSCs in HPLG promoted their osteogenic differentiation *in vitro* and bone formation *in vivo*. Interestingly, cell-free constructs of HPLG also showed ectopic mineralization – suggesting a possible 'osteoinductive' effect on the local host environment. This 'cross-species' osteoinductive effect of HPLG is particularly interesting and a paracrine mechanism of host cell-recruitment has been proposed [229]. The use of HPLG as an injectable MSC delivery system, as an alternative to PRP, warrants further investigation particularly for dental applications.

Acknowledgements

I would like to express my gratitude to the Department of Clinical Dentistry, Faculty of Medicine, University of Bergen, for the opportunity to carry out this PhD thesis. I am honoured to be associated with this institution.

I would like to thank my supervisors: *Kamal Mustafa* – for your generosity and guidance, *Anne Isine Bolstad* – for your kindness and support, and *Salwa Suliman* – for your valuable help, throughout this project. I am proud to have been part of the Tissue Engineering Research Group under your supervision. My special thanks to *Andreas Stavropoulos*, as much a friend as a supervisor, who stimulated my interest in research and encouraged me to pursue a PhD.

I would also like to thank my colleagues at various collaborating laboratories: the "BergenLys" team – *Tor Hervig, Einar Kristoffersen, Turid Helen Lunde* and *Tilo Eichler*; from the Gade's Institute – *Daniela Elena Costea, Harsh Dongre* and *Bendik Nordanger*; from the animal facility – *Joanna, Helen* and *Suzanne*; *Luiza Ghila* from KI; *Hege Dale* and *Heidi Espedal* from MIC. From the Dept. of Biophysics, NTNU – *Catharina de Lange Davies* and *Elin*, thanks for your help with the CAM experiments. From the School of Dentistry in Vienna – *Reinhard Gruber, Stefan Tangl, Carina Kampleitner, Patrick Heiml* and *Toni Dobsak* – thanks for a valuable learning experience and for making me feel welcome during my stay in Vienna.

To my colleagues at IKO – thank you for creating a positive and enjoyable working environment: *Andreas, Annika, Asgeir, Bodil, Cecilie, Christian, Dagmar, Elina, Elisabeth C, Elisabeth E, Ferda, Hassan, Hisham, Ibrahim, Inge, Jannika, June, Kaia, Marit Ø, Marit S, Maryam, Mihaela, Mo, Mona, Nageeb, Neha, Nils Roar, Niyaz, Odd Johan, Randi H, Randi S, Shaza, Shubham, Shuntaro, Siri, Siva, Sølve, Stein Atle, Sunita, Sushma, Tarig, Torbjørn, Ulrik, Victoria, Yassin* and *Ying*. Special thanks to *Siren*, our lab manager, and *Xin*, my office mate, for the fantastic help and support during my project. *Samih* and *Ahmad* – I am especially grateful for your help with my experiments. *Espen* og *Øyvind* – takk for at dere ikke ler når jeg snakker norsk.

To my friends in Bergen: *Lene, Håkon, Svein, Denise, Maria* and *Irene* – thanks for the good times. To *Iremlin* and *Liva* – you mean the world to me and I would not have survived Bergen without you. Thanks to you and *The Kalands* for adopting me. To my friends elsewhere – *Ankush, Hatim, Kauti, Vishaal, Ulrika, Gaurav, Ranjini, Jo, Connie, Victor* and *John* – thanks for the laughs along the way. To the music of *Tool* – thank you for inspiring me to be better.

Finally, to my family in India – thank you for always supporting me in every endeavour. I would not be half the person I am today without you in my life. Truly. *Maya, Vivek* and *Shreya* – this work is dedicated to you.

Siddharth Shanbhag
October 2020, Bergen

Bibliography

1. Clarke, B., *Normal bone anatomy and physiology.* Clin J Am Soc Nephrol, 2008. **3 Suppl 3**: p. S131-9.
2. Marsell, R. and T.A. Einhorn, *The biology of fracture healing.* Injury, 2011. **42**(6): p. 551-5.
3. Cameron, J.A., et al., *Employing the biology of successful fracture repair to heal critical size bone defects.* Curr Top Microbiol Immunol, 2013. **367**: p. 113-32.
4. Gibon, E., et al., *Inflammation, ageing, and bone regeneration.* J Orthop Translat, 2017. **10**: p. 28-35.
5. Rocchietta, I., L. Ferrantino, and M. Simion, *Vertical ridge augmentation in the esthetic zone.* Periodontology, 2018. **77**: p. 241-255.
6. Chanchareonsook, N., et al., *Tissue--engineered mandibular bone reconstruction for continuity defects: A systematic approach to the literature.* Tissue Engineering Part B Reviews, 2014. **20**: p. 147-162.
7. Janssen, N.G., et al., *Tissue engineering strategies for alveolar cleft reconstruction: A systematic review of the literature.* Clin Oral Investigations, 2014. **18**: p. 219-226.
8. Al-Nawas, B. and E. Schiegnitz, *Augmentation procedures using bone substitute materials or autogenous bone --a systematic review and meta--analysis.* European Journal of Oral Implantology, 2014. **7**(2): p. 219-234.
9. Dahlin, C. and A. Johansson, *Iliac crest autogenous bone graft versus alloplastic graft and guided bone regeneration in the reconstruction of atrophic maxillae: A 5--year retrospective study on cost--effectiveness and clinical outcome.* Clinical Implant Dentistry and Related Research, 2011. **13**: p. 305-310.
10. Sanz-Sánchez, I., et al., *Effectiveness of lateral bone augmentation on the alveolar crest dimension: A systematic review and meta--analysis.* Journal of Dental Research, 2015. **94**(9). p 128-142.
11. Shanbhag, S. and V. Shanbhag, *Clinical applications of cell-based approaches in alveolar bone augmentation: a systematic review.* Clin Implant Dent Relat Res, 2015. **17 Suppl 1**: p. e17-34.
12. Shanbhag, S., et al., *Alveolar bone tissue engineering in critical--size defects of experimental animal models: A systematic review and meta--analysis.* Journal of Tissue Engineering and Regenerative Medicine, 2016. **11**: p. 2935-2949.
13. Shanbhag, S., et al., *Bone tissue engineering in oral peri--implant defects in preclinical in vivo research: A systematic review and meta--analysis.* J Tissue Eng Regen Med, 2018. **12**: p. 336-349.
14. Shanbhag, S., et al., *Cell therapy for orofacial bone regeneration: A systematic review and meta-analysis.* J Clin Periodontol, 2019. **46 Suppl 21**: p. 162-182.
15. Hollinger, J.O. and J.C. Kleinschmidt, *The critical size defect as an experimental model to test bone repair materials.* J Craniofac Surg, 1990. **1**(1): p. 60-8.
16. Sanz, M., et al., *Biomaterials and regenerative technologies used in bone regeneration in the craniomaxillofacial region: Consensus report of group 2 of the 15th European Workshop on Periodontology on Bone Regeneration.* J Clin Periodontol, 2019. **46 Suppl 21**: p. 82-91.
17. Caplan, A.I., *Mesenchymal stem cells.* J Orthop Res, 1991. **9**(5): p. 641-50.
18. Friedenstein, A.J., et al., *Heterotopic of bone marrow. Analysis of precursor cells for osteogenic and hematopoietic tissues.* Transplantation, 1968. **6**: p. 230-247.
19. Pittenger, M.F., et al., *Multilineage potential of adult human mesenchymal stem cells.* D., et al, 1999. **284**: p. 143-147.

20. Pittenger, M.F., et al., *Mesenchymal stem cell perspective: cell biology to clinical progress.* NPJ Regen. Med, 2019. **4**: p. 22.

21. Dominici, M., et al., *Minimal criteria for defining multipotent mesenchymal stromal cells. The International Society for Cellular Therapy position statement.* Cytotherapy, 2006. **8**: p. 315-317.

22. Chahla, J., et al., *Bone marrow aspirate concentrate harvesting and processing technique.* Arthroscopy Techniques, 2017. **6**: p. 441-445.

23. Patterson, T.E., et al., *The efficiency of bone marrow aspiration for the harvest of connective tissue progenitors from the human iliac crest.* Journal of Bone and Joint Surgery. American Volume, 2017. **99**: p. 1673–1682.

24. Jager, M., et al., *Bridging the gap: Bone marrow aspiration concentrate reduces autologous bone grafting in osseous defects.* Journal of Orthopaedic Research, 2011. **29**: p. 173-180.

25. Rojewski, M.T., et al., *Translation of a standardized manufacturing protocol for mesenchymal stromal cells: A systematic comparison of validation and manufacturing data.* Cytotherapy, 2019. **21**(4): p. 468-482.

26. Gjerde, C., et al., *Cell therapy induced regeneration of severely atrophied mandibular bone in a clinical trial.* Stem Cell Res Ther, 2018. **9**(1): p. 213.

27. Ye, X., et al., *Ectopic bone regeneration by human bone marrow mononucleated cells, undifferentiated and osteogenically differentiated bone marrow mesenchymal stem cells in beta-tricalcium phosphate scaffolds.* Tissue Eng Part C Methods, 2012. **18**(7): p. 545-56.

28. Bolte, J., et al., *Two-step stem cell therapy improves bone regeneration compared to concentrated bone marrow therapy.* J Orthop Res, 2019. **37**(6): p. 1318-1328.

29. Wilson, A., et al., *Multiplicity of mesenchymal stromal cells: finding the right route to therapy. Front. Immunol.* 2019. **10**:1112.

30. Fraser, J.K., et al., *The Celution® system: Automated processing of adipose-- derived regenerative cells in a functionally closed system. Advance in Wound Care.* (New Rochelle) 2014. **3**(1): p. 38–45.

31. Patrikoski, M., B. Mannerstrom, and S. Miettinen, *Perspectives for Clinical Translation of Adipose Stromal/Stem Cells.* Stem Cells Int, 2019. **2019**: p. 5858247.

32. Prins, H.J., et al., *Bone Regeneration Using the Freshly Isolated Autologous Stromal Vascular Fraction of Adipose Tissue in Combination With Calcium Phosphate Ceramics.* Stem Cells Translational Medicine, 2016. **5**(10): p. 1362-1374.

33. Mohamed-Ahmed, S., et al., *Adipose-derived and bone marrow mesenchymal stem cells: a donor-matched comparison.* Stem Cell Res Ther, 2018. **9**(1): p. 168.

34. Patrikoski, M., et al., *Development of fully defined xeno-free culture system for the preparation and propagation of cell therapy-compliant human adipose stem cells.* Stem Cell Res Ther, 2013. **4**(2): p. 27.

35. Kyllonen, L., et al., *Effects of different serum conditions on osteogenic differentiation of human adipose stem cells in vitro.* Stem Cell Res Ther, 2013. **4**(1): p. 17.

36. Brocher, J., et al., *Inferior ectopic bone formation of mesenchymal stromal cells from adipose tissue compared to bone marrow: rescue by chondrogenic pre-induction.* Stem Cell Res, 2013. **11**(3): p. 1393-406.

37. Brennan, M.A., et al., *Inferior in vivo osteogenesis and superior angiogeneis of human adipose tissue: A comparison with bone marrow--derived stromal stem cells cultured in xeno--free conditions.* Stem Cells Translational Medicine, 2017. **6**: p. 2160-2172.

38. Fennema, E.M., et al., *Ectopic bone formation by aggregated mesenchymal stem cells from bone marrow and adipose tissue: A comparative study.* J Tissue Eng Regen Med, 2018. **12**(1): p. e150-e158.

39. Mohamed-Ahmed, S., et al., *Comparison of Bone Regenerative Capacity of Donor-matched Human Adipose-Derived and Bone Marrow Mesenchymal Stem Cells.* Cell Tissue Res., 2020. **doi**: 10.1007/s00441-020-03315-5.

40. Scherberich, A., et al., *Adipose tissue--derived progenitors for engineering osteogenic and vasculogenic grafts.* Journal of Cellular Physiology, 2010. **225**: p. 348-353.

41. Xu, L., et al., *Tissue source determines the differentiation potentials of mesenchymal stem cells: a comparative study of human mesenchymal stem cells from bone marrow and adipose tissue.* Stem Cell Res Ther, 2017. **8**(1): p. 275.

42. Muraglia, A., R. Cancedda, and R. Quarto, *Clonal mesenchymal progenitors from human bone marrow differentiate in vitro according to a hierarchical model.* J Cell Sci, 2000. **113 (Pt 7)**: p. 1161-6.

43. Hoch, A.I. and J.K. Leach, *Concise review: optimizing expansion of bone marrow mesenchymal stem/stromal cells for clinical applications.* Stem Cells Transl Med, 2015. **4**(4): p. 412.

44. Sharpe, P.T., *Dental mesenchymal stem cells.* Development, 2016. **143**: p. 2273-2280.

45. Xu, X., et al., *Gingivae contain neural-crest- and mesoderm-derived mesenchymal stem cells.* J. Dent. Res, 2013. **92**: p. 825-832.

46. Fournier, B.P., et al., *Multipotent progenitor cells in gingival connective tissue.* Tissue Eng. Part A, 2010. **16**: p. 2891-2899.

47. Mitrano, T.I., et al., *Culture and characterization of mesenchymal stem cells from human gingival tissue.* J. Periodontol, 2010. **81**: p. 917-925.

48. Yang, H., et al., *Comparison of mesenchymal stem cells derived from gingival tissue and periodontal ligament in different incubation conditions.* Biomaterials, 2013. **34**: p. 7033-7047.

49. Sun, Q., et al., *Comparison of gingiva-derived and bone marrow mesenchymal stem cells for osteogenesis.* J. Cell. Mol. Med, 2019. **23**: p. 7592-7601.

50. Wang, F., et al., *Gingivaderived mesenchymal stem cell-mediated therapeutic approach for bone tissue regeneration.* Stem Cells Dev, 2011. **20**: p. 2093-2102.

51. Ge, S., et al., *Isolation and characterization of mesenchymal stem cell-like cells from healthy and inflamed gingival tissue: potential use for clinical therapy.* Regen. Med, 2012. **7**: p. 819-832.

52. da Silva Meirelles, L., A.I. Caplan, and N.B. Nardi, *In search of the in vivo identity of mesenchymal stem cells.* Stem Cells, 2008. **26**(9): p. 2287-99.

53. Mostafa, N.Z., et al., *In vitro osteogenic induction of human gingival fibroblasts for bone regeneration.* Open Dent. J, 2011. **5**: p. 139-145.

54. Denu, R.A., et al., *Fibroblasts and mesenchymal stromal/stem cells are phenotypically indistinguishable.* Acta Haematol, 2016. **136**: p. 85-97.

55. Sanz, A.R., F.S. Carrion, and A.P. Chaparro, *Mesenchymal stem cells from the oral cavity and their potential value in tissue engineering.* Periodontol 2000, 2015. **67**(1): p. 251-67.

56. Stefanska, K., et al., *Stemness Potency of Human Gingival Cells-Application in Anticancer Therapies and Clinical Trials.* Cells, 2020. **9**(8): p. 1916.

57. Yamada, Y., et al., *Promising advances in clinical trials of dental tissue-derived cell-based regenerative medicine.* Stem Cell Res Ther, 2020. **11**(1): p. 175.

58. Tomar, G.B., et al., *Human gingiva-derived mesenchymal stem cells are superior to bone marrow-derived mesenchymal stem cells for cell therapy in regenerative medicine.* Biochem. Biophys. Res. Commun, 2010. **393**: p. 377-383.

59. Zorin, V.L., et al., *Octacalcium phosphate ceramics combined with gingiva-derived stromal cells for engineered functional bone grafts.* Biomed Mater, 2014. **9**(5): p. 055005.

60. Shi, A., et al., *Small molecule inhibitor of TGF-beta signaling enables robust osteogenesis of autologous GMSCs to successfully repair minipig severe maxillofacial bone defects.* Stem Cell Res Ther, 2019. **10**(1): p. 172.

61. Moshaverinia, A., et al., *Bone regeneration potential of stem cells derived from periodontal ligament or gingival tissue sources encapsulated in RGD-modified alginate scaffold.* Tissue Eng. A, 2014. **20**: p. 611-621.

62. Xu, Q.C., et al., *Systemically transplanted human gingiva-derived mesenchymal stem cells contributing to bone tissue regeneration.* Int J Clin Exp Pathol, 2014. **7**(8): p. 4922-9.

63. Diomede, F., et al., *Biotherapeutic effect of gingival stem cells conditioned medium in bone tissue restoration.* Int. J. Mol. Sci, 2018. **8**: p. 315-317.

64. Al-Qadhi, G., et al., *Gingival mesenchymal stem cells as an alternative source to bone marrow mesenchymal stem cells in regeneration of bone defects: In vivo study.* Tissue Cell, 2020. **63**: p. 101325.

65. Kandalam, U., et al., *Predifferentiated Gingival Stem Cell-Induced Bone Regeneration in Rat Alveolar Bone Defect Model.* Tissue Eng Part A, 2020. **doi**: 10.1089/ten.TEA.2020.0052.

66. Lee, M.W., et al., *Effect of ex vivo culture conditions on immunosuppression by human mesenchymal stem cells.* Biomed Res Int, 2013. **2013**: p. 154919.

67. Masterson, C.H., G.F. Curley, and J.G. Laffey, *Modulating the distribution and fate of exogenously delivered MSCs to enhance therapeutic potential: knowns and unknowns.* Intensive Care Med Exp, 2019. **7**(Suppl 1): p. 41.

68. Bieback, K., et al., *Clinical Protocols for the Isolation and Expansion of Mesenchymal Stromal Cells.* Transfus Med Hemother, 2008. **35**(4): p. 286-294.

69. Mendicino, M., et al., *MSC-based product characterization for clinical trials: an FDA perspective.* Cell Stem Cell, 2014. **14**(2): p. 141-5.

70. Hemeda, H., B. Giebel, and W. Wagner, *Evaluation of human platelet lysate versus fetal bovine serum for culture of mesenchymal stromal cells.* Cytotherapy, 2014. **16**: p. 170.

71. Spees, J.L., et al., *Internalized antigens must be removed to prepare hypoimmunogenic mesenchymal stem cells for cell and gene therapy.* Mol Ther, 2004. **9**: p. 747.

72. Sakamoto, N., et al., *Bovine apolipoprotein B-100 is a dominant immunogen in therapeutic cell populations cultured in fetal calf serum in mice and humans.* Blood, 2007. **110**: p. 501.

73. Haque, N., N.H. Abu Kasim, and M.T. Rahman, *Optimization of pre-transplantation conditions to enhance the efficacy of mesenchymal stem cells.* Int J Biol Sci, 2015. **11**(324).

74. Bieback, K., et al., *Human alternatives to fetal bovine serum for the expansion of mesenchymal stromal cells from bone marrow.* Stem Cells, 2009. **27**(9): p. 2331-41.

75. Tekkatte, C., et al., *''Humanized'' stem cell culture techniques: the animal serum controversy.* Stem Cells Int, 2011. **504723**.

76. Bieback, K., *Platelet lysate as replacement for fetal bovine serum in mesenchymal stromal cell cultures.* Transfus Med Hemother, 2013. **40**: p. 326.

77. Ikebe, C. and K. Suzuki, *Mesenchymal Stem Cells for Regenerative Therapy: Optimization of Cell Preparation Protocols.* Biomed Res Int, 2014. **2014**: p. 951512.

78. Agency, E.M., *Guideline on the use of bovine serum in the manufacture of human biological medicinal products*, in *EMA/CHMP/BWP/457920/2012 rev1. Amsterdam.* 2013.

79. Bieback, K., et al., *Gaps in the knowledge of human platelet lysate as a cell culture supplement for cell therapy: a joint publication from the AABB and the.* International Society for Cell & Gene Therapy. Transfusion, 2019. **59**: p. 3448-3460.

80. Strunk, D., et al., *International Forum on GMP-grade human platelet lysate for cell propagation: summary.* Vox Sang, 2018. **113**(1): p. 80-87.

81. Phinney, D.G., et al., *Manufacturing mesenchymal stromal cells for clinical applications: A survey of Good Manufacturing Practices at U.S. academic centers.* Cytotherapy, 2019. **21**(7): p. 782-792.

82. Wolff, J., et al., *GMP--level adipose stem cells combined with computer--aided manufacturing to reconstruct mandibular ameloblastoma resection defects: Experience with three cases.* Annals of Maxillofacial Surgery, 2013. **3**: p. 114-125.

83. Schallmoser, K., et al., *Production and Quality Requirements of Human Platelet Lysate: A Position Statement from the Working Party on Cellular Therapies of the International Society of Blood Transfusion.* Trends Biotechnol, 2020. **38**(1): p. 13-23.

84. Burnouf, T., et al., *Human platelet lysate: replacing fetal bovine serum as a gold standard for human cell propagation?* Biomaterials, 2016. **76**: p. 371-387.

85. Chou, M.L. and T. Burnouf, *Current methods to manufacture human platelet lysates for cell therapy and tissue engineering: possible trends in product safety and standardization.* ISBT Science Series, 2017. **12**(1): p. 168-175.

86. Bieback, K., et al., *Gaps in the knowledge of human platelet lysate as a cell culture supplement for cell therapy: a joint publication from the AABB and the International Society for Cell & Gene Therapy.* Transfusion, 2019. **59**(11): p. 3448-3460.

87. Henschler, R., et al., *Human platelet lysate current standards and future developments.* Transfusion, 2019. **59**(4): p. 1407-1413.

88. Strunk, D., et al., *International Forum on GMP-grade human platelet lysate for cell propagation.* Vox Sang, 2018. **113**(1): p. e1-e25.

89. Torreggiani, E., et al., *Exosomes: novel effectors of human platelet lysate activity.* Eur Cell Mater, 2014. **28**: p. 137.

90. Huang, C., J. Geng, and S. Jiang, *MicroRNAs in regulation of osteogenic differentiation of mesenchymal stem cells.* Cell Tissue Res, 2017. **368**(2): p. 229-238.

91. Mannerstrom, B., et al., *Publisher Correction: Extracellular small non-coding RNA contaminants in fetal bovine serum and serum-free media.* Sci Rep, 2020. **10**(1): p. 1369.

92. Witwer, K.W., et al., *Defining mesenchymal stromal cell (MSC)-derived small extracellular vesicles for therapeutic applications.* J Extracell Vesicles, 2019. **8**(1): p. 1609206.

93. Sammali, E., et al., *Intravenous infusion of human bone marrow mesenchymal stromal cells promotes functional recovery and neuroplasticity after ischemic stroke in mice.* Sci Rep, 2017. **7**(1): p. 6962.

94. Lucchini, G., et al., *Platelet-lysate-expanded mesenchymal stromal cells as a salvage therapy for severe resistant graft-versus-host disease in a pediatric population.* Biol Blood Marrow Transplant, 2010. **16**(9): p. 1293-301.

95. Castren, E., et al., *Osteogenic differentiation of mesenchymal stromal cells in two-dimensional and three-dimensional cultures without animal serum.* Stem Cell Res Ther, 2015. **6**: p. 167.

96. Li, C.Y., et al., *Comparative analysis of human mesenchymal stem cells from bone marrow and adipose tissue under xeno-free conditions for cell therapy.* Stem Cell Res Ther, 2015. **6**: p. 55.

97. Xia, W., et al., *Human platelet lysate supports ex vivo expansion and enhances osteogenic differentiation of human bone marrow-derived mesenchymal stem cells.* Cell Biol Int, 2011. **35**(6): p. 639-43.

98. Chevallier, N., et al., *Osteoblastic differentiation of human mesenchymal stem cells with platelet lysate.* Biomaterials, 2010. **31**(2): p. 270-8.

99. Kuterbekov, M., et al., *Design of experiments to assess the effect of culture parameters on the osteogenic differentiation of human adipose stromal cells.* Stem Cell Res Ther, 2019. **10**(1): p. 256.

100. Banfi, A., et al., *Proliferation kinetics and differentiation potential of ex vivo expanded human bone marrow stromal cells: Implications for their use in cell therapy.* Exp Hematol, 2000. **28**(6): p. 707-15.

101. Sart, S., et al., *Three-dimensional aggregates of mesenchymal stem cells: cellular mechanisms, biological properties, and applications.* Tissue Eng. B Rev, 2014. **20**: p. 365-380.

102. Follin, B., et al., *Increased Paracrine Immunomodulatory Potential of Mesenchymal Stromal Cells in Three-Dimensional Culture.* Tissue Eng Part B Rev, 2016. **22**(4): p. 322-9.

103. Ghazanfari, R., et al., *Human primary bone marrow mesenchymal stromal cells and their in vitro progenies display distinct transcriptional profile signatures.* Sci. Rep, 2017. **7**(1): p. 10338.

104. Petrenko, Y., E. Sykova, and S. Kubinova, *The therapeutic potential of three-dimensional multipotent mesenchymal stromal cell spheroids.* Stem Cell Res Ther. 2017. **8**(1): p. 94.

105. Braccini, A., et al., *Three-dimensional perfusion culture of human bone marrow cells and generation of osteoinductive grafts.* Stem Cells, 2005. **23**(8): p. 1066-72.

106. Rauh, J., et al., *Bioreactor systems for bone tissue engineering.* Tissue Eng Part B Rev, 2011. **17**(4): p. 263-80.

107. Haugen, H.J., et al., *Bone grafts: which is the ideal biomaterial?* J Clin Periodontol, 2019. **46 Suppl 21**: p. 92-102.

108. Hassan, M.N., et al., *The bone regeneration capacity of 3D-printed templates in calvarial defect models: A systematic review and meta-analysis.* Acta Biomater, 2019. **91**: p. 1-23.

109. Ahmadbeigi, N., et al., *The aggregate nature of human mesenchymal stromal cells in native bone marrow.* Cytotherapy, 2012. **14**: p. 917-924.

110. Bartosh, T.J., et al., *Dynamic compaction of human mesenchymal stem/precursor cells into spheres self-activates caspase-dependent IL1 signaling to enhance secretion of modulators of inflammation and immunity (PGE2, TSG6, and STC1).* Stem Cells 2013. **31**: p. 2443-56.

111. Bartosh, T.J. and J.H. Ylostalo, *Preparation of anti-inflammatory mesenchymal stem/precursor cells (MSCs) through sphere formation using hanging-drop culture technique.* Curr. Protoc. Stem Cell Biol, 2014. **28**:Unit 2B.6.

112. Cesarz, Z. and K. Tamama, *Spheroid Culture of Mesenchymal Stem Cells.* Stem Cells Int, 2016. **2016**: p. 9176357.

113. Edmondson, R., et al., *Three-dimensional cell culture systems and their applications in drug discovery and cell-based biosensors.* Assay Drug Dev Technol, 2014. **12**(4): p. 207-18.

114. Hall, B.K. and T. Miyake, *All for one and one for all: condensations and the initiation of skeletal development.* Bioessays, 2000. **22**: p. 138-147.

115. Kale, S., et al., *Three-dimensional cellular development is essential for ex vivo formation of human bone.* Nat. Biotechnol, 2000. **18**: p. 954-958.

116. Facer, S.R., et al., *Rotary culture enhances pre-osteoblast aggregation and mineralization.* J. Dent. Res, 2005. **84**: p. 542-547.

117. Kilian, K.A., et al., *Geometric cues for directing the differentiation of mesenchymal stem cells.* Proc Natl Acad Sci U S A, 2010. **107**(11): p. 4872-7.

118. Passanha, F.R., et al., *Cell culture dimensionality influences mesenchymal stem cell fate through cadherin-2 and cadherin-11*. Biomaterials, 2020. **254**: p. 120127.
119. He, S., D. Nakada, and S.J. Morrison, *Mechanisms of stem cell self-renewal*. Annu Rev Cell Dev Biol, 2009. **25**: p. 377-406.
120. Kolf, C.M., E. Cho, and R.S. Tuan, *Mesenchymal stromal cells. Biology of adult mesenchymal stem cells: regulation of niche, self-renewal and differentiation*. Arthritis Res Ther. 2007. **9**(1): p. 204.
121. Takahashi, K. and S. Yamanaka, *Induction of pluripotent stem cells from mouse embryonic and adult fibroblast cultures by defined factors*. Cell, 2006. **126**(4): p. 663-76.
122. Basu-Roy, U., et al., *The transcription factor Sox2 is required for osteoblast self-renewal*. Cell Death Diff, 2010. **17**: p. 1345-1353.
123. Guo, L., et al., *Epigenetic changes of mesenchymal stem cells in three-dimensional (3D) spheroids*. J. Cell. Mol. Med, 2014. **18**: p. 2009-2019.
124. Lo, L.M., M. Raghunath, and K.K.H. Lee, *Growing human dermal fibroblasts as spheroids renders them susceptible for early expression of pluripotency genes*. Adv Biosyst. 2019. 3: 1900094.
125. Yoo, J.U., et al., *The chondrogenic potential of human bone-marrow-derived mesenchymal progenitor cells*. J Bone Joint Surg Am, 1998. **80**(12): p. 1745-57.
126. Kabiri, M., et al., *3D mesenchymal stem/stromal cell osteogenesis and autocrine signalling*. Biochem. Biophys. Res. Commun, 2012. **419**: p. 142-147.
127. Suenaga, H., et al., *Bone regeneration in calvarial defects in a rat model by implantation of human bone marrow-derived mesenchymal stromal cell spheroids*. J. Mater. Sci. Mater. Med, 2015. **26**: p. 254.
128. Lee, S.H., et al., *Three-dimensional sphere-forming cells are unique multipotent cell population in dental pulp cells*. J. Endod, 2017. **43**: p. 1302-1308.
129. Moritani, Y., et al., *Spheroid culture enhances osteogenic potential of periodontal ligament mesenchymal stem cells*. J. Periodontal. Res, 2018. **53**: p. 870-882.
130. Langenbach, F., et al., *Generation and differentiation of microtissues from multipotent precursor cells for use in tissue engineering*. Nat Protoc, 2011. **6**(11): p. 1726-35.
131. Huang, G.S., et al., *Spheroid formation of mesenchymal stem cells on chitosan and chitosan-hyaluronan membranes*. Biomaterials, 2011. **32**(29): p. 6929-45.
132. Miyagawa, Y., et al., *A microfabricated scaffold induces the spheroid formation of human bone marrow-derived mesenchymal progenitor cells and promotes efficient adipogenic differentiation*. Tissue Eng Part A, 2011. **17**(3-4): p. 513-21.
133. Jing, Y. and Y. Jian-Xiong, *3-D spheroid culture of bone marrow mesenchymal stem cell of rhesus monkey with improved multi-differentiation potential to epithelial progenitors and neuron in vitro*. Clin Exp Ophthalmol, 2011. **39**(8): p. 808-19.
134. Haumer, A., et al., *Delivery of cellular factors to regulate bone healing*. Advanced Drug Delivery Reviews, 2018. **129**: p. 285-294.
135. Bartosh, T.J., et al., *Aggregation of human mesenchymal stromal cells (MSCs) into 3D spheroids enhances their antiinflammatory properties*. Proc Natl Acad Sci USA, 2010. **107**(31): p. 13724-9.
136. Ylostalo, J.H., et al., *Human mesenchymal stem/stromal cells cultured as spheroids are self-activated to produce prostaglandin E2 that directs stimulated macrophages into an anti-inflammatory phenotype*. Stem Cells, 2012. **30**(10): p. 2283-96.
137. Potapova, I.A., et al., *Mesenchymal stem cells support migration, extracellular matrix invasion, proliferation, and survival of endothelial cells in vitro*. Stem Cells, 2007. **25**: p. 1761-1768.

138. Potapova, I.A., et al., *Culturing of human mesenchymal stem cells as three-dimensional aggregates induces functional expression of CXCR4 that regulates adhesion to endothelial cells.* J Biol Chem, 2008. **283**(19): p. 13100-7.

139. Murphy, K.C., S.Y. Fang, and J.K. Leach, *Human mesenchymal stem cell spheroids in fibrin hydrogels exhibit improved cell survival and potential for bone healing.* Cell Tissue Res, 2014. **357**: p. 91-99.

140. Cesarz, Z., et al., *Soft elasticity-associated signaling and bone morphogenic protein 2 are key regulators of mesenchymal stem cell spheroidal aggregates.* Stem Cells Dev., 2016. **33**(5023–5035): p. 622-635.

141. Kim, J. and T. Adachi, *Cell condensation triggers the differentiation of osteoblast precursor cells to osteocyte-like cells.* Front. Bioeng. Biotechnol, 2019. **7**: 288.

142. Phimphilai, M., et al., *BMP signaling is required for RUNX2-dependent induction of the osteoblast phenotype.* J. Bone Miner. Res, 2006. **21**: p. 637-646.

143. Urist, M.R., *Bone morphogenetic protein: the molecularization of skeletal system development.* J Bone Miner Res, 1997. **12**: p. 343.

144. Farrell, E., et al., *In-vivo generation of bone via endochondral ossification by in-vitro chondrogenic priming of adult human and rat mesenchymal stem cells.* BMC Musculoskelet Disord, 2011. **12**: p. 31.

145. Chatterjea, A., et al., *Engineering new bone via a minimally invasive route using human bone marrow-derived stromal cell aggregates, microceramic particles, and human platelet-rich plasma gel.* Tissue Eng Part A, 2013. **19**(3-4): p. 340-9.

146. Chatterjea, A., et al., *Cell aggregation enhances bone formation by human mesenchymal stromal cells.* Eur Cell Mater, 2017. **33**: p. 121-129.

147. Ho, S.S., et al., *Increased Survival and Function of Mesenchymal Stem Cell Spheroids Entrapped in Instructive Alginate Hydrogels.* Stem Cells Transl Med, 2016. **5**(6): p. 773-81.

148. Ho, S.S., et al., *Cell Migration and Bone Formation from Mesenchymal Stem Cell Spheroids in Alginate Hydrogels Are Regulated by Adhesive Ligand Density.* Biomacromolecules, 2017. **18**(12): p. 4331-4340.

149. Yamaguchi, Y., et al., *Mesenchymal stem cell spheroids exhibit enhanced in-vitro and in-vivo osteoregenerative potential.* BMC Biotechnol, 2014. **14**: p. 105.

150. Ho, S.S., et al., *Hypoxic Preconditioning of Mesenchymal Stem Cells with Subsequent Spheroid Formation Accelerates Repair of Segmental Bone Defects.* Stem Cells, 2018. **36**(9): p. 1393-1403.

151. Iwasaki, K., et al., *Changes in characteristics of periodontal ligament stem cells in spheroid culture.* J Periodontal Res, 2019. **54**(4): p. 364-373.

152. Imamura, A., et al., *Three-dimensional spheroids of mesenchymal stem/stromal cells promote osteogenesis by activating stemness and Wnt/beta-catenin.* Biochem Biophys Res Commun, 2020. **523**(2): p. 458-464.

153. Kanczler, J.M. and R.O.C. Oreffo, *Osteogenesis and angiogenesis: the potential for engineering bone.* Eur Cell Mater, 2008. **15**: p. 100.

154. Jain, R.K., et al., *Engineering vascularized tissue.* Nat Biotechnol, 2005. **23**(821).

155. Nguyen, L.H., et al., *Vascularized bone tissue engineering: approaches for potential improvement.* Tissue Eng Part B Rev, 2012. **18**: p. 363.

156. Kalka, C., et al., *Transplantation of ex vivo expanded endothelial progenitor cells*, in *for therapeutic neovascularization. Proc Natl Acad Sci. USA* 2000. **97**: p. 3422.

157. Balaji, S., et al., *The role of endothelial progenitor cells in postnatal vasculogenesis: implications for therapeutic neovascularization and wound healing.* Adv Wound Care, 2013. **2**: p. 283.

158. Pedersen, T.O., et al., *Endothelial microvascular networks affect gene-expression profiles and osteogenic potential of tissue-engineered constructs. Stem Cell Res Ther.* 2013. **4**(2): 52.

159. Liu, Y., J.K. Chan, and S.H. Teoh, *Review of vascularised bone tissue-engineering strategies with a focus on co-culture systems.* J Tissue Eng Regen Med, 2015. **9**: p. 85.

160. Shanbhag, S., et al., *Cell Cotransplantation Strategies for Vascularized Craniofacial Bone Tissue Engineering: A Systematic Review and Meta-Analysis of Preclinical In Vivo Studies.* Tissue Eng Part B Rev, 2017. **23**(2): p. 101-117.

161. Power, S.M., D.B. Matic, and D.W. Holdsworth, *The effects of nonvascularized versus vascularized bone grafting on calvarial defect healing.* J Craniofac Surg, 2015. **26**: p. 290.

162. Chappell, J.C., D.M. Wiley, and V.L. Bautch, *How blood vessel networks are made and measured.* Cells Tissues Organs, 2012. **195**(1-2): p. 94-107.

163. Bauman, E., et al., *Xeno-free pre-vascularized spheroids for therapeutic applications.* Sci Rep, 2018. **8**(1): p. 230.

164. Mohamed-Ahmed, S., et al., *Adipose-derived and bone marrow mesenchymal stem cells: a donor-matched comparison.* Stem Cell. Res. Ther, 2018. **9**: p. 168.

165. Fujio, M., et al., *Conditioned media from hypoxic-cultured human dental pulp cells promotes bone healing during distraction osteogenesis.* J Tissue Eng Regen Med, 2017. **11**(7): p. 2116-2126.

166. Gharaei, M.A., et al., *Human dental pulp stromal cell conditioned medium alters endothelial cell behavior.* Stem Cell Res Ther, 2018. **9**(1): p. 69.

167. Pedersen, T.O., et al., *Endothelial microvascular networks affect gene-expression profiles and osteogenic potential of tissue-engineered constructs.* Stem Cell Res Ther, 2013. **4**(3): p. 52.

168. Pedersen, T.O., et al., *Mesenchymal stem cells induce endothelial cell quiescence and promote capillary formation.* Stem Cell Res Ther, 2014. **5**(1): p. 23.

169. Bartaula-Brevik, S., et al., *Angiogenic and Immunomodulatory Properties of Endothelial and Mesenchymal Stem Cells.* Tissue Eng Part A, 2016. **22**(3-4): p. 244-52.

170. Jain, S., et al., *Engineering 3D degradable, pliable scaffolds toward adipose tissue regeneration; optimized printability, simulations and surface modification.* Journal of Tissue Engineering, 2020. **11**: 2041731420954316.

171. Kilkenny, C., et al., *Improving bioscience research reporting: the ARRIVE guidelines for reporting animal research.* PLoS Biol, 2010. **8**: p. 1000412.

172. Moher, D., et al., *Preferred reporting items for systematic reviews and meta-- analyses: The PRISMA statement.* BMJ, 2009. **339**: p. 2535.

173. Hooijmans, C.R., et al., *SYRCLE's risk of bias tool for animal studies.* BMC Med Res Methodol, 2014. **14**: p. 43.

174. Thery, C., et al., *Isolation and characterization of exosomes from cell culture supernatants and biological fluids.* Curr Protoc Cell Biol, 2006. **Chapter 3**: Unit 3 22.

175. Aatonen, M.T., et al., *Isolation and characterization of platelet-derived extracellular vesicles.* J Extracell Vesicles, 2014. **doi:** 10.3402/jev.v3.24692.

176. Isern, J., et al., *Self-renewing human bone marrow mesenspheres promote hematopoietic stem cell expansion.* Cell Rep, 2013. **3**(5): p. 1714-24.

177. Baraniak, P.R. and T.C. McDevitt, *Scaffold-free culture of mesenchymal stem cell spheroids in suspension preserves multilineage potential.* Cell Tissue Res, 2012. **347**: p. 701-711.

178. Kuroda, Y., et al., *Unique multipotent cells in adult human mesenchymal cell populations.* Proc. Natl. Acad. Sci. USA, 2010. **107**: p. 8639-8643.

179. Robinson, S.T., et al., *A novel platelet lysate hydrogel for endothelial cell and mesenchymal stem cell-directed neovascularization.* Acta Biomater, 2016. **36**: p. 86-98.
180. Abiraman, S., et al., *Fibrin glue as an osteoinductive protein in a mouse model.* Biomaterials, 2002. **23**(14): p. 3023-31.
181. Bensaïd, W., et al., *A biodegradable fibrin scaffold for mesenchymal stem cell transplantation.* Biomaterials, 2003. **24**(14): p. 2497-2502.
182. Catelas, I., et al., *Human mesenchymal stem cell proliferation and osteogenic differentiation in fibrin gels in vitro.* Tissue Eng, 2006. **12**(8): p. 2385-96.
183. Ho, W., et al., *The behavior of human mesenchymal stem cells in 3D fibrin clots: dependence on fibrinogen concentration and clot structure.* Tissue Eng, 2006. **12**(6): p. 1587-95.
184. Trombi, L., et al., *Good manufacturing practice-grade fibrin gel is useful as a scaffold for human mesenchymal stromal cells and supports in vitro osteogenic differentiation.* Transfusion, 2008. **48**(10): p. 2246-51.
185. Kim, B.S., et al., *The effects of fibrinogen concentration on fibrin/atelocollagen composite gel: an in vitro and in vivo study in rabbit calvarial bone defect.* Clin Oral Implants Res, 2015. **26**(11): p. 1302-8.
186. Linsley, C.S., B.M. Wu, and B. Tawil, *Mesenchymal stem cell growth on and mechanical properties of fibrin-based biomimetic bone scaffolds.* J Biomed Mater Res A, 2016. **104**(12): p. 2945-2953.
187. Jaquiery, C., et al., *In vitro osteogenic differentiation and in vivo bone-forming capacity of human isogenic jaw periosteal cells and bone marrow stromal cells.* Ann Surg, 2005. **242**(6): p. 859-68.
188. Murphy, K.C., et al., *Engineered Fibrin Gels for Parallel Stimulation of Mesenchymal Stem Cell Proangiogenic and Osteogenic Potential.* Ann Biomed Eng, 2015. **43**(8): p. 2010-21.
189. Kim, B.S., et al., *Effects of fibrinogen concentration on fibrin glue and bone powder scaffolds in bone regeneration.* J Biosci Bioeng, 2014. **118**(4): p. 469-75.
190. Kim, B.S., F. Shkembi, and J. Lee, *In Vitro and In Vivo Evaluation of Commercially Available Fibrin Gel as a Carrier of Alendronate for Bone Tissue Engineering.* Biomed Res Int, 2017. **2017**: p. 6434169.
191. Yassin, M.A., et al., *3D and Porous RGDC-Functionalized Polyester-Based Scaffolds as a Niche to Induce Osteogenic Differentiation of Human Bone Marrow Stem Cells.* Macromol Biosci, 2019. **19**(6): p. e1900049.
192. Ribatti, D., *The chick embryo chorioallantoic membrane (CAM). A multifaceted experimental model.* Mech Dev, 2016. **141**: p. 70-77.
193. Donath, K. and G. Breuner, *A method for the study of undecalcified bones and teeth with attached soft tissues. The Sage-Schliff (sawing and grinding) technique.* J Oral Pathol, 1982. **11**(4): p. 318-26.
194. Stute, N., et al., *Autologous serum for isolation and expansion of human mesenchymal stem cells for clinical use.* Exp Hematol, 2004. **32**: 1212.
195. Shahdadfar, A., et al., *In vitro expansion of human mesenchymal stem cells: choice of serum is a determinant of cell proliferation, differentiation, gene expression, and transcriptome stability.* Stem Cells, 2005. **23**: 1357.
196. Perez-Ilzarbe, M., et al., *Comparison of ex vivo expansion culture conditions of mesenchymal stem cells for human cell therapy.* Transfusion (Paris), 2009. **49**(1901).
197. Shih, D.T.B. and T. Burnouf, *Preparation, quality criteria, and properties of human blood platelet lysate supplements for ex vivo stem cell expansion*. N Biotechnol, 2015. **32**(1): p. 199-211.

198. Agata, H., et al., *Feasibility and efficacy of bone tissue engineering using human bone marrow stromal cells cultivated in serum-free conditions.* Biochem Biophys Res Commun, 2009. **382**: 353.

199. Sato, K., et al., *Serum-free isolation and culture system to enhance the proliferation and bone regeneration of adipose tissue-derived mesenchymal stem cells.* In Vitro Cell Dev Biol Anim, 2015. **51**(5): p. 515-29.

200. Wuchter, P., et al., *Evaluation of GMPcompliant culture media for in vitro expansion of human bone marrow mesenchymal stromal cells.* Exp Hematol, 2016. **44**: 508.

201. Suliman, S., et al., *Impact of humanised isolation and culture conditions on stemness and osteogenic potential of bone marrow derived mesenchymal stromal cells.* Sci Rep, 2019. **9**(1): p. 16031.

202. Shanbhag, S., et al., *Efficacy of humanized mesenchymal stem cell cultures for bone tissue engineering: a systematic review with a focus on platelet derivatives.* Tissue Eng. Part B Rev, 2017. **23**: p. 552-569.

203. Yue, R., B. Shen, and S.J. Morrison, *Clec11a/osteolectin is an osteogenic growth factor that promotes the maintenance of the adult skeleton.* 2016: **eLife 5**: e18782.

204. Fekete, N., et al., *Platelet lysate from whole blood-derived pooled platelet concentrates and apheresis-derived platelet concentrates for the isolation and expansion of human bone marrow mesenchymal stromal cells: production process, content and identification of active components.* Cytotherapy, 2012. **14**(5): p. 540-54.

205. Widholz, B., et al., *Pooling of Patient-Derived Mesenchymal Stromal Cells Reduces Inter-Individual Confounder-Associated Variation without Negative Impact on Cell Viability, Proliferation and Osteogenic Differentiation.* Cells, 2019. **8**(6): 633.

206. Wu, R.X., et al., *Platelet lysate supports the in vitro expansion of human periodontal ligament stem cells for cytotherapeutic use.* J. Tissue Eng. Regen. Med, 2017. **11**: p. 2261-2275.

207. Samsonraj, R.M., et al., *Establishing criteria for human mesenchymal stem cell potency.* Stem Cells, 2015. **33**(6): p. 1878-91.

208. Corre, P., et al., *Determining a clinically relevant strategy for bone tissue engineering: an "all-in-one" study in nude mice.* PLoS One, 2013. **8**(12): p. e81599.

209. Brennan, M.A., et al., *Pre-clinical studies of bone regeneration with human bone marrow stromal cells and biphasic calcium phosphate.* Stem Cell Res Ther, 2014. **5**(5):114.

210. Kaul, H., et al., *Synergistic activity of polarised osteoblasts inside condensations cause their differentiation.* Sci. Rep, 2015. **5**: p. 11838.

211. Chen, F.M., et al., *Treatment of periodontal intrabony defects using autologous periodontal ligament stem cells: a randomized clinical trial.* Stem Cell Res Ther, 2016. **7**: p. 33.

212. Sanchez, N., et al., *Periodontal Regeneration using a Xenogeneic Bone Substitute seeded with Autologous Periodontal Ligament derived Mesenchymal Stem Cells: a 12-month quasi-randomized controlled pilot clinical trial.* J Clin Periodontol, 2020. **47**(11): p. 1391-1402.

213. Rodriguez, L.G., X. Wu, and J.L. Guan, *Wound-healing assay.* Methods Mol Biol, 2005. **294**: p. 23-9.

214. Zhang, Q., et al., *Three-dimensional spheroid culture of human gingivaderived mesenchymal stem cells enhances mitigation of chemotherapyinduced oral mucositis.* Stem Cells Dev, 2012. **21**: p. 937-947.

215. Miranda, J.P., et al., *The secretome derived from 3D-cultured umbilical cord tissue MSCs counteracts manifestations typifying rheumatoid arthritis. Front. Immunol.* 2019. **10**:18.

216. Joddar, B., S.A. Kumar, and A. Kumar, *A Contact-Based Method for Differentiation of Human Mesenchymal Stem Cells into an Endothelial Cell-Phenotype.* Cell Biochem Biophys, 2018. **76**(1-2): p. 187-195.

217. Rouwkema, J., J. de Boer, and C.A. Van Blitterswijk, *Endothelial cells assemble into a 3-dimensional prevascular network in a bone tissue engineering construct.* Tissue Eng, 2006. **12**: p. 2685.

218. Scott, M.A., et al., *Brief review of models of ectopic bone formation.* Stem Cells Dev, 2012. **21**(655).

219. Kuchler, U., et al., *Bone-conditioned medium modulates the osteoconductive properties of collagen membranes in a rat calvaria defect model.* Clin Oral Implants Res, 2018. **29**(4): p. 381-388.

220. Gamblin, A.L., et al., *Bone tissue formation with human mesenchymal stem cells and biphasic calcium phosphate ceramics: the local implication of osteoclasts and macrophages.* Biomaterials, 2014. **35**(36): p. 9660-7.

221. Mankani, M.H., S.A. Kuznetsov, and P.G. Robey, *Formation of hematopoietic territories and bone by transplanted human bone marrow stromal cells requires a critical cell density.* Exp Hematol, 2007. **35**(6): p. 995-1004.

222. Janicki, P., et al., *Prediction of in vivo bone forming potency of bone marrow-derived human mesenchymal stem cells.* Eur Cell Mater, 2011. **21**: p. 488-507.

223. Kasten, P., et al., *Influence of platelet-rich plasma on osteogenic differentiation of mesenchymal stem cells and ectopic bone formation in calcium phosphate ceramics.* Cells Tissues Organs, 2006. **183**(2): p. 68-79.

224. Zhang, S., T. Mao, and F. Chen, *Influence of platelet-rich plasma on ectopic bone formation of bone marrow stromal cells in porous coral.* Int J Oral Maxillofac Surg, 2011. **40**(9): p. 961-5.

225. Trouillas, M., et al., *A new platelet cryoprecipitate glue promoting bone formation after ectopic mesenchymal stromal cell-loaded biomaterial implantation in nude mice.* Stem Cell Res Ther, 2013. **4**(1): p. 1.

226. Yu, T., et al., *Autologous platelet-rich plasma induces bone formation of tissue-engineered bone with bone marrow mesenchymal stem cells on beta-tricalcium phosphate ceramics.* J Orthop Surg Res, 2017. **12**(1): p. 178.

227. Madden, V.J., *Microwave-Accelerated Decalcification*, in *Microwave Techniques and Protocols*, R.T. Giberson and R.S. Demaree, Editors. 2001, Humana Press: Totowa, NJ. p. 101-122.

228. Garske, D.S., et al., *Alginate Hydrogels for In Vivo Bone Regeneration: The Immune Competence of the Animal Model Matters.* Tissue Eng Part A, 2020. **26**(15-16): p. 852-862.

229. Leotot, J., et al., *Platelet lysate coating on scaffolds directly and indirectly enhances cell migration, improving bone and blood vessel formation.* Acta Biomater, 2013. **9**: p. 6630.

230. Huang, S. and Z. Wang, *Influence of platelet-rich plasma on proliferation and osteogenic differentiation of skeletal muscle satellite cells: an in vitro study.* Oral Surg Oral Med Oral Pathol Oral Radiol Endod, 2010. **110**(4): p. 453-62.

231. Longoni, A., et al., *Endochondral Bone Regeneration by Non-autologous Mesenchymal Stem Cells.* Front Bioeng Biotechnol, 2020. **8**: p. 651.

Original papers

Paper I

Efficacy of humanized mesenchymal stem cell cultures for bone tissue engineering: a systematic review with a focus on platelet-derivatives.

Shanbhag S, Stavropoulos A, Suliman S, Hervig T, Mustafa K.

Paper II

Influence of platelets storage time on human platelet lysates and platelet lysate-expanded mesenchymal stromal cells for bone tissue engineering.

Shanbhag S, Mohamed-Ahmed S, Lunde TH, Suliman S, Bolstad AI, Hervig T, Mustafa K.

Influence of platelet storage time on human platelet lysates and platelet lysate-expanded mesenchymal stromal cells for bone tissue engineering

Siddharth Shanbhag[1], Samih Mohamed-Ahmed[1], Turid Helen Felli Lunde[2], Salwa Suliman[1], Anne Isine Bolstad[1], Tor Hervig[2,3,4] and Kamal Mustafa[1*]

Abstract

Background: Human platelet lysate (HPL) is emerging as the preferred xeno-free supplement for the expansion of mesenchymal stromal cells (MSCs) for bone tissue engineering (BTE) applications. Due to a growing demand, the need for standardization and scaling-up of HPL has been highlighted. However, the optimal storage time of the source material, i.e., outdated platelet concentrates (PCs), remains to be determined. The present study aimed to determine the optimal storage time of PCs in terms of the cytokine content and biological efficacy of HPL.

Methods: Donor-matched bone marrow (BMSCs) and adipose-derived MSCs (ASCs) expanded in HPL or fetal bovine serum (FBS) were characterized based on in vitro proliferation, immunophenotype, and multi-lineage differentiation. Osteogenic differentiation was assessed at early (gene expression), intermediate [alkaline phosphatase (ALP) activity], and terminal stages (mineralization). Using a multiplex immunoassay, the cytokine contents of HPLs produced from PCs stored for 1–9 months were screened and a preliminary threshold of 4 months was identified. Next, HPLs were produced from PCs stored for controlled durations of 0, 1, 2, 3, and 4 months, and their efficacy was compared in terms of cytokine content and BMSCs' proliferation and osteogenic differentiation.

Results: BMSCs and ASCs in both HPL and FBS demonstrated a characteristic immunophenotype and multi-lineage differentiation; osteogenic differentiation of BMSCs and ASCs was significantly enhanced in HPL vs. FBS. Multiplex network analysis of HPL revealed several interacting growth factors, chemokines, and inflammatory cytokines. Notably, stem cell growth factor (SCGF) was detected in high concentrations. A majority of cytokines were elevated in HPLs produced from PCs stored for ≤ 4 months vs. > 4 months. However, no further differences in PC storage times between 0 and 4 months were identified in terms of HPLs' cytokine content or their effects on the proliferation, ALP activity, and mineralization of BMSCs from multiple donors.

* Correspondence: kamal.mustafa@uib.no
[1]Department of Clinical Dentistry, Faculty of Medicine, University of Bergen, Årstadveien 19, 5008 Bergen, Norway
Full list of author information is available at the end of the article

(Continued from previous page)

Conclusions: MSCs expanded in HPL demonstrate enhanced osteogenic differentiation, albeit with considerable donor variation. HPLs produced from outdated PCs stored for up to 4 months efficiently supported the proliferation and osteogenic differentiation of MSCs. These findings may facilitate the standardization and scaling-up of HPL from outdated PCs for BTE applications.

Keywords: Platelet lysate, Mesenchymal stromal cells, Bone tissue engineering, Regenerative medicine

Background

Adult mesenchymal stromal cells (MSCs) from various tissue sources, most frequently bone marrow (BMSCs) and adipose tissue (ASCs), are increasingly being used in bone tissue engineering (BTE) strategies for reconstruction of clinically challenging bone defects [1]. Although the use of whole tissue fractions, such as bone marrow concentrates and adipose stromal vascular fractions (SVFs), offers the feasibility of minimum cell manipulation and cost-effectiveness, the yield of MSCs obtained is relatively low. MSCs represent < 1% of the mononuclear cell fraction in the bone marrow and approximately 1.4% in adipose SVF [2]. This has encouraged ex vivo expansion strategies, which aim to exponentially amplify the number of BMSCs or ASCs available for implantation and thereby improve clinical outcomes.

The use of safe, standardized, and efficacious culture conditions is a critical aspect of Good Manufacturing Practice (GMP)-grade MSC expansion. Supplements providing growth factors (GFs), proteins, and enzymes for ex vivo MSC expansion are broadly categorized as xenogeneic (animal-derived), xeno-free (human-derived), or chemically defined [3, 4]. Although fetal bovine serum (FBS) is commonly used for MSC expansion [5], several limitations of FBS supplementation have been highlighted [3, 6]. European guidelines advocate the use of "non-ruminant" over "ruminant materials" for the manufacture of human medicinal products [7]. Accordingly, an increase in the use of "xeno-free" supplements, such as human platelet lysate (HPL), to develop GMP-compliant MSC expansion protocols has recently been reported [4, 8].

HPL is defined as a cell-free, protein- and GF-rich biological material produced from platelet concentrates (PCs) initially intended for transfusion [9]. Platelets release a wide range of physiological GFs and cytokines, which can significantly enhance cell growth and function. Pooled-and/or single-donor apheresis PCs are routinely prepared by blood establishments for transfusion and, depending on local regulations, stored for a maximum of 4–7 days before being discarded [9]. It is estimated that 5–20% of PCs produced in transfusion centers become "outdated" and utilizing these for HPL production is reported to be an ethically and economically optimal strategy, due to comparable efficacy of HPL produced from "fresh" and outdated PCs [6]. The current literature consistently demonstrates that HPL is at least comparable, and often

superior, to FBS in supporting MSC proliferation, stromal phenotype, chromosomal stability, and multi-lineage differentiation potential [10]. Interestingly, MSCs expanded in HPL have been reported to demonstrate enhanced osteoblastic differentiation potential, suggesting particular benefits of HPL expansion for BTE applications [4]. A clinically validated protocol for MSC expansion in HPL for BTE applications has recently been published [11].

The importance of HPL in GMP-grade MSC production is highlighted by the publication of several recent consensus statements [9, 12–14]. The most common themes in these reports are the need to scale-up HPL production by blood establishments and, more urgently, the need for standardization of HPL products. There is currently considerable large variation in the methods used to produce HPL, which is further complicated by the availability of several inadequately defined commercial HPL products. A need for standardization has been described at various levels of the HPL production process, such as the source material (pooled buffy coats vs. apheresis PCs and fresh vs. outdated PCs) and storage medium [plasma vs. platelet additive solution (PAS) or a combination]. Moreover, the pool sizes, i.e., the number of PC units or individual donations that are pooled to produce a single HPL product, method of platelet lysis, use of pathogen inactivation strategies, and quality control/release criteria for the final product vary between manufacturers [14].

Nevertheless, there is a clear consensus that the use of outdated pooled PCs as the source material is the optimal strategy for large-scale HPL production. Although the storage time of PCs varies between blood centers based on national regulations, recent recommendations call for immediate freezing of outdated PCs, i.e., within 7 days after collection, for subsequent HPL production—this represents an efficient use of resources and minimizes waste [9]. However, for many blood centers, it may not always be possible to initiate HPL production on the day of (or soon after) PC expiry, and the maximum duration for which PCs can be stored before being used to prepare an efficient HPL remains unknown. If outdated PCs can be stored for a standardized period to produce an optimal HPL product, it would facilitate logistical solutions and encourage more blood establishments to incorporate HPL production into their protocols. Thus, optimizing the storage time of PCs

would be a step towards addressing *both* the standardization *and* scaling-up of HPL production.

In the context of BTE, a recent study demonstrated differential effects of commercial HPL products on the mineralization capacity of BMSCs, although the mechanisms and HPL components contributing to these differences were not studied [15]. It would be of interest to investigate the effects of PC storage times on the cytokine contents of HPL, and subsequently the proliferation kinetics and osteogenic differentiation potential of HPL-expanded MSCs. Therefore, the objectives of this study were to characterize HPL in terms of its cytokine content and efficacy for MSC expansion (vs. FBS), particularly for BTE applications, and to investigate the effect of PC storage time on the cytokine content and efficacy of HPL in terms of MSC proliferation and osteogenic differentiation.

Materials and methods
Production of HPL
PC preparation and storage
The HPL herein (Bergenlys®, Bergen, Norway) is prepared from outdated pooled whole blood-derived PCs. The PCs are prepared at the Department of Immunology and Transfusion Medicine, Haukeland University Hospital, Bergen, Norway, according to established procedures and in line with national and EU quality requirements. Briefly, written informed consent is obtained from volunteer, healthy blood donors (aged 18–70 years) complying with national guidelines for blood donation. Whole blood is processed with the Reveos® Automated Blood Processing Unit (Terumo BCT, Lakewood, CO, USA). All donations are tested for ABO and RhD blood groups, infectious disease markers (HIV1/2, HBV, HCV), and sterility (aerobic bacteria). Donor information and manufacturing details are stored to ensure traceability of the final product. PCs (~ 300 mL) are generated by manually pooling five interim platelet units (IPUs) in 30% plasma and 70% platelet additive solution (Terumo BCT) and subsequently leukocyte-filtered (Immuflex®, Terumo BCT). Pooled PCs containing > 2 × 10^{11} platelets (and < 1 × 10^{6} leukocytes) are X-ray irradiated at a dose of 25 Gy and stored at 22 °C ± 2 °C under agitation for no longer than 7 days for use as transfusion units. All unused (or outdated) 7-day-old PCs are frozen at − 80 °C within 24 h for subsequent HPL production.

HPL production
Unused 7-day-old PCs were used for HPL production via the freeze/thaw lysis method [16]. Briefly, four different PCs (each PC containing buffy coats from five donors = 4 × 5 = 20 donors per HPL product) were exposed to multiple freezing (− 80 °C for at least 3 h) and thawing cycles [+ 37 °C in a plasma thawer (Plasmatherm®,

Barkey GmbH Co. KG, Leoppoldshoehe, Germany) for 15 min] to ensure platelet lysis before pooling. Pooled PCs were then centrifuged at 3000×g (4 °C, 15 min) to remove platelet fragments and aliquoted as the final HPL product. No fibrinogen depletion step was performed. HPL aliquots were stored at − 80 °C and thawed overnight at 4 °C for subsequent use in experiments.

Cell culture with HPL
Isolation and expansion of donor-matched BMSCs and ASCs
The biological efficacy of HPL was tested in various cellular assays using human BMSCs and ASCs. Donor-matched BMSCs and ASCs were isolated and expanded according to established protocols [17]. Briefly, human adipose tissue and bone marrow aspirates were obtained after informed parental consent and ethical approval (2013-1248/Regional Ethical Committee, South East, Norway) from patients aged 8–14 years undergoing surgery at the Department of Plastic Surgery, Haukeland University Hospital. For each donor, BMSCs and ASCs were isolated in 5% HPL and 10% FBS (GE Healthcare, South Logan, UT, USA) supplemented growth media [Dulbecco's modified Eagle's medium (DMEM, Invitrogen, Carlsbad, CA, USA) with 1% antibiotics (penicillin/streptomycin; GE Healthcare)]. In HPL-supplemented media, 1 IU/mL of heparin was added to prevent gelation and the medium was sterile filtered (0.2 μm) before use. Cells were sub-cultured and expanded according to a clinically validated protocol with a seeding density of 4000 cells/cm^2 [11]; passage 2–4 cells from at least three different donors were used in experiments. Cell number and viability were assessed using 0.4% Trypan blue stain (Invitrogen) and a Countess® Automated Cell Counter (Invitrogen).

Immunophenotype of BMSCs and ASCs
The immunophenotype of BMSCs and ASCs in HPL and FBS was assessed by flow cytometry based on the expression of specific surface antigens, as previously described [17] according to the "minimal criteria" for defining MSCs [18]. Briefly, the cells in HPL and FBS were incubated with conjugated antibodies against selected "negative" (CD34, CD45, HLA-DR) and "positive" (CD73, CD90, CD105) MSC markers (all from BD Biosciences, San Jose, CA, USA) and STRO-1 (Santa Cruz Biotechnology, Dallas, TX, USA) following the manufacturers' recommendations. Quantification was performed with a BD LSR Fortessa cell analyzer (BD Biosciences), and data were analyzed using flow cytometry software (FlowJo V10, Flowjo, LLC, Ashland, OR, USA).

Cell proliferation based on DNA quantification
BMSCs and ASCs in HPL and FBS were seeded in 24-well plates at a density of 4000 cells/cm^2. After 1, 7, and

14 days of culture, DNA quantification was performed using the Quant-IT® PicoGreen dsDNA Assay Kit (Thermo Fisher Scientific, Carlsbad, CA, USA) according to the manufacturer's instructions. Briefly, cells were lysed in 0.1% Triton X-100 and the PicoGreen staining solution was added and incubated for 5 min at RT protected from light, before fluorescence was measured at 480 nm (Ex)/520 nm (Em) with a microplate reader. DNA concentrations (ng/mL) were calculated based on known standards.

Multi-lineage differentiation of BMSCs and ASCs

The ability of BMSCs and ASCs to differentiate into multiple stromal lineages was tested as previously described [17]. Briefly, for adipogenic differentiation, cells in HPL and FBS were cultured in StemPro® adipogenic differentiation medium (Invitrogen) or standard growth medium (control). After 14 days, intracellular lipid formation was assessed via Oil red O (Sigma-Aldrich) staining. For quantification, the stain was extracted using 99% isopropanol (Sigma-Aldrich) and absorbance was measured at 540 nm using a microplate reader. For osteogenic differentiation, cells in HPL and FBS were cultured in osteogenic differentiation medium prepared by adding final concentrations of 0.05 mM L-ascorbic acid 2-phosphate, 10 nM dexamethasone, and 10 mM β glycerophosphate (all from Sigma-Aldrich) to the respective growth media. Cells in standard growth medium served as controls. After 21 days, extracellular calcium deposition was evaluated via Alizarin red S staining (Sigma-Aldrich). For quantification, the stain was dissolved in cetylpyridinium chloride (Sigma-Aldrich) and absorbance was measured at 540 nm using the microplate reader.

Gene expression

After 7 days of osteogenic induction, the expression of osteogenesis-related genes (Supplementary Table 1) was assessed in BMSCs and ASCs in HPL and FBS via quantitative real-time polymerase chain reaction (qPCR) using TaqMan® real-time PCR assays (Thermo Fisher Scientific). RNA extraction and cDNA synthesis were performed as previously described [17]. The expressions of the genes of interest were normalized to that of glyceraldehyde 3-phosphate dehydrogenase (GAPDH). Data were analyzed by the $\Delta\Delta Ct$ method, and results are presented as fold changes in HPL groups relative to FBS groups.

Alkaline phosphatase (ALP) activity

After 7 and 14 days, ALP activity in the cells was measured using the SIGMAFAST BCIP/NBT assay (Sigma-Aldrich). Following manufacturer's instructions, cells were lysed in 0.1% Triton-X100 buffer, mixed with a working solution containing a phosphatase substrate and alkaline buffer solution, and incubated at 37 °C for 15 min, and absorbance was measured at 405 nm using a microplate reader.

Cytokine content in HPL

Multiplex assay and cytokine network analysis

The concentrations of 48 cytokines (Supplementary Table 2) in HPL were measured using a multiplex immunoassay—Bio-Plex® Pro 48-plex Human Cytokine Screening Panel (Bio-Rad Laboratories, CA, USA) and a Bio-Plex® 200 System (Bio-Rad), according to the manufacturer's instructions. The cytokines included various GFs, inflammatory mediators, and chemokines involved in regulating MSC growth and function. To validate the multiplex data, concentrations of three selected GFs, namely platelet-derived growth factor BB (PDGF-BB), transforming growth factor-β1 (TGF-β1), and vascular endothelial growth factor (VEGF), were measured in representative batches of HPL via enzyme-linked immunosorbent assay (ELISA) kits (R&D Diagnostics, Wiesbaden, Germany) following the manufacturer's protocols. Interactions between cytokines were analyzed using the Search Tool for the Retrieval of Interacting Genes/Proteins (STRING) database and online software [19]. Cytokines were clustered according to the Markov Cluster algorithm and the STRING global score as previously reported [20].

Screening of different storage times to identify a threshold

The first multiplex assay included several HPL batches produced from PCs with different storage times (range 1–9 months). These HPLs, and corresponding PC units, were identified and screened retrospectively from a biobank, i.e., not collected and intentionally frozen for specific periods of time (as performed later in the study). In order to determine whether the duration of frozen storage of PCs affects the cytokine content of subsequently produced HPL, the storage times were divided into two categories: storage ≤ 4 months and > 4 months. Categorization was based on (a) recommendations regarding "quarantine storage" of GMP-grade blood products which state that the product must only be released if the donors have been tested negative for transmissible diseases twice, i.e., at the time of blood donation and re-tested as negative 4 months (or longer) thereafter [13, 21], and (b) current practices at the HPL production site (Haukeland Hospital Bloodbank), which are in line with the above recommendations.

Identifying a specific threshold for PC storage time

Since a preliminary threshold of 4 months was identified in the screening assay, a more focused custom-designed multiplex assay with 16 selected cytokines was performed to identify a specific threshold, if any, between 0 and 4 months. For this purpose, HPL batches were

specially produced from PCs frozen for controlled durations of 1, 2, 3, and 4 months. A reference HPL batch of PCs frozen and processed immediately ("0 months") was also included. The custom assay was a modification of the 48-plex panel (Bio-Rad) previously described. For both multiplex assays, data was analyzed using the Bio-Plex Manager Software (Bio-Rad) and final cytokine concentrations were derived in pg/mL.

Effect of frozen PC storage time on HPL efficacy
MSC morphology and proliferation kinetics
To investigate whether PC storage times affected the biological performance of HPL, cellular assays were performed using BMSCs. Previously cryopreserved passage 1 BMSCs were expanded for three additional passages in HPL produced from 0-, 1-, 2-, 3-, or 4-month PCs. At approximately 80% sub-confluence, cells from all conditions were harvested, counted, and re-seeded at 4000 cells/cm^2, following the same clinically validated protocol [11]. The population doubling (PD) rate was determined using the following formula [22]:

$$X = \frac{\log10(N_H) - \log10(N_I)}{\log10(2)}$$

N_H is the harvested cell number and N_I is the plated cell number. The PD for each passage was calculated and added to the PD of the previous passages to generate data for cumulative population doublings (CPD). Additionally, the population doubling time (PDT), i.e., the average time between two doublings, was calculated using the following formula [22]:

$$X = \frac{\log2 \times \Delta t}{\log10(N_H) - \log10(N_I)}$$

MSC osteogenic differentiation
To investigate whether PC freezing times affected the osteogenic differentiation potential of BMSCs, cells expanded for two passages with HPL produced from 0-, 1-, 2-, 3-, or 4-month PCs were plated for osteogenic differentiation assays. The differentiation medium was prepared by adding osteogenic supplements (as described above) to the respective growth media. Osteogenic differentiation was assessed via an ALP assay after 7 and 14 days (as described above) and via Alizarin red S staining of extracellular calcium deposits after 21 days (as described above) in osteogenically induced and non-induced BMSCs. Additionally, quantification of DNA per sample in the ALP experiment was performed as previously described. ALP activity was normalized to the amount of DNA per corresponding sample (ng/mL).

Statistical analysis
Statistical analyses were performed using the IBM SPSS version 17.0 software package (SPSS Inc., Chicago, IL, USA). Data are represented as arithmetic means ± SD, unless specified. For gene expression, statistical analyses are based on delta-Ct values and data are presented as relative fold changes. The student t test and one-way analysis of variance (ANOVA), followed by a post hoc Tukey's test for multiple comparisons, were applied when appropriate and $p < 0.05$ was considered statistically significant.

Results
Characterization of HPL efficacy
Isolation and characterization of BMSCs and ASCs
Donor-matched BMSCs and ASCs demonstrating characteristic plastic adherence and fibroblastic morphology were successfully expanded in both HPL- and FBS-supplemented media. Distinct morphological differences were observed between cells in HPL and FBS—the former being smaller and more spindle-shaped; these differences were more apparent at earlier passages (Fig. 1a). BMSCs and ASCs in both HPL and FBS demonstrated the characteristic MSC phenotype, i.e., > 95% of the cells were positive for the stromal markers CD73, CD90, and CD105, while < 5% of the cells expressed HLA-DR or the hematopoietic markers CD34 and CD45 (Fig. 1b, Supplementary figure 1). A trend for higher expression of STRO-1 was observed in HPL-cultured BMSCs and ASCs (Fig. 1c). Cell proliferation over 14 days was significantly greater in HPL-cultured BMSCs and ASCs based on DNA quantification (Fig. 1c).

Multi-lineage differentiation of BMSCs and ASCs
BMSCs and ASCs in both HPL- and FBS-supplemented media demonstrated the capacity to differentiate into adipocytes and osteoblasts, with some differences. Osteogenic differentiation in HPL and FBS was assessed at the gene, protein, and functional levels. Expression of early osteogenesis-related genes RUNX2 and BMP2 was significantly upregulated in HPL-cultured BMSCs and ASCs after 7 days (Fig. 3a). Interestingly, expressions of SPP1 and BGLAP, typically associated with later stages of osteogenesis, were also upregulated in HPL-cultured cells; BGLAP was significantly upregulated in ASCs. Intracellular ALP activity after 7 and 14 days was higher in HPL- vs. FBS-cultured BMSCs and ASCs; these differences were more pronounced in ASCs (Fig. 3b). While BMSCs generally presented higher ALP activity compared to ASCs at 7 days, the activity at 14 days was comparable between the two cell types. Significantly greater mineral deposition via Alizarin red S staining was observed in HPL- vs. FBS-cultured BMSCs and ASCs after 21 days, suggesting an enhanced osteogenic differentiation capacity of these cells (Fig. 3c). A trend for superior

Fig. 1 Characterization of BMSCs and ASCs in HPL. **a** Morphology of BMSCs and ASCs from one representative donor (scale bar 100 μm). **b** Surface marker expression of BMSCs and ASCs based on flow cytometry; data represent means ± SD ($n = 3$ donors). **c** Proliferation of BMSCs and ASCs over 14 days based on DNA quantification; data represent means ± SD ($n = 3$ donors); $**p < 0.001$
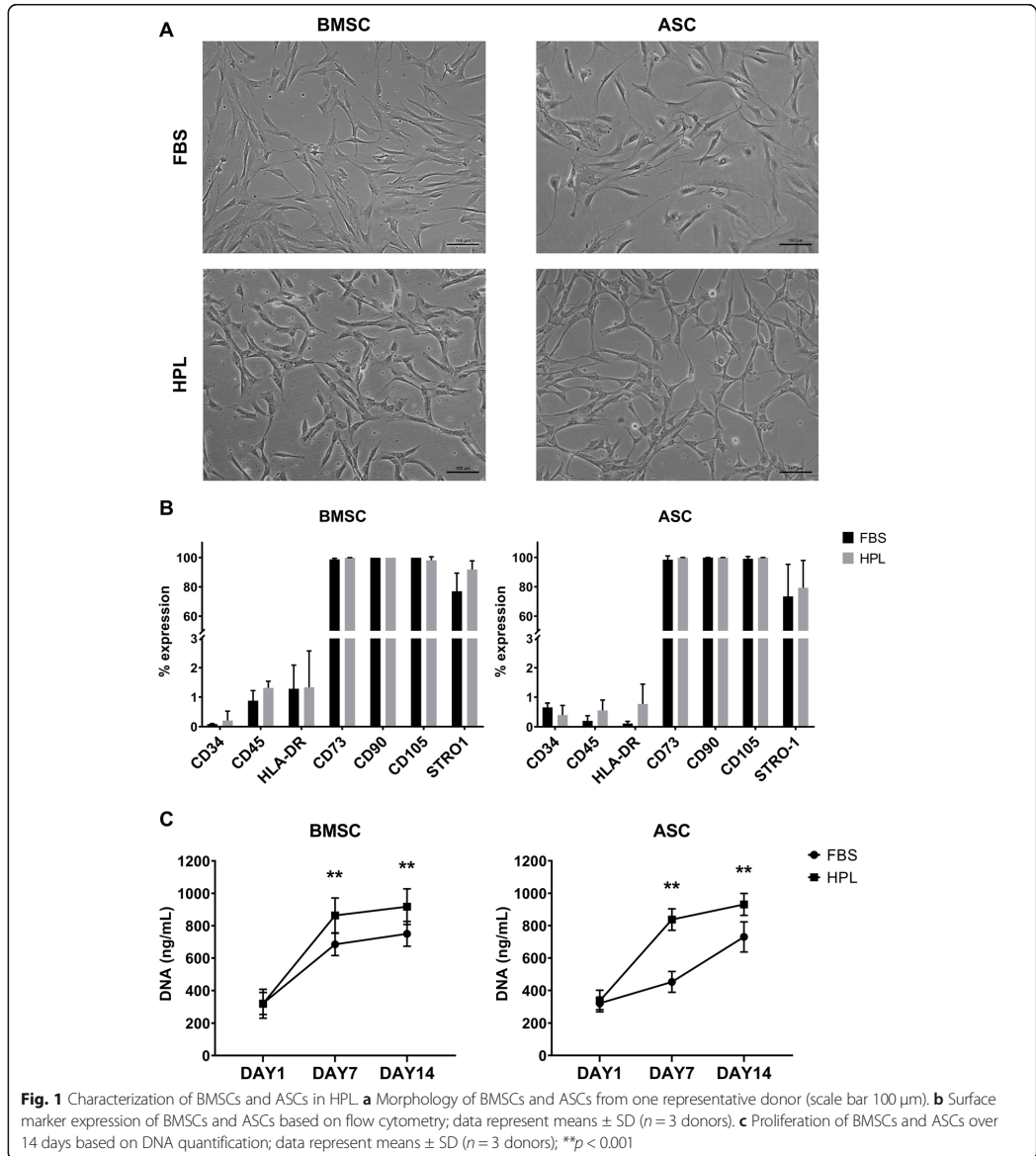
mineralization was observed in BMSCs as compared to ASCs. After 14 days of induction, ASCs demonstrated superior adipogenic differentiation, i.e., greater accumulation of intracellular lipid vesicles, compared to BMSCs, as revealed by quantification of Oil red O staining (Fig. 2e). HPL-cultured ASCs and BMSCs demonstrated similar adipogenic differentiation vs. their FBS-cultured counterparts (Fig. 2f).

No adipogenic or osteogenic differentiation of cells was observed in the standard growth media (data not shown).

Characterization of HPL cytokine content
Multiplex assay and cytokine network analysis
A multiplex immunoassay was performed using HPLs produced from frozen PCs stored for 1–9 months. Thirty
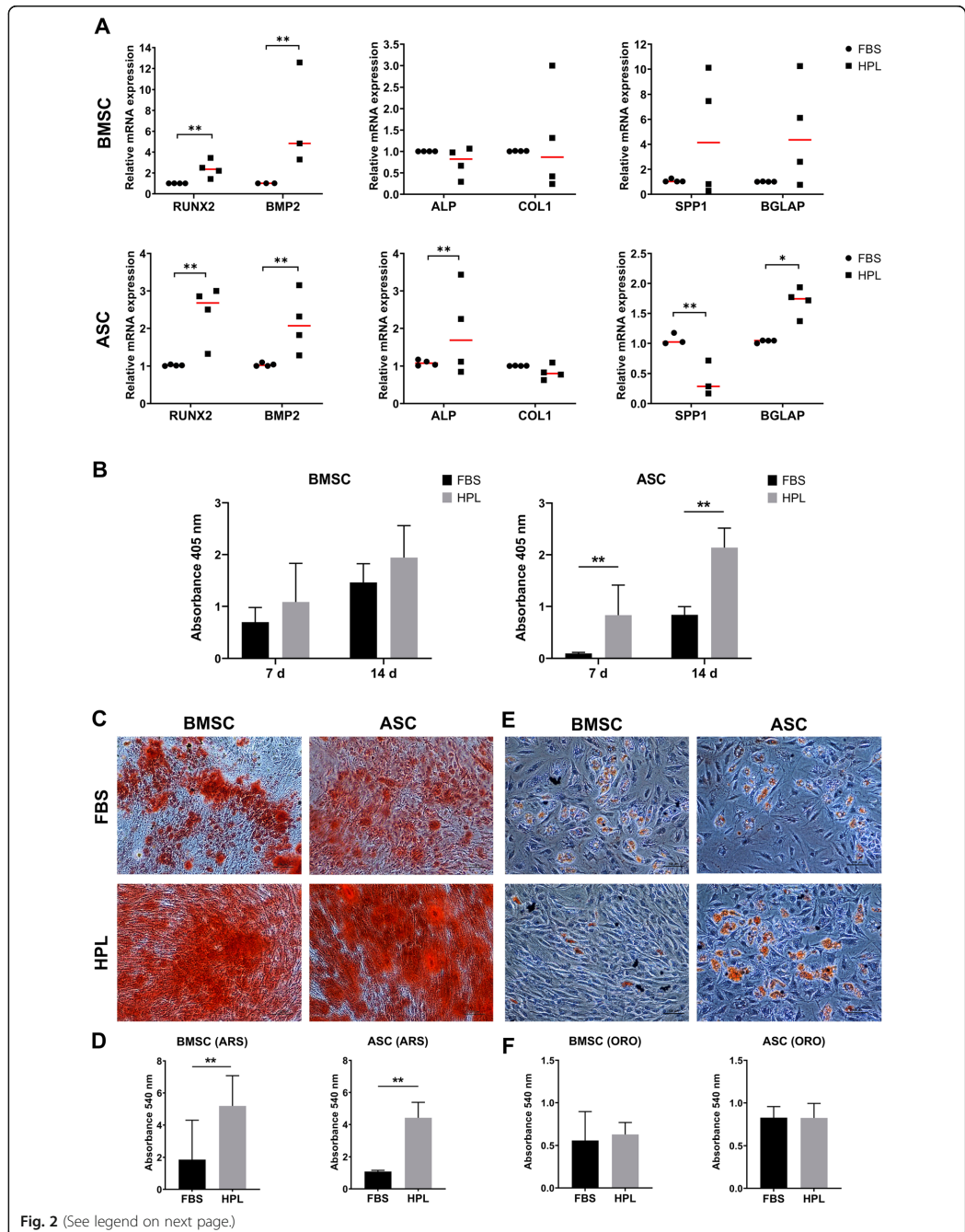
Fig. 2 (See legend on next page.)

of the 48 cytokines tested, including various GFs ($n = 11$), chemokines ($n = 9$), and inflammatory mediators ($n = 10$), were reliably detected in all tested HPLs. Cytokine concentrations, in comparison to previous studies, are reported in Table 1. Concentrations of three selected GFs, i.e., PDGF-BB, TGF-1, and VEGF, were validated via ELISA (Supplementary figure 2). The cytokine network analysis identified two major clusters of GFs, and chemokine/inflammatory mediators; stem cell growth factor (SCGF/CLEC11A) and stem cell factor (SCF/KITLG) were clustered separately (Fig. 3). Clear and abundant interactions were identified between the clusters including synergistic relations between several proteins that contribute to MSC proliferation, chemotaxis, and osteogenic differentiation.

Screening of different storage times to identify a threshold
Of these 30 cytokines, the concentrations of 27 cytokines were significantly reduced in the > 4-month group while only one cytokine, i.e., regulated upon activation, normal T cell expressed and secreted (RANTES), was significantly increased vs. the ≤ 4-month group. In addition to the known predominant cytokines PDGF-BB and TGF-β1, high levels of SCGF and macrophage inhibitory factor (MIF) were detected in HPL. Other GFs, such as basic fibroblast growth factor (b-FGF), hepatocyte growth factor (HGF), SCF, VEGF, and all inflammatory mediators [various interleukins (IL), tumor necrosis factor-α (TNF-α), and TNF-β] were present in relatively lower concentrations (Fig. 4).

Identifying a specific threshold for PC storage time
After a preliminary threshold of 4 months was identified, a second multiplex immunoassay with 16 selected cytokines was performed to identify a specific threshold, if any, for cytokine degradation between 0 and 4 months. Significantly lower concentrations were detected at 0 and 1 months for SCF and at 2 months for GCSF (Fig. 5). No significant differences were observed between the different storage times for any of the other tested cytokines, and no definitive threshold below 4 months could be identified.

Effect of frozen PC storage time on HPL efficacy
MSC morphology and proliferation kinetics
PC storage time did not seem to affect the biological performance of HPL; no differences in BMSC morphology were observed between the different storage times over three serial passages (Fig. 6a). The proliferation data revealed lower PD rate (fewer doublings) and higher PDT with increasing passages. No significant differences were observed with regard to kinetics-related variables (PD, CPD, PDT) or absolute DNA amounts between the different PC storage times (Fig. 6b).

MSC osteogenic differentiation
To investigate whether PC storage times affected the osteogenic differentiation potential of BMSCs, ALP activity (7, 14 days) and mineralization (21 days) were assessed. When combining data from all donors, no significant differences in ALP (Fig. 7a) or mineralization (Fig. 7b) were observed between the different PC storage times. Considerable variation was observed between the different BMSC donors in all groups—a trend for higher mean ALP activity (at 7 days) and mineralization, with lower inter-donor variation, was observed in the 3-month storage group. When analyzing data from individual donors, some differences in ALP activity and mineralization were observed, i.e., BMSCs from the same donor showed different activities in HPLs from different PC storage times, although these differences did not reach statistical significance for any of the donors. Overall, donor-related properties rather than PC storage time seemed to influence the osteogenic potential of HPL-cultured BMSCs.

Discussion
HPL is emerging as the preferred xeno-free supplement for the GMP-grade expansion of MSCs for BTE applications [1, 11]. Accordingly, there is a growing need for standardization and scaling-up of HPL production [12, 14]. Current GMP guidelines call for HPL release criteria to include testing for specific cytokines and biological efficacy based on cellular assays [9, 12]. In the present study, a scalable and GMP-compliant HPL was produced based on previously published methods and characterized for its cytokine content and efficacy for MSC expansion. Consistent with previous reports, HPL supported the expansion, stromal phenotype, and multilineage, particularly osteogenic, differentiation of MSCs in comparison to FBS [17].

A strength of the present study was the comparison of donor-matched cells from two different tissue sources,

Shanbhag *et al. Stem Cell Research & Therapy*   (2020) 11:351

Page 9 of 18

Table 1 Multiplex-based measurements of cytokine concentrations (pg/mL) in HPL

Reference	(21)*	(39)	(41)	(42)	(43)	(44)**	Present study
Starting material	< 5 d BC or AP	< 24 h AP	Fresh BC	Exp BC	7 d BC (3 w at − 80C), pathogen inactivated	5–7 d BC	7 d BC
Donors (n)	< 12 (BC) or 1 (AP)	1	16	245 + 16	16	40	20
Lysis method	1–2× F/T	2× F/T	3× F/T	1× F/T	3× F/T	3× F/T	3× F/T
Cytokines (n)	23	12	27	22	37	45	48
PDGF-AA	239,412 $\pm$ 53,690			10,287 + 1820	11,433.75 + 3083.45		
PDGF-AB/BB	571,730 + 381,036	1244 + 478.46	13,534.4 + 326.9	27,407 + 5365	25,941.5 + 1891.06	11,121 + 1126	11,783.482 + 917.39
TGF-β1	139,029 + 18,854						306,801.77 + 81,171.87
b-FGF	495 + 27	77.09 + 21.33	256.6 + 7.6		407 + 105	569 + 10	56.48 + 9.85
HGF			1594.7 + 172.3			2631 + 204	542.39 + 42.21
VEGF-A/D	325 + 34	660.88 + 221.90	421.9 + 1.9		424.5 + 88.91	1742 + 133/ 398 + 60	440.175 + 40.35
EGF			754.9 + 89.9		997.5 + 825.58	1104 + 224	
IGF						1122 + 54	
b-NGF		85.55 + 24.27				936 + 28	19.05 + 9.29
BDNF						3169 + 213	
SCGF/CLEC11a							186,005.65 + 12,463.91
SCF/KITLG						260 + 35	30.45 + 4.35
G-CSF	74 + 19		131.4 + 9.4		40 + 15.36		108.68 + 13.17
GM-CSF	34 + 16		98.1 + 3.8		22 + 6.27	2423 + 0	7.42 + 2.28
M-CSF				129,689 + 14,654			129.65 + 55.04
MCP1/CCL2		585.75 + 200.47	64.5 + 5.0		152.5 + 30.65	1060 + 73	16.00 + 3.26
MIP-1α/CCL3	47 + 4		12.5 + 0.5	29,337 + 2030	27.25 + 5.12	531 + 37	1.59 + 0.24
MIP-1β/CCL4	51 + 5		134.9 + 2.3	17,087 + 2385	124.25 + 33.93	1641 + 289	169.77 + 13.01
RANTES/CCL5	2,705,600 + 496,076	67.71 + 18.33	15,810.8 + 717.7	376,730 + 56,734		1453 + 24	8788.00 + 644.50
MCP3/CCL7					397 + 126.25		OOR<
Eotaxin/CCL11			72.6 + 3.3		91.5 + 31.2	196 + 64	44.68 + 5.86
CTACK/CCL27							311.83 + 44.73
MSP/MST1				688,589 + 132,037			
MDC					470.25 + 300.42		
MIF				287,188 + 51,282			6645.36 + 768.15
LIF						1473 + 114	79.47 + 18.88
GROa/CXCL1	11,126 + 6480			40,947 + 3148		866 + 109	1203.04 + 98.03
IL-8/CXCL8	80 + 6	17.15 + 5.22	112.5 + 5.3		57 + 16.53	ND	21.98 + 3.82
MIG/CXCL9							96.33 + 8.36
IP-10/CXCL10			284.7 + 3.1		82.5 + 33.37	527 + 65	384.76 + 11.42
SDF1α/CXCL12						16,102 + 1506	753.49 + 49.21
Fractalkine/ CX3CL1					174.75 + 54.59		

Shanbhag *et al. Stem Cell Research & Therapy*   (2020) 11:351
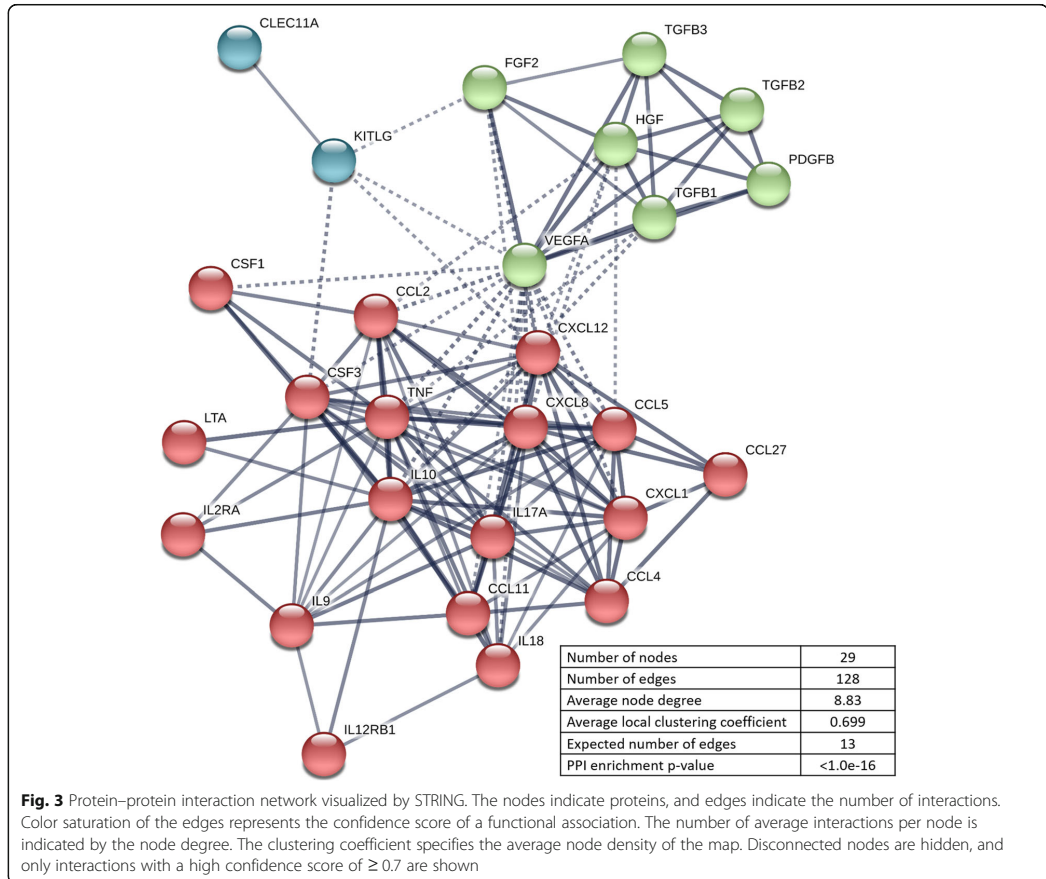
Page 10 of 18

Table 1 Multiplex-based measurements of cytokine concentrations (pg/mL) in HPL *(Continued)*

Reference	(21)*	(39)	(41)	(42)	(43)	(44)**	Present study
IL-1α	41 + 6	88.78 + 33.30		4854 + 533	39.25 + 18.44	ND	
IL-1β	3 + 2	24.89 + 9.22	6.7 + 0.4		4.47 + 1.77	ND	2.82 + 0.39
IL-1ra			235.3 + 4.8	3997 + 589	717.25 + 283.94	10,580 + 605	
IL-2	OOR<		OOR<		4.92 + 2.59	ND	OOR<
IL-2ra							209.18 + 81.59
IL-3					4.97 + 1.55		OOR<
IL-4			14.2 + 0.5	3840 + 639	30.75 + 12.91	ND	OOR<
IL-5			OOR <		53.25 + 26.34	ND	180.33 + 67.29
IL-6	3 + 0	159.75 + 61.57	22.5 + 0.6		9 + 4.42	1847 + 178	54.19 + 21.40
IL-7	32 + 16		41.8 + 1.1		27 + 7.39	145 + 24	31.43 + 5.57
IL-9			129.9 + 6.3		6.9 + 2.5	942 + 49	208.42 + 20.72
IL-10	3 + 2		60.2 + 2.4		10.85 + 7.74	186 + 25	OOR <
IL-12(p40)					51.5 + 13.91		135.82 + 25.12
IL-12(p70)			113.9 + 5.1		8.85 + 3.08	ND	12.85 + 4.61
IL-13			7.7 + 1.1		291 + 131.16	ND	OOR<
IL-15			OOR <		7.7 + 3.52	568 + 29	689.27 + 228.99
IL-17			1022.5 + 56.4		10.87 + 4.04	622 + 91	11.25 + 1.76
IL-18						2466 + 349	34.37 + 11.56
IL-21						ND	
IL-22						ND	
IL-23						ND	
IL-27						2658 + 1053	
IL-31						ND	
TNF-α	8 + 2	427.25 + 167.01	133.3 + 10.4		20.25 + 5.56	2942 + 0	46.97 + 5.8
TNF-β					390.5 + 164.81	ND	246.03 + 25.05
TRAIL/TNFSF10							86.28 + 5.33
IFN-γ	14 + 4	6.61 + 2.27	154.6 + 7.4		12.125 + 2.59	ND	23.41 + 3.19
IFN-a2					63.25 + 19.72	64 + 40	8.44 + 1.29
VCAM-1	1,789,695 + 1,108,320						
ICAM-1	137,300 + 93,670						
Angiopoietin-1				121,156 + 22,164			
Angiogenin				102,085 + 17,627			
IGFBP3				530,240 + 75,663			
CD40L	29,738 + 8361			151,662 + 17,153			
TIMP-1				231,407 + 39,966			

BC buffy coats, *AP* apheresis, *PI* pathogen inactivated, *F/T* freeze/thaw cycles, *d* days, *w* weeks, *OOR* out of range

Data represent means ± SD

*No significant differences between buffy coat- and apheresis-derived HPL
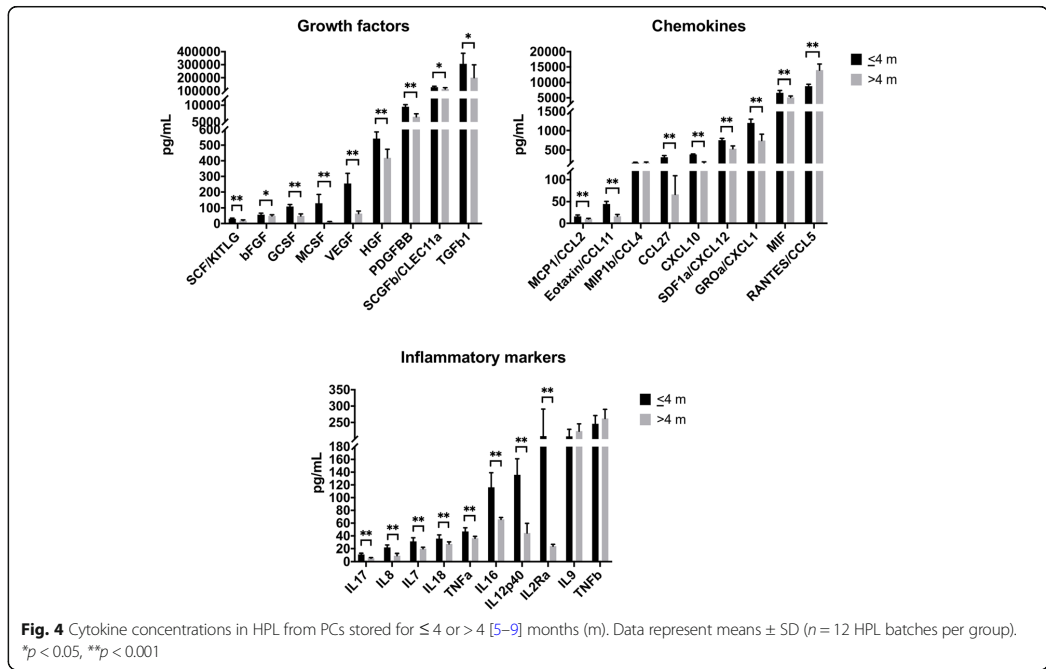
**Cytokine concentrations in medium supplemented with 10% HPL

Shanbhag *et al. Stem Cell Research & Therapy*   (2020) 11:351

Page 11 of 18

Fig. 3 Protein–protein interaction network visualized by STRING. The nodes indicate proteins, and edges indicate the number of interactions. Color saturation of the edges represents the confidence score of a functional association. The number of average interactions per node is indicated by the node degree. The clustering coefficient specifies the average node density of the map. Disconnected nodes are hidden, and only interactions with a high confidence score of ≥ 0.7 are shown

Number of nodes	29
Number of edges	128
Average node degree	8.83
Average local clustering coefficient	0.699
Expected number of edges	13
PPI enrichment p-value	<1.0e-16

i.e., BMSCs and ASCs, to evaluate HPL efficacy. Moreover, MSCs from each tissue type were cultured in HPL- and FBS-supplemented media from the time of isolation (passage 0), thus allowing true and standardized comparisons between xeno-free and xenogeneic-cultured cells [23]. Since the focus herein was BTE, the in vitro osteogenic differentiation of BMSCs and ASCs was studied in detail and was shown to be significantly enhanced in HPL vs. FBS at the early (expression of osteogenic genes), intermediate (ALP activity) and late stages (mineral deposition). Moreover, a trend for higher expression of STRO-1, a marker associated increased osteogenic potential [24], was observed in HPL- vs. FBS-cultured BMSCs and ASCs. When comparing the two cell types, osteogenic differentiation appeared to be accelerated in HPL-cultured BMSCs vs. ASCs, based on gene expression and ALP activity during the "early" differentiation stages, while adipogenic differentiation of HPL-cultured

ASCs was superior to that of BMSCs. One possible explanation could be the "tissue source variability" of BMSCs and ASCs [17, 25]. In context, previous studies have reported similar or enhanced differentiation of ASCs compared to BMSCs in vitro, but inferior bone formation in vivo, in both xenogeneic [26, 27] and HPL-supplemented cultures [28].

A substantial body of evidence points to the enhanced osteogenic potential of MSCs cultured in HPL [29–36], although the specific components contributing to this phenomenon are unknown. In the present study, the cytokine content of HPL was analyzed via a quantitative multiplex immunoassay to identify potentially relevant cytokines contributing to MSC osteogenesis. Although previous studies have measured cytokines in HPL via semi-quantitative assays [22, 36–40], to our knowledge, only five studies have reported quantitative multiplex-based assessments [21, 39, 41–44]. Considerable

Fig. 4 Cytokine concentrations in HPL from PCs stored for ≤ 4 or > 4 [5–9] months (m). Data represent means ± SD (*n* = 12 HPL batches per group). **p* < 0.05, ***p* < 0.001
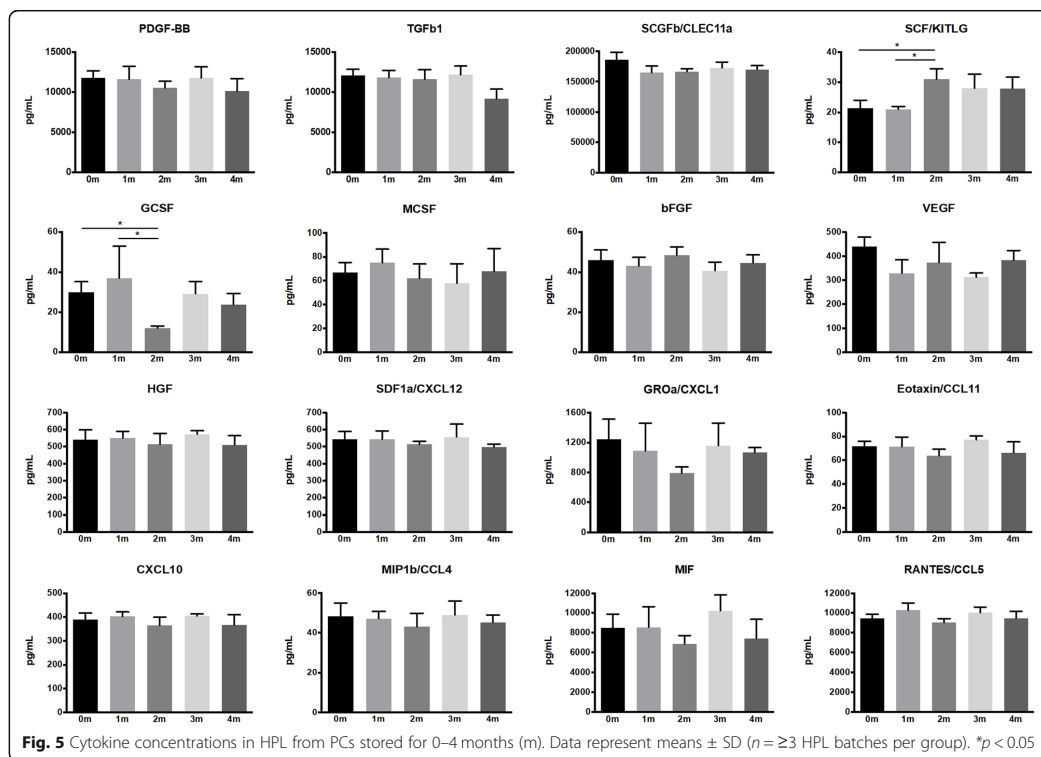
differences in cytokine concentrations are observed across the different studies (Table 1). Moreover, it is presently unclear which cytokines in HPL are most important, what are the optimal (minimum and/or maximum) concentrations of specific cytokines, and what are the effects of HPL preparation methods on individual cytokine concentrations [10]. Nevertheless, some cytokines such as PDGF-BB, TGF-β1, and b-FGF have been consistently identified in HPL in substantial quantities. A previous study identified PDGF-BB, TGF-β1, and b-FGF to be necessary for the optimal proliferation of MSCs in HPL [21]. However, these three factors on their own were not sufficient to promote MSC proliferation [21]. These data are consistent with findings that combinations of cytokines, rather than single GFs, are important to exert maximal effects on MSC migration and proliferation [45]. However, in another study, even the use of defined combinations of several recombinant GFs and chemokines was inferior to HPL supplementation for MSC expansion [46]. Since measurement of selected cytokine concentrations has been cited as a "quality control" measure for GMP-grade HPL [12], further information is needed on which cytokines (for specific MSC applications, e.g., BTE) should be tested along with "target" concentration ranges.

In addition to established factors such as PDGF-BB and TGF-β1, high concentrations of stem cell growth factor (SCGF)—a cytokine not previously identified in HPL—were detected in the multiplex analysis herein. SCGF is a protein encoded by the CLEC11A gene (C-type lectin domain family 11, member A) and is associated with the growth of hematopoietic progenitor cells [47]. In the context of the bone, SCGF/CLEC11A is reportedly expressed in the bone marrow by a variety of stromal cells [47, 48]. Interestingly, CLEC11A was recently shown to be expressed by murine BMSCs, and its overexpression promoted their in vitro osteogenic differentiation and in vivo osteogenesis in a fracture healing model [47]. However, a more recent study showed contrasting results in human BMSCs, where silencing, rather than overexpression, of CLEC11A promoted their in vitro osteogenic differentiation [49]. In another study, SCGF was detected in the secretome of BMSCs undergoing osteogenic differentiation and was found to be downregulated on days 1, 7, and 14 compared to day 0 [50]. Thus, in addition to PDGF-BB and TGF-β1, SCGF/CLEC11A signaling may be involved in the regulation of osteogenic differentiation of HPL-cultured MSCs.

Consistent with results from the above study [49], the in silico network analysis herein identified only a single interaction for SCGF/CLEC11A, which was with the chemokine stem cell factor (SCF), a ligand for the c-kit receptor (KITLG) [51]. Like SCGF, SCF is also typically associated with hematopoietic cell proliferation [51].

Fig. 5 Cytokine concentrations in HPL from PCs stored for 0–4 months (m). Data represent means ± SD ($n = \geq 3$ HPL batches per group). $*p < 0.05$
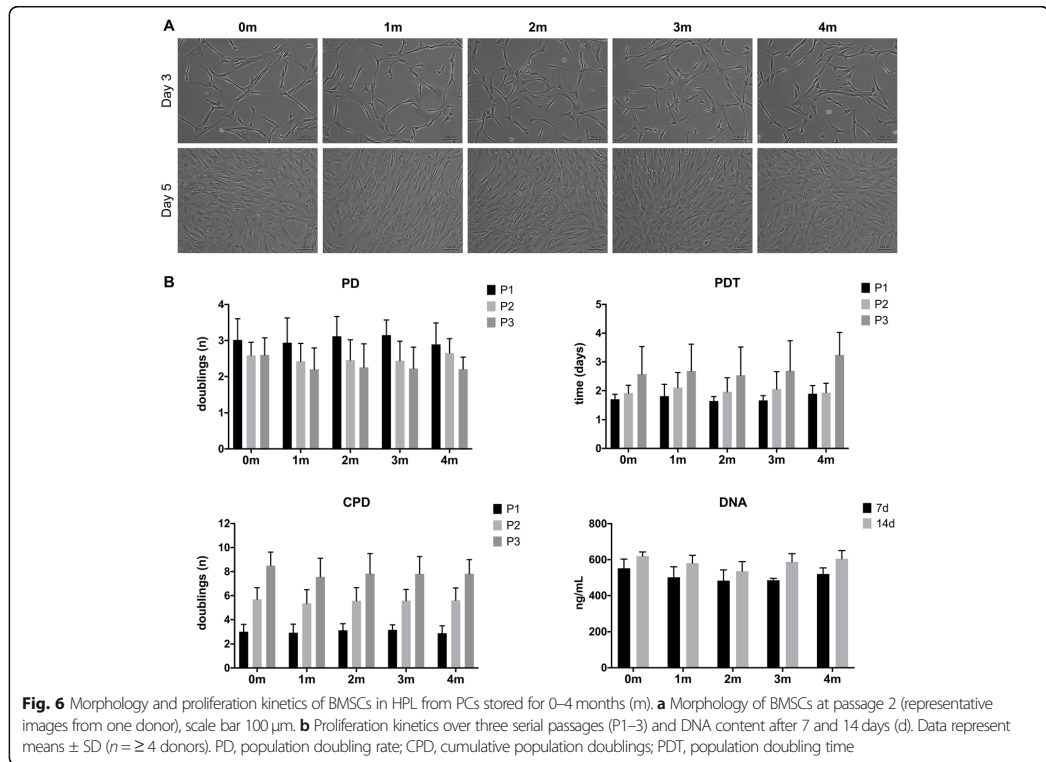
Although SCF was detected at a relatively lower concentration compared to SCGF, the network analysis revealed several interactions with the cytokine/chemokine and GF clusters. Recently, SCF signaling has been implicated in the mobilization, and subsequent osteogenic differentiation, of BMSCs in vitro and in in vivo models of fracture healing [52] and dental pulp/dentin regeneration [53]. Further studies are needed to elucidate the nature of the interaction(s) between SCGF, SCF, and other cytokines in the context of MSCs' osteogenic differentiation.

In addition to GFs, HPL also contains a wide range of chemokines, which regulate MSC migration, proliferation, and differentiation. Several chemokines of the CCL and CXCL families have been identified in HPL (Table 1). Of these, stromal derived factor-1 (SDF-1/CXCL12) is the most extensively studied and is involved in the recruitment of endogenous BMSCs to injury sites [54]. Platelets have been shown to release SDF1 and recruit progenitor cells to initiate wound healing at sites of vascular injury [55]. In the context of the bone, SDF1 was shown to play a critical role in the recruitment of murine BMSCs to the injury site during the early stages of fracture healing, and inhibition of SDF1 led to reduced in vivo bone formation [56]. Moreover, SDF1

regulated BMP2-induced osteogenic differentiation of mouse and human BMSCs; blocking SDF1 signaling led to significantly reduced ALP activity and mineralization of the cells [57]. Recent studies have also demonstrated enhanced in vivo bone regeneration following delivery of SDF1 via recruitment of endogenous MSCs to regeneration sites [58–61], thus highlighting the role of SDF1 in regulating MSCs' osteogenic differentiation.

Emerging evidence suggests that MSCs exert their regenerative effects primarily via paracrine mechanisms and modulation of immune cells, including osteoclasts [62]. Osteoblast-osteoclast interactions are known to be critical for bone regeneration. This is especially relevant in BTE, where MSCs are often delivered using biomaterial scaffolds, which elicits an initial inflammatory/resorptive response by macrophages/osteoclasts prior to bone formation by MSCs/osteoblasts [63]. It is therefore also of interest to consider the cytokines in HPL that may be involved in the regulation of osteoclastic activity. The most consistently reported of these are RANTES/CCL5 and associated cytokines, monocyte chemotactic protein-1 (MCP-1/CCL2), macrophage inflammatory protein 1 (MIP-1α/CCL3 and MIP-β/CCL4), and macrophage migration inhibitory factor (MIF). All of these

Fig. 6 Morphology and proliferation kinetics of BMSCs in HPL from PCs stored for 0–4 months (m). **a** Morphology of BMSCs at passage 2 (representative images from one donor), scale bar 100 μm. **b** Proliferation kinetics over three serial passages (P1–3) and DNA content after 7 and 14 days (d). Data represent means ± SD (*n* = ≥ 4 donors). PD, population doubling rate; CPD, cumulative population doublings; PDT, population doubling time
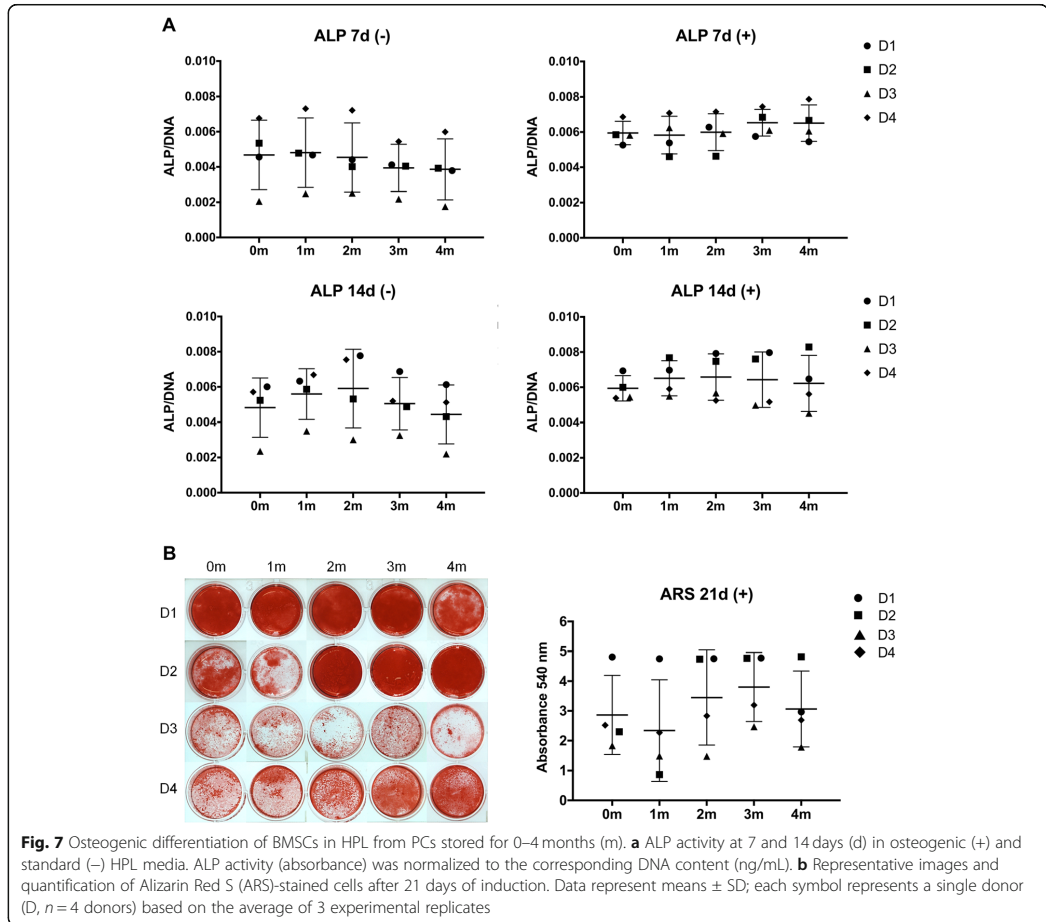
have been implicated in the recruitment and differentiation of osteoclasts and/or their precursors [64–66]. Moreover, it has been demonstrated that RANTES secreted by osteoclasts promotes the migration of osteoblasts and MSCs in vitro [64, 67, 68] and mineralization in vivo [68, 69].

In addition to GFs and chemokines, a number of inflammatory cytokines were identified in the HPL herein. The evidence for the effects of inflammatory cytokines on MSCs is conflicting since these effects appear to be (a) tissue/site-specific, (b) MSC type-specific, and (c) dose-dependent, based on which a particular cytokine may exert pro- or anti-inflammatory and pro- or anti-osteogenic effects [54]. The most commonly reported of these are TNF-α and IL-1, predominant during the acute inflammatory phase of healing. The combination of HPL and exogenous IL-1α was shown to result in a transient increase in the inflammatory response accompanied by an increase in proliferation, without loss of differentiation potential, in human osteoblasts [70] and ASCs [71]. Interferon-γ (IFN-γ), another major pro-inflammatory cytokine, has consistently more anti-osteogenic effects [54]. Nevertheless, several studies have reported

advantages of "pre-conditioning" MSCs with IFN-γ, either alone or in combination with other cytokines such as TNF-α and IL-1, in terms of their immunomodulatory and regenerative potential [72].

Recent studies have reported differences in MSC proliferation and osteogenic differentiation when cultured in different HPL formulations, expressing differences in their protein compositions [15, 73]. MSC proliferation, i.e., PD rate/time, is considered a "key parameter" during ex vivo expansion [11], and ALP and mineralization assays are routinely used to test the in vitro osteogenic capacity of MSCs. In the context of BTE, the in vitro PD time and ALP activity of MSCs are reported to most likely correlate with their in vivo mineralization capacity [74]. Accordingly, in the present study, the growth kinetics and osteogenic potential of BMSCs were tested in HPLs produced from the different PC storage times; BMSCs from multiple donors were used to account for donor-related variations. No significant differences were observed between the different PC storage times in terms of either BMSC proliferation or ALP activity/mineralization. However, considerable donor-related variation was observed in relation to the latter. Notably, the highest relative mean ALP activity and mineralization, with the

Fig. 7 Osteogenic differentiation of BMSCs in HPL from PCs stored for 0–4 months (m). **a** ALP activity at 7 and 14 days (d) in osteogenic (+) and standard (−) HPL media. ALP activity (absorbance) was normalized to the corresponding DNA content (ng/mL). **b** Representative images and quantification of Alizarin Red S (ARS)-stained cells after 21 days of induction. Data represent means ± SD; each symbol represents a single donor (D, $n = 4$ donors) based on the average of 3 experimental replicates

least inter-donor variation, was observed in the 3-month PC storage group. The results herein are consistent with a recent study reporting on MSCs from a similar donor cohort (healthy young patients), which reported large inter-donor variations in xenogeneic MSCs [17]. It is well-known that several biological (age, sex), behavioral (alcohol/tobacco use), and disease-related (obesity, diabetes) factors influence MSC properties including proliferation and osteogenic differentiation [75]. Nevertheless, it must be acknowledged that the observed donor variation may have confounded the detection of significant differences between PC storage times in the present study.

Among various aspects of HPL production which require standardization is the storage time of the source material, i.e., PCs produced by blood establishments. Current recommendations call for blood centers to freeze outdated PCs (within 7 days of collection) for later

HPL production, although "the maximum period time that PCs can be used after expiry to prepare an efficient HPL for cell expansion is unknown" [9]. International blood authorities advise a minimum interval of 3 months between blood donations to allow for repeated viral testing to minimize the risk of disease transmission via platelet products. In the context of HPL, this is especially relevant when smaller PC-pool sizes are used (≤ 16 donors) and where pathogen reduction is not applied [6]. In the present study, HPL produced from PCs stored for > 4 months showed a significant deterioration of several cytokines relevant for MSCs. No significant differences between PC storage times < 4 months were observed in terms of HPL cytokine concentrations, i.e., a clear trend for cytokine deterioration with time, or corresponding MSC proliferation and osteogenic differentiation. Thus, the data herein did not allow for the

detection of any statistical associations between specific HPL cytokines and the degree of MSC osteogenic differentiation. Nevertheless, our observation that outdated PCs can be safely frozen for up to 4 months (preferably 3 months when the focus is BTE) may facilitate the implementation of routines enabling more blood banks to produce HPL. This would address the need for standardization and scaling-up of HPL production, while also benefiting blood bank economies.

Conclusions
The expansion of human MSCs in HPL represents a favorable strategy for BTE. MSCs expanded in HPL demonstrate a high in vitro osteogenic differentiation potential, albeit with considerable donor variation. Exactly which components of HPL contribute to enhancing the osteogenic potential of MSCs is unclear, since HPL contains a complex mixture of cytokines, chemokines, and inflammatory mediators presenting with synergistic effects. Based on the proteomic analysis herein, further investigation of the role of certain cytokines, particularly SCGF, in the regulation of MSCs' osteogenic differentiation is warranted. Finally, a maximum frozen storage time of 4 months is recommended for outdated PCs assigned for HPL production at blood establishments.

Supplementary information
Supplementary information accompanies this paper at https://doi.org/10.1186/s13287-020-01863-9.

Additional file 1 : Supplementary Table 1. Real-time PCR assays. **Supplementary Table 2**. Multiplex human cytokine screening panel. **Supplementary Figure 1**. Immunophenotype of BMSCs and ASCs in FBS and HPL. **Supplementary Figure 2**. Cytokine concentrations in HPL.

Abbreviations
BTE: Bone tissue engineering; MSCs: Mesenchymal stromal cells; BMSCs: Bone marrow-derived mesenchymal stromal cells; ASCs: Adipose tissue-derived mesenchymal stromal cells; SVF: Stromal vascular fraction; GMP: Good manufacturing practice; FBS: Fetal bovine serum; HPL: Human platelet lysate; PCs: Platelet concentrates; qPCR: Quantitative real-time polymerase chain reaction; ELISA: Enzyme-linked immunosorbent assay; ALP: Alkaline phosphatase; GFs: Growth factors; PD: Population doubling rate; PDT: Population doubling time; CPD: Cumulative population doubling

Authors' contributions
S.S. designed the study, performed the experiments, analyzed the data, and drafted the manuscript. S.M.A., T.H.F.L., and S.S. contributed to the design, experiments, data analysis, and manuscript writing. A.I.B., T.H., and K.M. contributed to the design, data analysis, and manuscript writing. The authors read and approved the final manuscript.

Author details
[1]Department of Clinical Dentistry, Faculty of Medicine, University of Bergen, Årstadveien 19, 5008 Bergen, Norway. [2]Department of Immunology and Transfusion Medicine, Haukeland University Hospital, Bergen, Norway. [3]Laboratory of Immunology and Transfusion Medicine, Haugesund Hospital, Fonna Health Trust, Haugesund, Norway. [4]Department of Clinical Science, University of Bergen, Bergen, Norway.

References
1. Shanbhag S, Suliman S, Pandis N, Stavropoulos A, Sanz M, Mustafa K. Cell therapy for orofacial bone regeneration: a systematic review and meta-analysis. J Clin Periodontol. 2019;46(Suppl 21):162–82.
2. Prins HJ, Schulten EAJM, Ten Bruggenkate CM, Klein-Nulend J, Helder MN. Bone regeneration using the freshly isolated autologous stromal vascular fraction of adipose tissue in combination with calcium phosphate ceramics. Stem Cell Transl Med. 2016;5(10):1362–74.
3. Karnieli O, Friedner OM, Allickson JG, Zhang N, Jung S, Fiorentini D, et al. A consensus introduction to serum replacements and serum-free media for cellular therapies. Cytotherapy. 2017;19(2):155–69.
4. Shanbhag S, Stavropoulos A, Suliman S, Hervig T, Mustafa K. Efficacy of humanized mesenchymal stem cell cultures for bone tissue engineering: a systematic review with a focus on platelet derivatives. Tissue Eng Part B Rev. 2017;23(6):552–69.
5. Mendicino M, Bailey AM, Wonnacott K, Puri RK, Bauer SR. MSC-based product characterization for clinical trials: an FDA perspective. Cell Stem Cell. 2014;14(2):141–5.
6. Bieback K, Fernandez-Munoz B, Pati S, Schafer R. Gaps in the knowledge of human platelet lysate as a cell culture supplement for cell therapy: a joint publication from the AABB and the International Society for Cell & Gene Therapy. Transfusion. 2019;59(11):3448–60.
7. European Medicines Agency. Guideline on the use of bovine serum in the manufacture of human biological medicinal products. EMA/CHMP/BWP/457920/2012 rev 1. Amsterdam: European Medicines Agency; 2013.
8. Phinney DG, Galipeau J, Msc Committee of the International Society of C, Gene T. Manufacturing mesenchymal stromal cells for clinical applications: a survey of good manufacturing practices at U.S. academic centers. Cytotherapy. 2019;21(7):782–92.
9. Schallmoser K, Henschler R, Gabriel C, Koh MBC, Burnouf T. Production and quality requirements of human platelet lysate: a position statement from the working party on cellular therapies of the International Society of Blood Transfusion. Trends Biotechnol. 2020;38(1):13–23.
10. Burnouf T, Strunk D, Koh MB, Schallmoser K. Human platelet lysate: replacing fetal bovine serum as a gold standard for human cell propagation? Biomaterials. 2016;76:371–87.
11. Rojewski MT, Lotfi R, Gjerde C, Mustafa K, Veronesi E, Ahmed AB, et al. Translation of a standardized manufacturing protocol for mesenchymal

stromal cells: a systematic comparison of validation and manufacturing data. Cytotherapy. 2019;21(4):468–82.

12. Henschler R, Gabriel C, Schallmoser K, Burnouf T, Koh MBC. Human platelet lysate current standards and future developments. Transfusion. 2019;59(4): 1407–13.

13. Strunk D, Lozano M, Marks DC, Loh YS, Gstraunthaler G, Schennach H, et al. International Forum on GMP-grade human platelet lysate for cell propagation. Vox Sang. 2018;113(1):e1–e25.

14. Strunk D, Lozano M, Marks DC, Loh YS, Gstraunthaler G, Schennach H, et al. International Forum on GMP-grade human platelet lysate for cell propagation: summary. Vox Sang. 2018;113(1):80–7.

15. Boraldi F, Burns JS, Bartolomeo A, Dominici M, Quaglino D. Mineralization by mesenchymal stromal cells is variously modulated depending on commercial platelet lysate preparations. Cytotherapy. 2018;20(3):335–42.

16. Schallmoser K, Strunk D. Generation of a pool of human platelet lysate and efficient use in cell culture. Methods Mol Biol. 2013;946:349–62.

17. Mohamed-Ahmed S, Fristad I, Lie SA, Suliman S, Mustafa K, Vindenes H, et al. Adipose-derived and bone marrow mesenchymal stem cells: a donor-matched comparison. Stem Cell Res Ther. 2018;9(1):168.

18. Dominici M, Le Blanc K, Mueller I, Slaper-Cortenbach I, Marini F, Krause D, et al. Minimal criteria for defining multipotent mesenchymal stromal cells. The International Society for Cellular Therapy position statement. Cytotherapy. 2006;8:315–7.

19. Szklarczyk D, Gable AL, Lyon D, Junge A, Wyder S, Huerta-Cepas J, et al. STRI NG v11: protein-protein association networks with increased coverage, supporting functional discovery in genome-wide experimental datasets. Nucleic Acids Res. 2019;47(D1):D607–D13.

20. Munir A, Døskeland A, Avery SJ, Fuoco T, Mohamed-Ahmed S, Lygre H, et al. Efficacy of copolymer scaffolds delivering human demineralised dentine matrix for bone regeneration. J Tissue Eng. 2019;10: 2041731419852703.

21. Fekete N, Gadelorge M, Furst D, Maurer C, Dausend J, Fleury-Cappellesso S, et al. Platelet lysate from whole blood-derived pooled platelet concentrates and apheresis-derived platelet concentrates for the isolation and expansion of human bone marrow mesenchymal stromal cells: production process, content and identification of active components. Cytotherapy. 2012;14(5):540–54.

22. Bieback K, Hecker A, Kocaomer A, Lannert H, Schallmoser K, Strunk D, et al. Human alternatives to fetal bovine serum for the expansion of mesenchymal stromal cells from bone marrow. Stem Cells. 2009;27(9):2331–41.

23. Suliman S, Ali HRW, Karlsen TA, Amiaud J, Mohamed-Ahmed S, Layrolle P, et al. Impact of humanised isolation and culture conditions on stemness and osteogenic potential of bone marrow derived mesenchymal stromal cells. Sci Rep. 2019;9(1):16031.

24. Gronthos S, Graves SE, Ohta S, Simmons PJ. The STRO-1+ fraction of adult human bone marrow contains the osteogenic precursors. Blood. 1994; 84(12):4164–73.

25. Xu L, Liu Y, Sun Y, Wang B, Xiong Y, Lin W, et al. Tissue source determines the differentiation potentials of mesenchymal stem cells: a comparative study of human mesenchymal stem cells from bone marrow and adipose tissue. Stem Cell Res Ther. 2017;8(1):275.

26. Fennema EM, Tchang LAH, Yuan H, van Blitterswijk CA, Martin I, Scherberich A, et al. Ectopic bone formation by aggregated mesenchymal stem cells from bone marrow and adipose tissue: a comparative study. J Tissue Eng Regen Med. 2018;12(1):e150–e8.

27. Brocher J, Janicki P, Voltz P, Seebach E, Neumann E, Mueller-Ladner U, et al. Inferior ectopic bone formation of mesenchymal stromal cells from adipose tissue compared to bone marrow: rescue by chondrogenic pre-induction. Stem Cell Res. 2013;11(3):1393–406.

28. Brennan MA, Renaud A, Guilloton F, Mebarki M, Trichet V, Sensebé L, et al. Inferior in vivo osteogenesis and superior angiogenesis of human adipose-derived stem cells compared with bone marrow-derived stem cells cultured in xeno-free conditions. Stem Cell Transl Med. 2018;7(3):315.

29. Castren E, Sillat T, Oja S, Noro A, Laitinen A, Konttinen YT, et al. Osteogenic differentiation of mesenchymal stromal cells in two-dimensional and three-dimensional cultures without animal serum. Stem Cell Res Ther. 2015;6:167.

30. Li CY, Wu XY, Tong JB, Yang XX, Zhao JL, Zheng QF, et al. Comparative analysis of human mesenchymal stem cells from bone marrow and adipose tissue under xeno-free conditions for cell therapy. Stem Cell Res Ther. 2015;6:55.

31. Xia W, Li H, Wang Z, Xu R, Fu Y, Zhang X, et al. Human platelet lysate supports ex vivo expansion and enhances osteogenic differentiation of

human bone marrow-derived mesenchymal stem cells. Cell Biol Int. 2011; 35(6):639–43.

32. Chevallier N, Anagnostou F, Zilber S, Bodivit G, Maurin S, Barrault A, et al. Osteoblastic differentiation of human mesenchymal stem cells with platelet lysate. Biomaterials. 2010;31(2):270–8.

33. Kuterbekov M, Machillot P, Baillet F, Jonas AM, Glinel K, Picart C. Design of experiments to assess the effect of culture parameters on the osteogenic differentiation of human adipose stromal cells. Stem Cell Res Ther. 2019; 10(1):256.

34. Shansky YD, Sergeeva NS, Sviridova IK, Karalkin PA, Kirsanova VA, Akhmedova SA, et al. Human platelet lysate sustains the osteogenic/ adipogenic differentiation potential of adipose-derived mesenchymal stromal cells and maintains their DNA integrity in vitro. Cells Tissues Organs. 2019;207(3–4):149–64.

35. Cowper M, Frazier T, Wu X, Curley L, Ma MH, Mohuiddin OA, et al. Human platelet lysate as a functional substitute for fetal bovine serum in the culture of human adipose derived stromal/stem cells. Cells. 2019;8(7):724.

36. Mangum LH, Natesan S, Stone R 2nd, Wrice NL, Larson DA, Florell KF, et al. Tissue source and cell expansion condition influence phenotypic changes of adipose-derived stem cells. Stem Cells Int. 2017;2017:7108458.

37. Horn P, Bokermann G, Cholewa D, Bork S, Walenda T, Koch C, et al. Impact of individual platelet lysates on isolation and growth of human mesenchymal stromal cells. Cytotherapy. 2010;12(7):888–98.

38. Copland IB, Garcia MA, Waller EK, Roback JD, Galipeau J. The effect of platelet lysate fibrinogen on the functionality of MSCs in immunotherapy. Biomaterials. 2013;34(32):7840–50.

39. Renn TY, Kao YH, Wang CC, Burnouf T. Anti-inflammatory effects of platelet biomaterials in a macrophage cellular model. Vox Sang. 2015;109(2):138–47.

40. Canestrari E, Steidinger HR, McSwain B, Charlebois SJ, Dann CT. Human platelet lysate media supplement supports lentiviral transduction and expansion of human T lymphocytes while maintaining memory phenotype. J Immunol Res. 2019;2019:3616120.

41. Sovkova V, Vocetkova K, Rampichova M, Mickova A, Buzgo M, Lukasova V, et al. Platelet lysate as a serum replacement for skin cell culture on biomimetic PCL nanofibers. Platelets. 2018;29(4):395–405.

42. Viau S, Lagrange A, Chabrand L, Lorant J, Charrier M, Rouger K, et al. A highly standardized and characterized human platelet lysate for efficient and reproducible expansion of human bone marrow mesenchymal stromal cells. Cytotherapy. 2019;21(7):738–54.

43. Christensen C, Jonsdottir-Buch S, Sigurjonsson O. Effects of amotosalen treatment on human platelet lysate bioactivity; 2019.

44. Laner-Plamberger S, Oeller M, Mrazek C, Hartl A, Sonderegger A, Rohde E, et al. Upregulation of mitotic bookmarking factors during enhanced proliferation of human stromal cells in human platelet lysate. J Transl Med. 2019;17(1):432.

45. Ozaki Y, Nishimura M, Sekiya K, Suehiro F, Kanawa M, Nikawa H, et al. Comprehensive analysis of chemotactic factors for bone marrow mesenchymal stem cells. Stem Cells Dev. 2007;16(1):119–29.

46. Fekete N, Rojewski MT, Lotfi R, Schrezenmeier H. Essential components for ex vivo proliferation of mesenchymal stromal cells. Tissue Eng Part C Methods. 2014;20(2):129–39.

47. Yue R, Shen B, Morrison SJ. Clec11a/osteolectin is an osteogenic growth factor that promotes the maintenance of the adult skeleton. Elife. 2016;5:e18782.

48. Ito C, Sato H, Ando K, Watanabe S, Yoshiba F, Kishi K, et al. Serum stem cell growth factor for monitoring hematopoietic recovery following stem cell transplantation. Bone Marrow Transpl. 2003;32(4):391–8.

49. Chaboya C. Elucidating the signaling pathways for the c-type lectin clec11a in human mesenchymal stromal cells. Sacramento: California State University; 2019.

50. Kristensen LP, Chen L, Nielsen MO, Qanie DW, Kratchmarova I, Kassem M, et al. Temporal profiling and pulsed SILAC labeling identify novel secreted proteins during ex vivo osteoblast differentiation of human stromal stem cells. Mol Cell Proteomics. 2012;11(10):989–1007.

51. Grabarek J, Groopman JE, Lyles YR, Jiang S, Bennett L, Zsebo K, et al. Human kit ligand (stem cell factor) modulates platelet activation in vitro. J Biol Chem. 1994;269(34):21718–24.

52. Matsumoto T, Ii M, Nishimura H, Shoji T, Mifune Y, Kawamoto A, et al. Lnk-dependent axis of SCF-cKit signal for osteogenesis in bone fracture healing. J Exp Med. 2010;207(10):2207–23.

53. Ruangsawasdi N, Zehnder M, Patcas R, Ghayor C, Siegenthaler B, Gjoksi B, et al. Effects of stem cell factor on cell homing during functional pulp

Shanbhag *et al. Stem Cell Research & Therapy*   (2020) 11:351

Page 18 of 18

regeneration in human immature teeth. Tissue Eng Part A. 2017;23(3–4): 115–23.

54. Deshpande S, James AW, Blough J, Donneys A, Wang SC, Cederna PS, et al. Reconciling the effects of inflammatory cytokines on mesenchymal cell osteogenic differentiation. J Surg Res. 2013;185(1):278–85.

55. Massberg S, Konrad I, Schurzinger K, Lorenz M, Schneider S, Zohlnhoefer D, et al. Platelets secrete stromal cell-derived factor 1alpha and recruit bone marrow-derived progenitor cells to arterial thrombi in vivo. J Exp Med. 2006; 203(5):1221–33.

56. Kitaori T, Ito H, Schwarz EM, Tsutsumi R, Yoshitomi H, Oishi S, et al. Stromal cell-derived factor 1/CXCR4 signaling is critical for the recruitment of mesenchymal stem cells to the fracture site during skeletal repair in a mouse model. Arthritis Rheum. 2009;60(3):813–23.

57. Hosogane N, Huang Z, Rawlins BA, Liu X, Boachie-Adjei O, Boskey AL, et al. Stromal derived factor-1 regulates bone morphogenetic protein 2-induced osteogenic differentiation of primary mesenchymal stem cells. Int J Biochem Cell Biol. 2010;42(7):1132–41.

58. Liu H, Li M, Du L, Yang P, Ge S. Local administration of stromal cell-derived factor-1 promotes stem cell recruitment and bone regeneration in a rat periodontal bone defect model. Mater Sci Eng C Mater Biol Appl. 2015;53: 83–94.

59. Yang F, Xue F, Guan J, Zhang Z, Yin J, Kang Q. Stromal-cell-derived factor (SDF) 1-alpha overexpression promotes bone regeneration by osteogenesis and angiogenesis in osteonecrosis of the femoral head. Cell Physiol Biochem. 2018;46(6):2561–75.

60. Ando Y, Ishikawa J, Fujio M, Matsushita Y, Wakayama H, Hibi H, et al. Stromal cell-derived factor-1 accelerates bone regeneration through multiple regenerative mechanisms. J Oral Maxillofac Surg Med Pathol. 2019; 31(4):245–50.

61. Huang J, Chi H, Chi H, Qiu L, Wang Y, Qiu Z, et al. Stromal cell-derived factor 1 promotes cell migration to enhance bone regeneration after hypoxic preconditioning. Tissue Eng Part A. 2019;25(17–18):1300–9.

62. Haumer A, Bourgine PE, Occhetta P, Born G, Tasso R, Martin I. Delivery of cellular factors to regulate bone healing. Adv Drug Deliv Rev. 2018;129:285–94.

63. Gamblin AL, Brennan MA, Renaud A, Yagita H, Lezot F, Heymann D, et al. Bone tissue formation with human mesenchymal stem cells and biphasic calcium phosphate ceramics: the local implication of osteoclasts and macrophages. Biomaterials. 2014;35(36):9660–7.

64. Yano S, Mentaverri R, Kanuparthi D, Bandyopadhyay S, Rivera A, Brown EM, et al. Functional expression of beta-chemokine receptors in osteoblasts: role of regulated upon activation, normal T cell expressed and secreted (RANT ES) in osteoblasts and regulation of its secretion by osteoblasts and osteoclasts. Endocrinology. 2005;146(5):2324–35.

65. Kim MS, Magno CL, Day CJ, Morrison NA. Induction of chemokines and chemokine receptors CCR2b and CCR4 in authentic human osteoclasts differentiated with RANKL and osteoclast like cells differentiated by MCP-1 and RANTES. J Cell Biochem. 2006;97(3):512–8.

66. Onodera S, Sasaki S, Ohshima S, Amizuka N, Li M, Udagawa N, et al. Transgenic mice overexpressing macrophage migration inhibitory factor (MIF) exhibit high-turnover osteoporosis. J Bone Miner Res. 2006;21(6):876–85.

67. Ponte AL, Marais E, Gallay N, Langonne A, Delorme B, Herault O, et al. The in vitro migration capacity of human bone marrow mesenchymal stem cells: comparison of chemokine and growth factor chemotactic activities. Stem Cells. 2007;25(7):1737–45.

68. Liu YC, Kao YT, Huang WK, Lin KY, Wu SC, Hsu SC, et al. CCL5/RANTES is important for inducing osteogenesis of human mesenchymal stem cells and is regulated by dexamethasone. Biosci Trends. 2014;8(3):138–43.

69. Lee JS, Lee JB, Cha JK, Choi EY, Park SY, Cho KS, et al. Chemokine in inflamed periodontal tissues activates healthy periodontal-ligament stem cell migration. J Clin Periodontol. 2017;44(5):530–9.

70. Ruggiu A, Ulivi V, Sanguineti F, Cancedda R, Descalzi F. The effect of platelet lysate on osteoblast proliferation associated with a transient increase of the inflammatory response in bone regeneration. Biomaterials. 2013;34(37): 9318–30.

71. Romaldini A, Mastrogiacomo M, Cancedda R, Descalzi F. Platelet lysate activates human subcutaneous adipose tissue cells by promoting cell proliferation and their paracrine activity toward epidermal keratinocytes. Front Bioeng Biotechnol. 2018;6:203.

72. Noronha NC, Mizukami A, Caliári-Oliveira C, Cominal JG, JLM R, Covas DT, et al. Priming approaches to improve the efficacy of mesenchymal stromal cell-based therapies. Stem Cell Res Ther. 2019;10(1):131.

73. Juhl M, Tratwal J, Follin B, Sondergaard RH, Kirchhoff M, Ekblond A, et al. Comparison of clinical grade human platelet lysates for cultivation of mesenchymal stromal cells from bone marrow and adipose tissue. Scand J Clin Lab Invest. 2016;76(2):93–104.

74. Janicki P, Boeuf S, Steck E, Egermann M, Kasten P, Richter W. Prediction of in vivo bone forming potency of bone marrow-derived human mesenchymal stem cells. Eur Cell Mater. 2011;21:488–507.

75. Widholz B, Tsitlakidis S, Reible B, Moghaddam A, Westhauser F. Pooling of patient-derived mesenchymal stromal cells reduces inter-individual confounder-associated variation without negative impact on cell viability, proliferation and osteogenic differentiation. Cells. 2019;8(6):633.

Publisher's Note

Supplementary table 1: Real-time PCR assays

Gene	TaqMan® Assay ID	Amplicon length
GAPDH	Hs 02758991_g1	93
RUNX2	Hs01047973_m1	86
BMP2	Hs00154192_m1	60
ALPL	Hs01029144_m1	79
COL1A2	Hs00164099_m1	68
SPP1	Hs00959010_m1	84
BGLAP	Hs01587814_g1	138

GAPDH glyceraldehyde 3-phosphate dehydrogenase, *RUNX2* runt-related transcription factor 2, *BMP2* Bone morphogenetic protein 2, *ALPL* alkaline phosphatase, *COL1A2* Collagen type 1, *SPP1* Osteopontin, *BGLAP* Osteocalcin

Supplementary table 2: Multiplex human cytokine screening panel

| Abbreviation	Cytokine
b-FGF	Basic fibroblast growth factor
Eotaxin/CCL11	C-C chemokine 11
G-CSF	Granulocyte colony stimulating factor
GM-CSF	Granulocyte-macrophage colony-stimulating factor
IFN-γ	Interferon-γ
IL-1β	Interleukin-1β
IL-1ra	Interleukin 1 receptor antagonist
IL-1α	Interleukin-1α
IL-2Rα	Interleukin-2 receptor α
IL-3	Interleukin-3
IL-12 (p40)	Interleukin-12 subunit beta
IL-16	Interleukin-16
IL-2	Interleukin-2
IL-4	Interleukin-4
IL-5	Interleukin-5
IL-6	Interleukin-6
IL-7	Interleukin-7
IL-8	Interleukin-8
IL-9	Interleukin-9
GRO-α/CXCL1	CXC ligand 1
HGF	Hepatocyte growth factor
IFN-α2	Interferon-α2
LIF	Leukemia inhibitory factor
MCP-3/CCL7	Monocyte chemotactic protein-3
IL-10	Interleukin-10
IL-12 (p70)	Interleukin-12
IL-13	Interleukin-13
IL-15	Interleukin-15
IL-17A	Interleukin-17
IL-18	Interleukin-18
IP-10/CXCL10	Interferon gamma-induced protein 10/CXC chemokine 10
MCP-1/CCL2	Monocyte Chemoattractant Protein-1
MIG/CXCL9	Monokine induced by gamma interferon/CXC ligand 9
β-NGF	Nerve growth factor
SCF/KITLG	Stem cell factor/KIT-ligand
SCGF-β	Stem cell growth factor
SDF-1α/CXCL12	Stromal cell-derived factor 1
MIP-1α/CCL3	Macrophage inflammatory protein
MIP-1β/CCL4	Macrophage inflammatory protein
PDGF-BB	Platelet-derived growth factor-BB
RANTES/CCL5	Regulated on activation, normal T cell expressed and secreted
TNF-α	Tumor Necrosis Factor-α
TNF-β	Tumor necrosis factor-β
VEGF	Vascular endothelial growth factor
CTACK/CCL27	Cutaneous T-Cell Attracting Chemokine
MIF	Macrophage migration inhibitory factor
TRAIL	TNF-related apoptosis-inducing ligand
M-CSF	Macrophage colony-stimulating factor

Supplementary Figure 1: Immunophenotype of BMSCs and ASCs in FBS and HPL

Representative histograms from the flow cytometry analysis of one donor showing surface expression of (A) positive and negative stromal markers, and (B) STRO-1. Expression of stained cells *(red)* and corresponding antibody controls *(blue)*.

Supplementary Figure 2: Cytokine concentrations in HPL
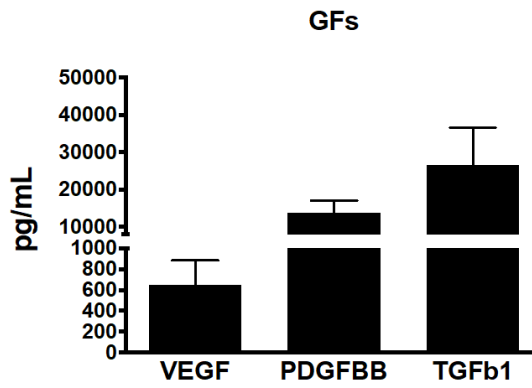
Growth factor (GF) concentrations in HPL determined by ELISA. Data represent means $\pm$ SD (n=$\geq$3 batches)

Paper III

Xeno-free spheroids of human gingiva-derived progenitor cells for bone tissue engineering.

Shanbhag S, Suliman S, Bolstad AI, Stavropoulos A, Mustafa K.

Xeno-Free Spheroids of Human Gingiva-Derived Progenitor Cells for Bone Tissue Engineering

Siddharth Shanbhag[1]*, Salwa Suliman[1], Anne Isine Bolstad[1], Andreas Stavropoulos[2,3] and Kamal Mustafa[1]*

[1] Department of Clinical Dentistry, Faculty of Medicine, University of Bergen, Bergen, Norway, [2] Department of Periodontology, Faculty of Odontology, Malmö University, Malmö, Sweden, [3] Division of Regenerative Medicine and Periodontology, University Clinics of Dental Medicine, University of Geneva, Geneva, Switzerland

Gingiva has been identified as a minimally invasive source of multipotent progenitor cells (GPCs) for use in bone tissue engineering (BTE). To facilitate clinical translation, it is important to characterize GPCs in xeno-free cultures. Recent evidence indicates several advantages of three-dimensional (3D) spheroid cultures of mesenchymal stromal cells (MSCs) over conventional 2D monolayers. The present study aimed to characterize human GPCs in xeno-free 2D cultures, and to test their osteogenic potential in 3D cultures, in comparison to bone marrow MSCs (BMSCs). Primary GPCs and BMSCs were expanded in human platelet lysate (HPL) or fetal bovine serum (FBS) and characterized based on *in vitro* proliferation, immunophenotype and multi-lineage differentiation. Next, 3D spheroids of GPCs and BMSCs were formed via self-assembly and cultured in HPL. Expression of stemness- (SOX2, OCT4, NANOG) and osteogenesis-related markers (BMP2, RUNX2, OPN, OCN) was assessed at gene and protein levels in 3D and 2D cultures. The cytokine profile of 3D and 2D GPCs and BMSCs was assessed via a multiplex immunoassay. Monolayer GPCs in both HPL and FBS demonstrated a characteristic MSC-like immunophenotype and multi-lineage differentiation; osteogenic differentiation of GPCs was enhanced in HPL vs. FBS. CD271$^+$ GPCs in HPL spontaneously acquired a neuronal phenotype and strongly expressed neuronal/glial markers. 3D spheroids of GPCs and BMSCs with high cell viability were formed in HPL media. Expression of stemness- and osteogenesis-related genes was significantly upregulated in 3D vs. 2D GPCs/BMSCs; the latter was independent of osteogenic induction. Synthesis of SOX2, BMP2 and OCN was confirmed via immunostaining, and *in vitro* mineralization via Alizarin red staining. Finally, secretion of several growth factors and chemokines was enhanced in GPC/BMSC spheroids, while that of pro-inflammatory cytokines was reduced, compared to monolayers. In summary, monolayer GPCs expanded in HPL demonstrate enhanced osteogenic differentiation potential, comparable to that of BMSCs. Xeno-free spheroid culture further enhances stemness- and osteogenesis-related gene expression, and cytokine secretion in GPCs, comparable to that of BMSCs.

Keywords: platelet lysate, mesenchymal stromal cells, gingival stem cells, spheroid culture, bone tissue engineering, regenerative medicine

fbioe-08-00968   August 17, 2020   Time: 16:41   # 2

Shanbhag et al.   Xeno-Free Spheroids of Gingival Progenitor Cells

INTRODUCTION

Adult mesenchymal stromal cells (MSCs) are increasingly being used in bone tissue engineering (BTE) for the reconstruction of clinically challenging bone defects. MSCs were originally identified in the bone marrow (BMSCs), and these are still the most frequently tested cells in clinical studies (Friedenstein et al., 1968; Pittenger et al., 2019). However, the yield of BMSCs obtained from the marrow mononuclear cell fraction is relatively low ($\leq$0.01%) (Pittenger et al., 1999). Moreover, considerable donor-related variations in BMSCs, in addition to the morbidity associated with bone marrow harvesting, have prompted the investigation of 'MSC-like' cells from other, relatively less invasive, tissue sources (Mohamed-Ahmed et al., 2018; Wilson et al., 2019).

Oral tissues, such as dental pulp, mucosa, periodontal ligament (PDL) and gingiva, represent alternative sources of 'MSC-like' progenitor cells (Sharpe, 2016). Gingiva, in particular, can be harvested with minimal morbidity and rapid scarless healing, and is reported to contain a subpopulation of multipotent progenitor cells (GPCs) (Fournier et al., 2010; Mitrano et al., 2010). GPCs demonstrate the characteristic MSC-phenotype, immunomodulatory properties, and multi-lineage differentiation, possibly owing to their neural crest origins (Xu et al., 2013). Notably, GPCs have demonstrated superior properties in comparison to other MSCs in vitro (Yang et al., 2013; Sun et al., 2019), and the ability to regenerate bone in vivo (Wang et al., 2011; Ge et al., 2012). However, in all of these studies, GPCs were cultured in xenogeneic media.

A critical aspect in the clinical translation of MSC-based therapies is the use of safe and standardized culture conditions. Although commonly used for MSC expansion, several limitations of xenogeneic fetal bovine serum (FBS) supplementation have been highlighted, and current recommendations from health authorities advocate the use of 'xeno-free' protocols whenever possible (Bieback et al., 2019). Accordingly, xeno-free alternatives to FBS, such as human platelet lysate (HPL), have emerged (Shanbhag et al., 2017). HPL is shown to be comparable, and often superior, to FBS for the proliferation and multi-lineage differentiation of MSCs from various tissues (Burnouf et al., 2016). Moreover, MSCs expanded in HPL demonstrate enhanced osteoblastic differentiation, suggesting particular benefits for BTE (Shanbhag et al., 2017). However, no studies have yet reported on HPL-cultured GPCs.

In order to obtain clinically relevant cell numbers, current strategies demand the large-scale ex vivo expansion of MSCs, most commonly via plastic adherent/monolayer culture. However, this two-dimensional (2D) culture system is not representative of the 3D in vivo microenvironment (Sart et al., 2014; Petrenko et al., 2017). Moreover, expansion of MSCs via serial passaging in plastic-adherent cultures may alter their phenotype and diminish their regenerative and immunomodulatory potential (Follin et al., 2016; Ghazanfari et al., 2017). In contrast, the self-assembly or spontaneous aggregation of MSCs into 3D structures, mediated by unique cell-cell and cell-extracellular matrix (ECM) interactions, biomechanical cues and signaling pathways, more closely simulates their in vivo microenvironment or niche (Ahmadbeigi et al., 2012; Sart et al., 2014). The cytoskeletal changes induced by 3D culture have also been linked to 'mesenchymal cell condensation' (MCC) – a critical event during embryonic skeletal development via endochondral ossification, which can be recapitulated ex vivo (Hall and Miyake, 2000; Kale et al., 2000; Facer et al., 2005; Kim and Adachi, 2019).

While a majority of the literature is focused on BMSCs, 3D cultures have also been reported to enhance the survival, stemness, paracrine/immunomodulatory activity, and multi-lineage differentiation of oral tissue-derived MSCs (Zhang et al., 2012; Lee et al., 2017; Moritani et al., 2018; Subbarayan et al., 2018). However, few studies have characterized MSC spheroids in xeno-free cultures to facilitate clinical translation (Ylostalo et al., 2017; Dong et al., 2019). Therefore, the objectives of the present study were to establish xeno-free monolayer (2D) cultures of human GPCs in HPL, and subsequently, to test their osteogenic potential in 3D spheroid cultures in comparison to BMSCs.

MATERIALS AND METHODS

Monolayer (2D) Cell Culture

GPCs were isolated as previously described (Fournier et al., 2010). Briefly, human gingival biopsies were collected after ethical approval (Regional Ethical Committee-North, Norway, 2016-1266) and informed consent from systemically healthy patients aged 18–31 years ($n = 5$) undergoing surgery at the Department of Clinical Dentistry, University of Bergen, Bergen, Norway. From each donor, primary connective tissue-explant cultures of GPCs were established in 5% HPL (Bergenlys®, Bergen, Norway) and 10% FBS (GE Healthcare, South Logan, UT, United States) supplemented growth media [Dulbecco's Modified Eagle's medium (DMEM, Invitrogen, Carlsbad, CA, United States) with 1% antibiotics (penicillin/streptomycin; GE Healthcare)]. BMSCs (from different patients) were isolated and cultured in HPL media as previously described (Mohamed-Ahmed et al., 2018). Details of HPL production are provided in the **Supplementary data**. Cells were sub-cultured and expanded in their respective growth media in humidified 5% CO_2 at 37°C; passage 2–4 cells from at least three different donors were used in experiments. Proliferation of GPCs in HPL and FBS over 7 days was determined via an alamar blue assay (Invitrogen); at each time point, 10% vol. dye was added to the cells, incubated for 4 h and fluorescence was measured (540 Ex/590 Em).

Immunophenotype of 2D GPCs

The immunophenotype of HPL- and FBS-cultured GPCs was assessed by flow cytometry based on expression of specific surface antigens according to the "minimal criteria" for defining MSCs (Dominici et al., 2006). Briefly, cells in HPL and FBS were incubated with conjugated antibodies against selected 'negative' (CD34, CD45, HLA-DR) and 'positive' (CD73, CD90, CD105) MSC markers, and additionally CD271 (all from BD Biosciences, San Jose, CA, United States), following the manufacturers' recommendations. Quantification was performed with a BD LSR Fortessa analyzer and fluorescence activated cell sorting (FACS)

of CD271$^+$ GPCs with a BD FACS Aria sorter (both from BD Biosciences). Data were analyzed using flow cytometry software (Flowjo v10, Flowjo, LLC, Ashland, OR, United States).

Gene Expression in 2D GPCs

The expression of adipogenesis- and osteogenesis-related genes (**Supplementary Table 1**) in HPL- and FBS-cultured GPCs after 7 days in the appropriate induction media (see below), was assessed via quantitative real-time polymerase chain reaction (qPCR) using TaqMan® real-time PCR assays (Thermo Fisher Scientific, Carlsbad, CA, United States). RNA extraction and cDNA synthesis were performed as previously described (Mohamed-Ahmed et al., 2018). The expressions of the genes of interest were normalized to that of glyceraldehyde 3-phosphate dehydrogenase (GAPDH). Data were analyzed by the $\Delta\Delta Ct$ method and results are presented as fold changes in HPL groups relative to FBS groups.

Adipogenic Differentiation of 2D GPCs

The ability of GPCs to differentiate into multiple stromal lineages was tested as previously described (Mohamed-Ahmed et al., 2018). Briefly, for adipogenic differentiation, cells in HPL and FBS were cultured in StemPro® adipogenic differentiation medium (Invitrogen) or standard growth medium (control). After 21 days, cells were fixed with 4% paraformaldehyde (PFA) for 10 min at RT and intracellular lipid formation was assessed via Oil red O staining (Sigma-Aldrich, St. Louis, MO, United States).

Osteogenic Differentiation of 2D GPCs

For osteogenic differentiation, cells in HPL and FBS were cultured in osteogenic differentiation medium prepared by adding final concentrations of 0.05 mM L-ascorbic acid 2-phosphate, 10 nM dexamethasone and 10 mM β glycerophosphate (all from Sigma-Aldrich) to the respective growth media. After 21 days, cells were fixed and extracellular calcium deposition was evaluated via Alizarin red S staining (Sigma-Aldrich). The osteogenic potential of HPL-cultured GPCs was also tested on previously validated poly(L-lactide-co-ε-caprolactone) [poly(LLA-co-CL)] copolymer scaffolds (Yassin et al., 2017) (10^6 cells/scaffold); HPL-cultured BMSCs were used as a reference. Cell attachment and spreading on the scaffolds after 24 h was observed via scanning electron microscopy (SEM; Jeol JSM 7400F, Tokyo, Japan), as previously described (Yassin et al., 2017). After 14 days of induction, Alizarin red S staining was performed as described above. In all differentiation experiments, corresponding non-induced HPL- and/or FBS-cultured cells served as controls.

Neurogenic Differentiation and Immunofluorescence (IF) Staining of 2D GPCs

Since FACS isolated CD271$^+$ GPCs showed a neuronal-like morphology, the expression of neuronal [βIII-tubulin (TUJ1)] and glial markers [glial fibrillary acidic protein (GFAP)] was assessed via IF staining. Briefly, cells were fixed with PFA, permeabilized with 0.1% Triton X-100 and blocked with 10% goat serum in phosphate-buffered saline (PBS; Invitrogen). Cells were incubated with primary antibodies; mouse monoclonal anti-TUJ1 (Abcam, Cambridge, United Kingdom, dilution 1:100) and chicken monoclonal anti-GFAP (Abcam, dilution 1:100) overnight at 4°C. Corresponding secondary antibodies were incubated for 1 h at RT (Thermo Fisher Scientific, dilution 1:200). After washing with PBS, the nuclei were stained with 4′,6-diamidino-2-phenylindole (DAPI) (Sigma-Aldrich, dilution 1:2000). Imaging was performed using a confocal microscope (Andor Dragonfly, Oxford Instruments, Abingdon, United Kingdom).

3D Spheroid Culture

Formation of GPC and BMSC spheroids was assessed via two methods: mesenspheres (Isern et al., 2013) and aggregates (Baraniak and McDevitt, 2012). Briefly, dissociated passage 1–2 monolayer GPCs and BMSCs in HPL media were seeded (1000 cells/cm^2) in low-attachment dishes (Corning®, Corning, NY, United States) for 7 days to obtain mesenspheres, or in microwell-patterned 24-well plates (Sphericalplate®, Kugelmeiers Ltd, Erlenbach, CH) for 24 h to obtain spheroid aggregates of 1000–2000 cells. The novel design of these microwell plates was optimized for embryoid body formation (Silin, 2012). Since aggregate spheroids could be formed more predictably than mesenspheres, only the former were used in subsequent experiments. Cell viability in spheroids was assessed after 7 days via a live/dead assay (Thermo Fisher Scientific). Hereafter, the terms 2D or monolayer culture and 3D or spheroid culture are used interchangeably throughout the manuscript.

Gene Expression and Osteogenic Differentiation in 3D Spheroids

The expression of pluripotency/stemness-related genes (**Supplementary Table 1**) was assessed in 3D and 2D GPCs and BMSCs after 7 days of suspension and adherent culture, respectively, via qPCR. Similarly, the expression of osteogenesis-related genes (**Supplementary Table 1**) was assessed after 7 days in standard (non-induced) and osteogenically induced cultures (as described above). Gene expression experiments were performed using spheroids and monolayers generated from both independent and pooled donor-cells and data are presented as fold changes in 3D groups relative to 2D groups. Protein expression of osteogenic markers was determined after 14 days via IF (see below). Alizarin red S staining was performed after 21 days to detect mineralization in induced and non-induced spheroids and monolayers; spheroids were stained in suspension, and following paraffin embedding and histological sectioning (3–5 μm).

IF Staining in 3D Spheroids

The protein expression of stemness [sex determining region Y-box 2 (SOX2)] and osteogenic markers [bone morphogenetic protein 2 (BMP2), osteocalcin (OCN)] was assessed in GPC and BMSC spheroids after 10 or 14 days of suspension culture via IF staining. The primary antibodies rabbit polyclonal anti-SOX2 (Abcam, dilution 1:1000), mouse monoclonal anti-BMP2 (Bio-Techne, Abingdon, United Kingdom, dilution 1:100), and rabbit polyclonal anti-OCN (Abcam, dilution 1:100) were incubated ON at 4°C. Corresponding secondary antibodies were incubated for 1 h at RT (Thermo Fisher Scientific; dilution 1:200), and

nuclei were stained with DAPI (Sigma-Aldrich; dilution 1:2000) before imaging with a confocal microscope (Andor Dragonfly). Cell autofluorescence and non-specific staining was confirmed in control samples incubated with neither or only secondary antibodies, respectively (data not shown).

Multiplex Cytokine Assay

Conditioned media (CM) from 2D and 3D GPCs and BMSCs were collected after 48 h culture in HPL-free medium and the concentrations of several cytokines (**Supplementary Table 2**) were measured using a custom multiplex assay and a Bio-Plex® 200 System (both from Bio-Rad Laboratories, CA, United States), according to the manufacturer's instructions. Although the initial number of cells seeded in 2D and 3D cultures was the same, to account for differences in the rates of cell proliferation between the conditions, cytokine concentrations (pg/mL) were normalized to the corresponding total DNA (ng/mL). DNA quantification was performed using the Quant-IT® PicoGreen dsDNA Assay Kit (Thermo Fisher Scientific) according to the manufacturer's instructions.

Statistical Analysis

Statistical analyses were performed using GraphPad Prism v 8.0 (GraphPad Software, San Diego, CA, United States). Data are presented as means ($\pm$ SD), unless specified. Analyses of gene expression data are based on delta-CT values and results are presented as relative (log/non-linear) fold changes using scatter plots. Multiplex proteomic data are presented on a logarithmic ($\log_{10}$) scale. All other linear data are presented as bar graphs. Normality testing was performed via the Shapiro–Wilk test. The student t-test, Mann–Whitney U-test or one-way analysis of variance (ANOVA followed by a *post hoc* Tukey's test for multiple comparisons), were applied as appropriate, and $p < 0.05$ was considered statistically significant.

RESULTS

Characterization of 2D GPCs

GPCs demonstrating characteristic plastic adherence and fibroblastic morphology were isolated from gingiva explants in both HPL- and FBS-media. GPCs in HPL appeared smaller and more spindle-shaped, especially in early passages (**Figure 1A**), and demonstrated a higher proliferation rate ($p < 0.05$) (**Figure 1B**). Both HPL- and FBS-expanded GPCs demonstrated a characteristic MSC phenotype, i.e., > 95% of the cells were positive for CD73, CD90 and CD105, and < 5% of the cells expressed the hematopoietic markers CD34 and CD45; HLA-DR expression was < 8% (**Figure 1C**). Expression of CD271 was observed in < 5% of GPCs in both conditions.

Adipogenic Differentiation of 2D GPCs

GPCs in both HPL and FBS demonstrated the capacity to differentiate into adipocytes. The expression of genes associated with adipogenic differentiation, peroxisome proliferator-activated receptor-gamma (PPARG) and lipoprotein lipase (LPL), was significantly upregulated in HPL- vs. FBS-cultured

GPCs after 7 days of adipogenic induction; LPL was also upregulated in non-induced HPL-cultured GPCs ($p < 0.05$; **Figure 1D**). Accumulation of intracellular lipid vesicles after 21 days was confirmed via Oil red O staining of GPCs in both conditions (**Figure 1E**). No differentiation of control cells was observed in the standard growth media.

Osteogenic Differentiation of 2D GPCs

GPCs in both HPL and FBS demonstrated the capacity to differentiate into osteoblasts. Genes associated with both early [runt-related transcription factor 2 (RUNX2), alkaline phosphatase (ALP)] and late osteogenic differentiation [collagen I (COL1), osteocalcin (OCN/BGLAP)] were upregulated in HPL- vs. FBS-cultured GPCs after 7 days; these genes were also upregulated in non-induced HPL-cultured GPCs ($p < 0.05$; **Figure 1D**). Extracellular calcium deposition was confirmed via Alizarin red S staining after 21 days; greater calcium deposition was observed in HPL-cultured GPCs (**Figure 1E**). Next, the osteogenic differentiation of HPL-cultured GPCs was tested on copolymer scaffolds in comparison to that of BMSCs. Cell attachment and spreading on the scaffold surface was confirmed after 24 h via SEM. After 14 days of osteogenic induction the entire scaffold surface was covered with mineralized matrix as revealed by Alizarin red S staining; staining was comparable between GPCs and BMSCs (**Supplementary Figure 1**).

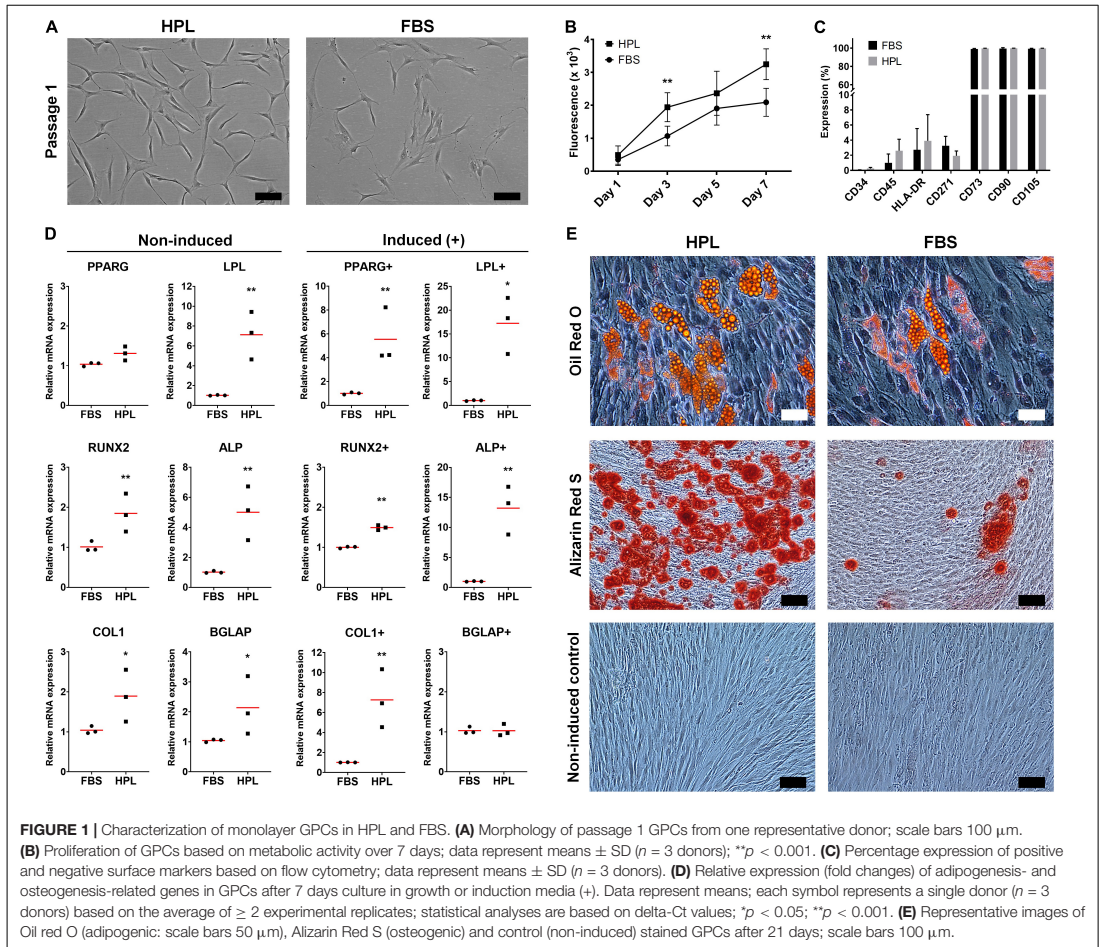### Neurogenic Differentiation of 2D GPCs

To investigate whether CD271 represents a marker to enrich osteogenic cells, CD271$^+$ GPCs in HPL and FBS media were isolated via FACS. Interestingly, these cells acquired a neuronal morphology, which was more evident in HPL- than FBS-cultures (**Figure 2A**). Subsequently, IF staining revealed an abundant expression of neuronal (TUJ1) and glial markers (GFAP) in HPL-cultured CD271$^+$ GPCs, while only a few FBS-cultured cells appeared to express these markers (**Figure 2B**).

Formation and Viability of 3D Spheroids

3D spheroids of GPCs and BMSCs were formed as menspheres or aggregates in HPL media (**Figure 3A**). Since the former method relies on the self-renewal capacity of individual cells, the size and shape of mesenspheres varied considerably ($\phi < 100$ μm) and the frequency of sphere formation was low; sphere formation in GPCs was considerably lower than in BMSCs. In contrast to mesenspheres, highly consistent spheroids of GPCs and BMSCs were obtained via spontaneous aggregation in microwells ($\sim$1000 cells/spheroid, ϕ 100–300 μm; **Figure 3B**). Viability of a majority of cells within the aggregate spheroids was confirmed via live/dead staining (**Figure 3C**).

Gene Expression and Osteogenic Differentiation in 3D Spheroids

The expression of stemness- and osteogenesis-related genes was assessed in 3D and 2D GPCs and BMSCs after 7 days of suspension culture. SOX2 and octamer-binding transcription factor 4 (OCT4) were significantly upregulated in GPC/BMSC spheroids vs. monolayers ($p < 0.05$); nanog homeobox factor (NANOG) was upregulated only in GPC spheroids (**Figure 4A**).

FIGURE 1 | Characterization of monolayer GPCs in HPL and FBS. **(A)** Morphology of passage 1 GPCs from one representative donor; scale bars 100 μm. **(B)** Proliferation of GPCs based on metabolic activity over 7 days; data represent means ± SD (n = 3 donors); $^{**}p < 0.001$. **(C)** Percentage expression of positive and negative surface markers based on flow cytometry; data represent means ± SD (n = 3 donors). **(D)** Relative expression (fold changes) of adipogenesis- and osteogenesis-related genes in GPCs after 7 days culture in growth or induction media (+). Data represent means; each symbol represents a single donor (n = 3 donors) based on the average of ≥ 2 experimental replicates; statistical analyses are based on delta-Ct values; $^{*}p < 0.05$; $^{**}p < 0.001$. **(E)** Representative images of Oil red O (adipogenic: scale bars 50 μm), Alizarin Red S (osteogenic) and control (non-induced) stained GPCs after 21 days; scale bars 100 μm.

A relatively higher degree of gene upregulation was observed in spheroids of GPCs as compared to BMSCs. SOX2 and OCT4 were also upregulated in independent donor GPC and BMSC spheroids (**Supplementary Figure 2A**). Expression of SOX2 in 3D GPCs and BMSCs was confirmed via IF staining (**Figure 4B**).

With regards to osteogenesis, genes associated with both early (BMP2) and late stages [OCN/BGLAP, osteopontin (OPN/SPP1)] of osteogenic differentiation were upregulated in 3D GPCs and BMSCs ($p < 0.05$) (**Figure 5A**); RUNX2 was upregulated in independent donor, but not pooled, spheroids (**Supplementary Figure 2B**). In contrast to stemness-related genes, a relatively higher degree of upregulation of osteogenesis-related genes was observed in 3D BMSCs as compared to GPCs. With regards to the effects of osteogenic induction, although BMP2, OPN and OCN were also significantly upregulated in 3D GPCs and BMSCs vs. monolayers after 7 days of osteogenic induction, upregulation of these genes was relatively higher in

non-induced spheroids (**Figure 5A**). Protein expression of BMP2 and OCN after 14 days was confirmed via IF staining (**Figure 5B**, **Supplementary Figure 3**); expression of BMP2 was further confirmed via western blotting (**Supplementary Figure 4**).

After 21 days of osteogenic induction, 3D and 2D GPCs and BMSCs were positively stained for mineral deposition with Alizarin red (**Figure 6A**). In 2D cultures, the staining appeared to be marginally more intense in BMSCs, while in 3D cultures, the staining appeared comparable between GPC and BMSC spheroids. Mineral staining within the core of the spheroids was confirmed via histology, revealing a mature and organized ECM (**Figure 6B**).

Cytokine Profile of 3D Spheroids

The concentrations of various growth factors, chemokines and inflammatory cytokines (**Supplementary Table 2**) were measured in the 48 h CM of spheroid and monolayer
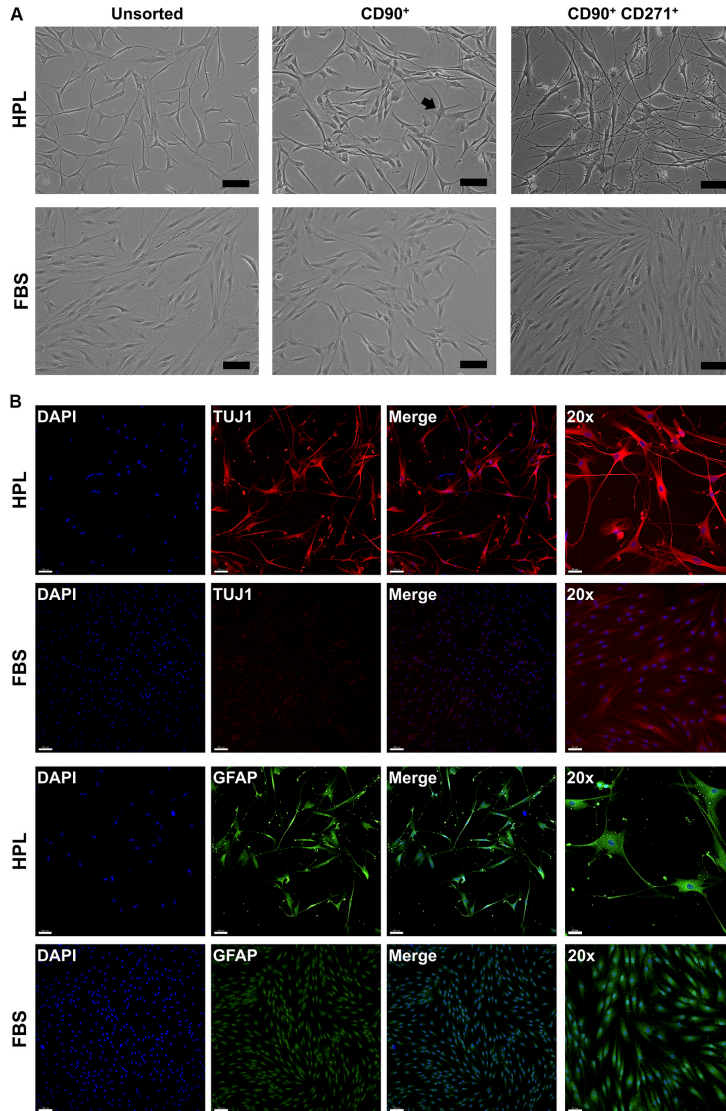
FIGURE 2 | Characterization of CD271$^+$ GPCs. **(A)** Selection of CD271$^+$ GPCs via FACS revealed a neuronal morphology in HPL-, but not FBS-cultured cells; *unsorted* cells represent the total plastic adherent gingival cell population; CD90 was used as a 'reference' marker (some cells with neuronal morphology are visible – *arrow*); scale bars 100 μm. **(B)** IF staining for βIII-tubulin (TUJ1) and GFAP in CD271$^+$ GPCs; scale bars 100 μm (50 μm for 20× images).

GPCs and BMSCs. Several growth factors (FGF2, PDGF-BB, TGF-β1, HGF, SCF, GCSF) were elevated in spheroid cultures; VEGF was elevated in GPC, but not BMSC spheroids (**Figure 6**). Notably, both spheroid and monolayer GPCs and BMSCs produced high concentrations of SCGF-β. A number of chemokines (CCL2, CCL3, CCL4, CCL5/RANTES, LIF,

MIF) were also elevated in the CM of spheroid GPCs, while others (CCL11, CXCL10, CXCL12) were higher in monolayers; CXCL1 was markedly elevated in the CM of BMSC spheroids. Interestingly, several pro-inflammatory cytokines (IL-1α, 1IL-1β, IL-2, TNF-α, IFN-γ) were downregulated in the CM of GPC and BMSC spheroids, while IL-8 was markedly
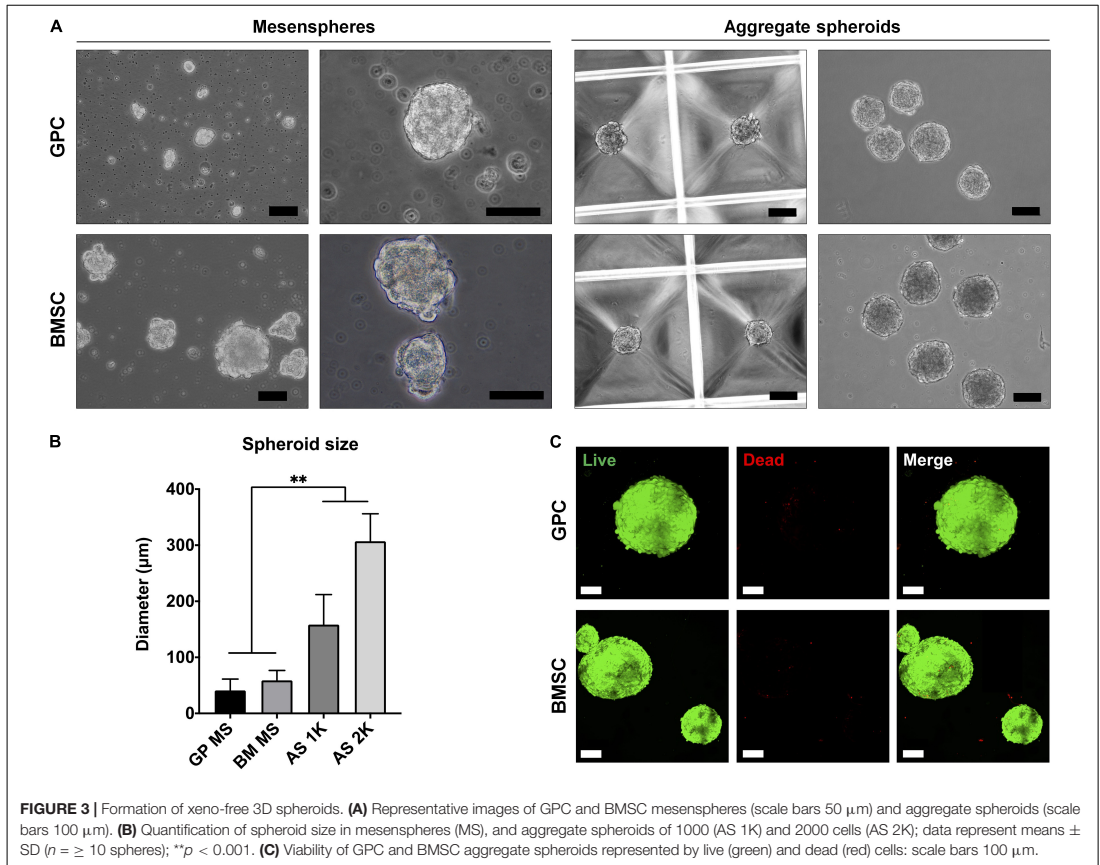
FIGURE 3 | Formation of xeno-free 3D spheroids. **(A)** Representative images of GPC and BMSC mesenspheres (scale bars 50 μm) and aggregate spheroids (scale bars 100 μm). **(B)** Quantification of spheroid size in mesenspheres (MS), and aggregate spheroids of 1000 (AS 1K) and 2000 cells (AS 2K); data represent means ± SD ($n = \geq 10$ spheres); $**p < 0.001$. **(C)** Viability of GPC and BMSC aggregate spheroids represented by live (green) and dead (red) cells: scale bars 100 μm.
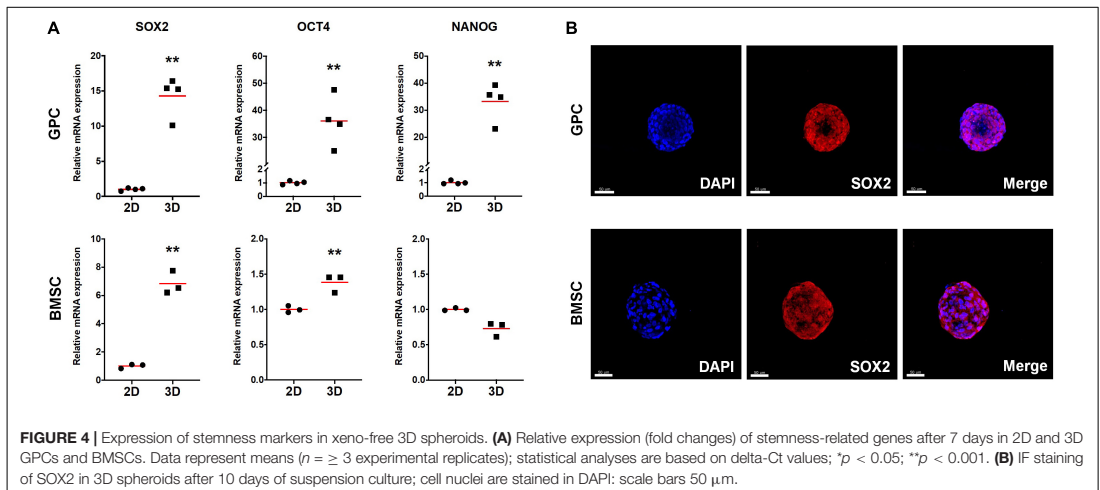

FIGURE 4 | Expression of stemness markers in xeno-free 3D spheroids. **(A)** Relative expression (fold changes) of stemness-related genes after 7 days in 2D and 3D GPCs and BMSCs. Data represent means ($n = \geq 3$ experimental replicates); statistical analyses are based on delta-Ct values; $*p < 0.05$; $**p < 0.001$. **(B)** IF staining of SOX2 in 3D spheroids after 10 days of suspension culture; cell nuclei are stained in DAPI: scale bars 50 μm.
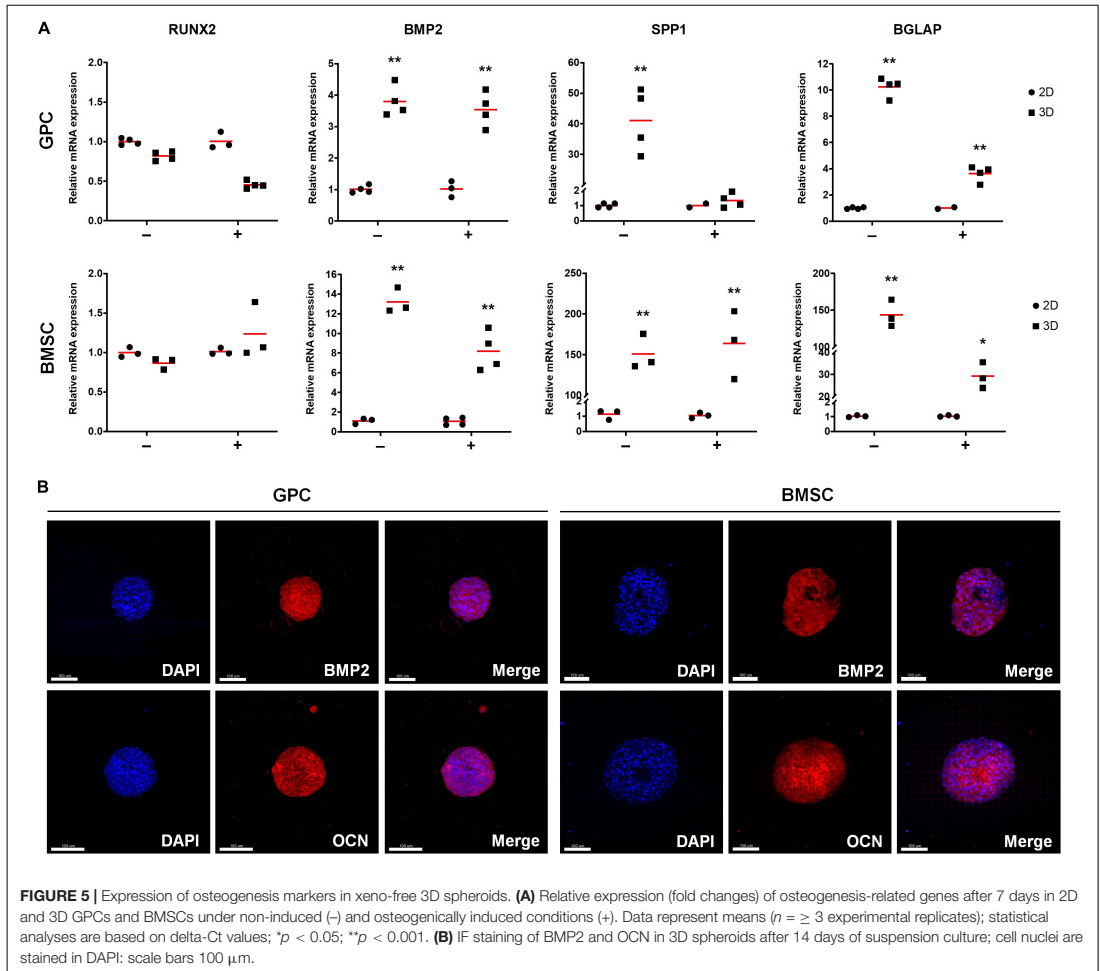
FIGURE 5 | Expression of osteogenesis markers in xeno-free 3D spheroids. **(A)** Relative expression (fold changes) of osteogenesis-related genes after 7 days in 2D and 3D GPCs and BMSCs under non-induced (–) and osteogenically induced conditions (+). Data represent means ($n = \geq 3$ experimental replicates); statistical analyses are based on delta-Ct values; $^*p < 0.05$; $^{**}p < 0.001$. **(B)** IF staining of BMP2 and OCN in 3D spheroids after 14 days of suspension culture; cell nuclei are stained in DAPI: scale bars 100 µm.

elevated, especially in BMSCs. The anti-inflammatory IL-10 was upregulated in monolayers in both GPCs and BMSCs (**Figure 7**).

DISCUSSION

Gingiva represents a minimally invasive source of multipotent progenitor cells (GPCs) with promising potential for BTE (Wang et al., 2011). To facilitate the clinical translation of GPCs, it is important to characterize their properties in xeno-free cultures compliant with current Good Manufacturing Practices (cGMP). Although previous studies have reported xeno-free culture of cells from other oral tissues using HPL (Naveau et al., 2011; Chen et al., 2012; Wu et al., 2017), to our knowledge, no studies have yet reported on HPL-cultured GPCs. In the present study, GPCs from matched donors were cultured in HPL- or FBS-supplemented media, thus allowing true and standardized comparisons between xeno-free and xenogeneic cultured cells. Overall, the GPCs herein demonstrated superior proliferation and osteogenic differentiation in HPL-supplemented media.

Monolayer GPCs demonstrated a 'classical' MSC-immunophenotype (Dominici et al., 2006) with no remarkable differences between HPL- and FBS-cultured cells. However, the specificity of the 'classical' surface markers to identify true MSC fractions in heterogeneous cell populations, especially those not derived from bone marrow, has been questioned (Halfon et al., 2011; Lv et al., 2014). CD271 or low-affinity nerve growth factor receptor (LNGFR) is reportedly a more specific marker for isolating a primitive subset of BMSCs with high clonogenicity and multi-lineage, specifically osteogenic, differentiation potential (Cuthbert et al., 2015). Osteogenic enrichment has also
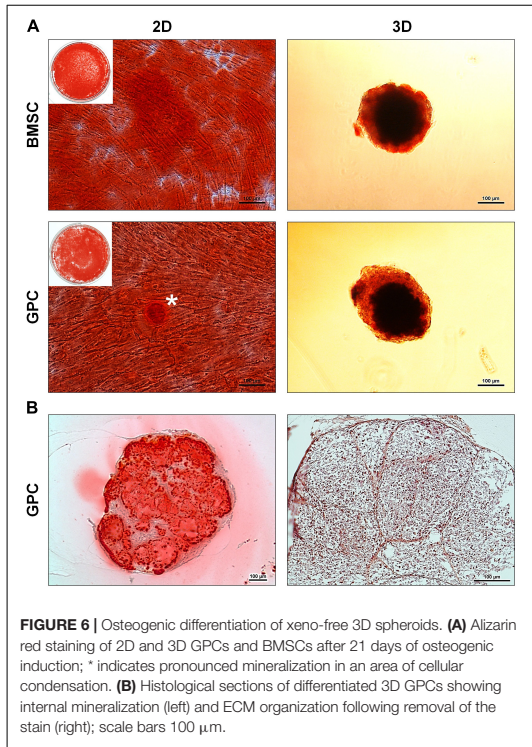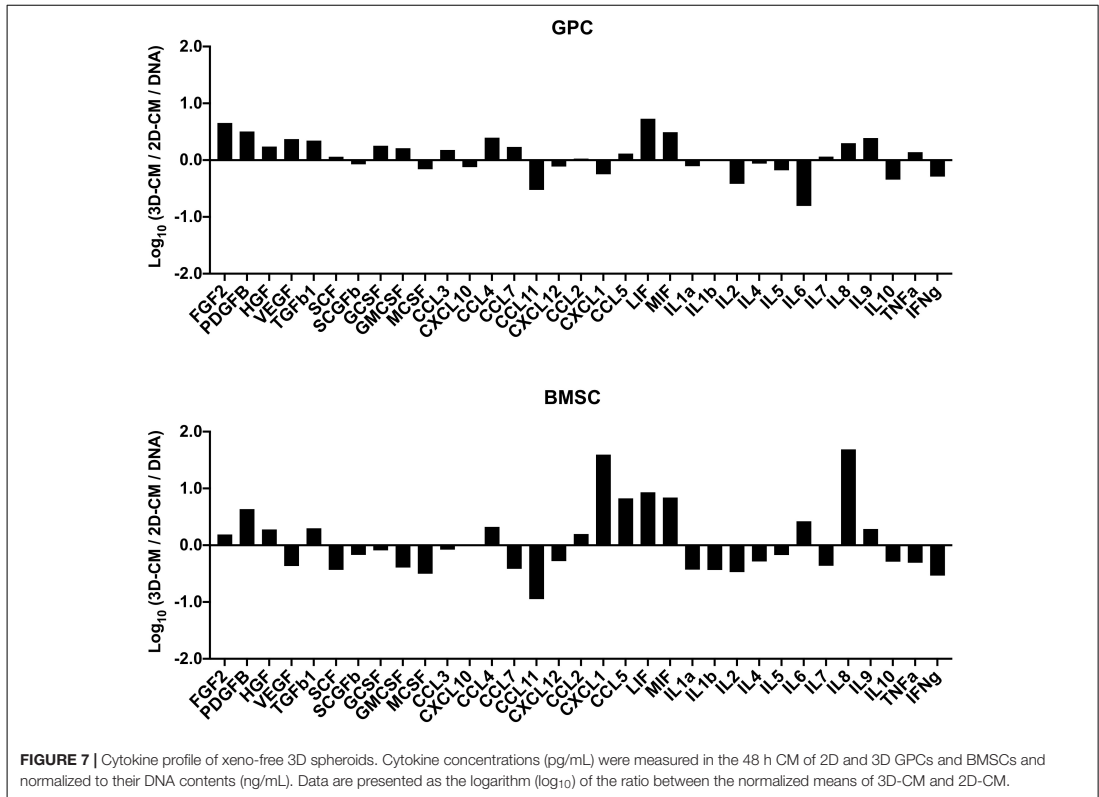
FIGURE 6 | Osteogenic differentiation of xeno-free 3D spheroids. **(A)** Alizarin red staining of 2D and 3D GPCs and BMSCs after 21 days of osteogenic induction; * indicates pronounced mineralization in an area of cellular condensation. **(B)** Histological sections of differentiated 3D GPCs showing internal mineralization (left) and ECM organization following removal of the stain (right); scale bars 100 μm.

been reported in CD271$^+$ subsets (< 5%) of dental pulp (DPCs) (Alvarez et al., 2015a) and PDL cells (PDLCs) (Alvarez et al., 2015b). Indeed, a small fraction (1–3%) of CD271$^+$ cells was identified in HPL- and FBS-cultured GPCs herein. Interestingly, these cells acquired a neuronal-like morphology; cells in HPL appeared more differentiated with limited proliferation capacity and more homogenous expression of neuronal/glial markers vs. FBS-cultured cells. Indeed, CD271 is reported to be a marker of neural stem/progenitor cells (van Strien et al., 2014). Moreover, craniofacial tissues, including gingiva, have a neural crest origin and therefore contain a subpopulation of cells with the capacity for neurogenic differentiation (Xu et al., 2013). Previous studies have reported the neuronal differentiation of unsorted GPCs when stimulated with neurogenic supplements (Subbarayan et al., 2017; Gugliandolo et al., 2019), although which fraction of the total GPC population actually differentiated, and to what extent, is unclear. Based on the findings herein, the CD271+ GPCs may represent a subpopulation with a propensity for neurogenic differentiation, which is further enhanced in HPL culture. In context, a recent study reported enhanced survival and differentiation of neuronal precursor cells in HPL (Nebie et al., 2020). However, further research is needed to confirm the phenotype and neurogenic potential of CD271+ GPCs.

Concerning multi-lineage differentiation, both HPL- and FBS-cultured monolayer GPCs could be differentiated into adipocytes and osteoblasts *in vitro*. The osteogenic differentiation of GPCs was significantly enhanced in HPL vs. FBS cultures at early and terminal stages, as revealed by gene expression and calcium deposition, respectively. Similar findings have been reported in relation to HPL-cultured DPCs (Chen et al., 2012) and PDLCs (Abuarqoub et al., 2015). Interestingly, the expression of osteogenic genes was also upregulated in non-induced HPL-cultured GPCs after 7 days. It may be hypothesized that this upregulation is related to the presence of several cytokines in HPL, which may influence MSCs' osteogenic differentiation (Shanbhag et al., 2017). HPL-cultured GPCs also demonstrated attachment and mineralization on copolymer scaffolds, in a comparable manner to BMSCs, highlighting their relevance for BTE applications. Regarding their *in vivo* mineralization capacity, previous studies have reported variable results using FBS-cultured GPCs, ranging from well- to poorly-mineralized tissues (Fournier et al., 2010; Tomar et al., 2010; Wang et al., 2011; Ge et al., 2012; Yang et al., 2013; Moshaverinia et al., 2014). Whether HPL culture enhances the *in vivo* mineralization of monolayer GPCs, remains to be determined.

To overcome the limitations of traditional 2D/monolayer cultures, several studies have demonstrated the benefits of 3D spheroid cultures in terms of promoting the self-renewal, differentiation and paracrine/immunomodulatory activity of MSCs (Murphy et al., 2014; Sart et al., 2014; Follin et al., 2016). Various methods for spheroid culture have been reported (Sart et al., 2014), and can broadly be categorized as *mensespheres* or *aggregates*. In the *mensespheres* approach, sphere formation occurs via self-renewal of primary non-expanded (Isern et al., 2013) or early-passage expanded MSCs (Kuroda et al., 2010) seeded in low-density non-adherent cultures. These sphere-forming cells represent 'true' stem cells with a capacity for self-renewal and differentiation both *in vitro* and *in vivo* (Basu-Roy et al., 2010; Isern et al., 2013). A small fraction of passage one GPCs herein demonstrated the capacity to form mensespheres in HPL media. However, the frequency of sphere-forming GPCs was low and of a heterogeneous nature compared to that of BMSCs under similar conditions. One explanation for the low frequency of mensespheres could be the media composition; mensespheres have previously only been generated in complex media formulations (Isern et al., 2013) in comparison to the standard HPL media used herein. Nevertheless, obtaining clinically relevant MSC numbers may be challenging with this approach, especially from tissues other than bone marrow.

In contrast to mensespheres, the more common *aggregates* approach utilizes monolayer expanded cells to form 3D spheroids, either via self-assembly (Baraniak and McDevitt, 2012; Bartosh and Ylostalo, 2014) or forced aggregation (Iwasaki et al., 2019). In the present study, aggregate spheroids were generated via 'guided' self-assembly in novel microwell-patterned tissue culture plates – no studies have yet reported this particular micro-well design to generate MSC spheroids. Spheroids with controlled size and morphology were formed after 24 h and showed favorable cell viability with few dead

FIGURE 7 | Cytokine profile of xeno-free 3D spheroids. Cytokine concentrations (pg/mL) were measured in the 48 h CM of 2D and 3D GPCs and BMSCs and normalized to their DNA contents (ng/mL). Data are presented as the logarithm ($\log_{10}$) of the ratio between the normalized means of 3D-CM and 2D-CM.

cells after 7 days in HPL-supplemented media. Self-assembly of cells has been linked to events during organogenesis, e.g., MCC during skeletal development (Hall and Miyake, 2000). MCC is known to be a critical event during endochondral ossification and these condensations represent "the earliest sign of the initiation of a skeletal element or elements" (Hall and Miyake, 2000). Indeed, aggregate cultures are routinely used to induce chondrogenic differentiation of MSCs *in vitro,* and often show signs of 'hypertrophy' suggestive of endochondral ossification. Even in osteogenically differentiated monolayer MSCs, mineral deposition is observed most prominently in regions of high cellular 'confluence' or condensation (**Figure 6**), after prolonged (2–4 weeks) *in vitro* culture (Kaul et al., 2015). Aggregates of MSCs/osteoprogenitors are reported to mimic such condensations *in vitro,* thereby recapitulating embryonic events during endochondral ossification (Kale et al., 2000; Kim and Adachi, 2019). Moreover, the cytoskeletal changes induced by self-assembly of MSCs into 3D structures, as reviewed elsewhere (Sart et al., 2014), induce "epigenetic" changes which enhance their self-renewal and differentiation potential (Guo et al., 2014).

In *pluripotent* embryonic stem cells (ESCs), self-renewal and maintenance of pluripotency are regulated by three main transcription factors – SOX2, OCT4 and NANOG (He et al., 2009). In *multipotent* cells, such as MSCs, these factors are associated with self-renewal (or 'stemness') and maintenance of an undifferentiated cellular state, even in 2D/monolayer cultures (Kolf et al., 2007). In more differentiated 2D cells, e.g., fibroblasts, *ectopic* (over)expression of pluripotency factors triggers cellular reprogramming back to a pluripotent state, as in induced pluripotent stem cells (iPSCs) (He et al., 2009). However, simply changing the microenvironment from 2D to 3D/spheroid culture is known to cause an *intrinsic* upregulation of pluripotency factors in MSCs/osteoprogenitors, suggesting enhanced self-renewal and differentiation potential (Basu-Roy et al., 2010; Guo et al., 2014). Consistently, a significant upregulation of pluripotency factors was observed in 3D vs. 2D GPCs and BMSCs herein. Interestingly, similar observations were recently reported in PDLCs (Moritani et al., 2018) and dermal fibroblasts (Lo et al., 2019). In the latter study, transcriptome analyses revealed differential regulation of 3304 genes in 3D vs. 2D cultures, and the authors concluded that even in naturally heterogeneous populations, such as fibroblasts, the mere shift from a 2D to 3D microenvironment induces gene expression patterns suggestive of "dedifferentiation" or "reprogramming" towards pluripotency

(Lo et al., 2019). Both PDL and gingiva are connective tissues with large fibroblast populations. Indeed, fibroblasts from various tissues, including gingiva, are reportedly indistinguishable from MSCs *in vitro*, based on the current "minimal criteria" (Mostafa et al., 2011; Denu et al., 2016). This identical pattern of pluripotency gene-upregulation further supports the evidence for a certain plasticity between 'MSCs' and more differentiated cells (Ichim et al., 2018). However, whether upregulation of pluripotency factors in 3D spheroids of GPCs directly translates to enhanced *in vivo* survival, requires further investigation.

In addition to pluripotency markers, an upregulation of early (RUNX2, BMP2) and late osteogenesis-related genes (OPN, OCN) was observed in GPC/BMSC spheroids, even in the absence of osteogenic supplements. As already discussed, a similar upregulation of osteogenic genes was observed in non-induced *HPL*-cultured 2D GPCs. However, *post hoc* analyses of *FBS*-cultured GPC spheroids revealed a similar pattern of osteogenic gene upregulation (**Supplementary Figure 5**), suggesting that this was primarily an effect of 3D culture. In context, a recent study reported upregulation of osteogenesis-related genes in FBS-cultured spheroids of murine pre-osteoblastic (MC3T3-E1) cells, where a stronger effect of "cell condensation" than osteogenic induction was highlighted, and attributed to recapitulation of 'MCC-like' events (Kim and Adachi, 2019). BMPs, including BMP2, are known to mediate MCC during skeletal development *in vivo* (Hall and Miyake, 2000), and are also well-established regulators of MSC osteogenic differentiation *in vitro*, via both extrinsic and autocrine signaling (Phimphilai et al., 2006). BMP2 is also reported to be among the most strongly upregulated genes in 3D spheroids of MSCs (Potapova et al., 2007; Cesarz et al., 2016) and other cells, e.g., fibroblasts (Lo et al., 2019). A previous study reported the 'early' *intrinsic* upregulation of BMP2 in FBS-cultured BMSC spheroids, independent of osteogenic induction, which translated to superior *in vitro* ECM production and mineralization vs. 2D BMSCs (Kabiri et al., 2012). The spontaneous upregulation of other bone-related markers (OPN, OCN), along with BMP2, as observed in the GPC/BMSC spheroids herein, further compliments these reports. OPN and OCN are important bone ECM proteins which subsequently undergo mineralization, and their expression is typically associated with later stages of osteogenic differentiation (Liu and Lee, 2013). However, positive staining (Alizarin red) for mineral deposits was only observed in osteogenically induced GPC/BMSC spheroids herein. Indeed, previous studies have reported superior *in vivo* bone regeneration by osteogenically induced spheroids of human BMSCs (Suenaga et al., 2015), DPCs (Lee et al., 2017) and PDLCs (Moritani et al., 2018), vs. monolayers. Thus, it may be hypothesized that MCC-like assemblies induced by spheroid culture *intrinsically* 'prime' MSCs towards osteoblastic commitment, although *extrinsic* signals/supplements may be necessary for terminal differentiation and/or matrix mineralization (Kale et al., 2000; Facer et al., 2005).

It is of relevance to discuss the simultaneous upregulation of pluripotency and osteogenesis-related genes in *in vitro*

3D spheroids, in the context of other literature. A similar observation was reported in a previous study comparing the transcriptome of 2D and 3D BMSCs – genes related to pluripotency (SOX2, OCT4, NANOG) and osteogenesis (BMP2, RUNX2, OPN) were upregulated in 3D BMSCs after 3 days of *in vitro* culture (Potapova et al., 2007). The pluripotency factors SOX2, OCT4 and NANOG are known to mediate somatic cell-reprogramming, and intrinsic BMP-signaling is also involved in the early stages this process (Samavarchi-Tehrani et al., 2010). With regard to 2D MSCs, SOX2 and BMP2 were found to be upregulated in subsets of BMSCs with high self-renewal and differentiation potential (Mareddy et al., 2010). Moreover, in 'reprogrammed' BMSCs (via forced expression of SOX2 or NANOG), osteogenic differentiation is enhanced, reportedly via BMP-signaling (Go et al., 2008; Ogasawara et al., 2013). In 3D MSCs, the switch to spheroid culture (without extrinsic supplements) leads to an epigenetic upregulation of not only the pluripotency factors, but also BMP2. BMPs, including BMP2, are known to mediate MCC *in vivo,* and MSC spheroids are considered to be the *in vitro* counterparts of 'MCC-like' condensations. In the MSC osteogenic differentiation cascade, BMP2 is a potent autocrine regulator of RUNX2, which in turn regulates the downstream expression of osteoblast-specific markers, e.g., OPN and OCN (Liu and Lee, 2013). Indeed, RUNX2, OPN and OCN were found to be upregulated in 3D GPCs and BMSCs herein. Thus, based on the literature, it may be hypothesized that BMP-signaling may act as a 'link' between these two distinct processes, i.e., self-renewal and (osteogenic) lineage commitment (**Supplementary Figure 6**). The co-existence of self-renewing *stem* cells and more-committed *progenitor* cells is a characteristic feature of the stem cell-*niche* (Kolf et al., 2007; He et al., 2009), which appears to be recapitulated in 3D spheroids. However, the role of BMP2 as hypothesized above was not experimentally confirmed herein, and demands further investigation.

Another advantage of 3D culture is the reported enhancement of MSCs' paracrine and immunomodulatory activity (Follin et al., 2016). Emerging concepts in BTE highlight paracrine- and immune-modulation as primary mechanisms for MSC-mediated bone regeneration (Pittenger et al., 2019). Consistent with previous reports (Zhang et al., 2012; Miranda et al., 2019), the secretome of GPC/BMSC spheroids was enriched in terms of upregulation of several growth factors and chemokines/immune-modulatory cytokines, and downregulation of several pro-inflammatory cytokines. This could, at least partly, explain the observed *in vivo* benefits of spheroid MSCs in regeneration and inflammation models (Zhang et al., 2012; Miranda et al., 2019). Moreover, the enrichment of several cytokines implicated in MSC recruitment and osteogenic differentiation, suggests that transplantation of HPL-cultured 3D GPCs, or their CM, may induce a favorable *in vivo* host-response. Indeed, the CM of 2D GPCs expanded in FBS (Qiu et al., 2020) or defined serum-free medium (Diomede et al., 2018) has recently been shown to promote *in vivo* bone regeneration. Interestingly, both 2D and 3D GPCs (and BMSCs) herein, secreted high concentrations of

fbioe-08-00968   August 17, 2020   Time: 16:41   # 12

Shanbhag et al.   Xeno-Free Spheroids of Gingival Progenitor Cells

stem cell growth factor (SCGF) – a protein encoded by the CLEC11A gene, which has been shown to promote osteogenic differentiation and *in vivo* fracture healing in murine MSC-models (Yue et al., 2016). Since high concentrations of SCGF were also detected in HPL (data not shown), this could be another benefit of HPL supplementation for BTE applications. Finally, whether the combination of HPL supplementation and 3D culture enhances the *in vivo* bone regeneration capacity of GPCs, should be investigated in future studies.

CONCLUSION

Monolayer GPCs expanded in HPL vs. FBS demonstrate enhanced *in vitro* osteogenic differentiation, comparable to that of BMSCs. When cultured as 3D spheroids in HPL, both GPCs and BMSCs express significantly higher levels of pluripotency genes as compared to monolayers, suggesting a higher potential for self-renewal. Simultaneously, the expression of osteogenesis-related genes is also significantly increased in GPC and BMSC spheroids, independent of osteogenic induction; *in vitro* mineralization was comparable between GPCs and BMSCs Finally, the secretome of GPC and BMSC spheroids is enriched, in terms of several growth factors, chemokines and immune-modulatory cytokines, in comparison to that of monolayers. In summary, while xeno-free cultured spheroids of GPCs are comparable to BMSCs *in vitro*, GPCs offer the advantage of less-invasive tissue harvesting and are thus promising candidates for BTE applications.

DATA AVAILABILITY STATEMENT

All datasets presented in this study are included in the article/**Supplementary Material**. Additional data can be made available by the authors upon request.

REFERENCES

SUPPLEMENTARY MATERIAL

The Supplementary Material for this article can be found online at: https://www.frontiersin.org/articles/10.3389/fbioe. 2020.00968/full#supplementary-material

Abuarqoub, D., Awidi, A., and Abuharfeil, N. (2015). Comparison of osteo/odontogenic differentiation of human adult dental pulp stem cells and stem cells from apical papilla in the presence of platelet lysate. *Arch. Oral Biol.* 60, 1545–1553. doi: 10.1016/j.archoralbio.2015.07.007

Ahmadbeigi, N., Soleimani, M., Babaeijandaghi, F., Mortazavi, Y., Gheisari, Y., Vasei, M., et al. (2012). The aggregate nature of human mesenchymal stromal cells in native bone marrow. *Cytotherapy* 14, 917–924. doi: 10.3109/14653249. 2012.689426

Alvarez, R., Lee, H. L., Hong, C., and Wang, C. Y. (2015a). Single CD271 marker isolates mesenchymal stem cells from human dental pulp. *Int. J. Oral Sci.* 7, 205–212. doi: 10.1038/ijos.2015.29

Alvarez, R., Lee, H. L., Wang, C. Y., and Hong, C. (2015b). Characterization of the osteogenic potential of mesenchymal stem cells from human periodontal ligament based on cell surface markers. *Int. J. Oral Sci.* 7, 213–219. doi: 10.1038/ ijos.2015.42

Baraniak, P. R., and McDevitt, T. C. (2012). Scaffold-free culture of mesenchymal stem cell spheroids in suspension preserves multilineage potential. *Cell Tissue Res.* 347, 701–711. doi: 10.1007/s00441-011-1215-5

Bartosh, T. J., and Ylostalo, J. H. (2014). Preparation of anti-inflammatory mesenchymal stem/precursor cells (MSCs) through sphere formation using

hanging-drop culture technique. *Curr. Protoc. Stem Cell Biol.* 28:Unit2B.6. doi: 10.1002/9780470151808.sc02b06s28

Basu-Roy, U., Ambrosetti, D., Favaro, R., Nicolis, S. K., Mansukhani, A., and Basilico, C. (2010). The transcription factor Sox2 is required for osteoblast self-renewal. *Cell Death Diff.* 17, 1345–1353. doi: 10.1038/cdd.2010.57

Bieback, K., Fernandez-Munoz, B., Pati, S., and Schafer, R. (2019). Gaps in the knowledge of human platelet lysate as a cell culture supplement for cell therapy: a joint publication from the AABB and the International Society for Cell & Gene Therapy. *Transfusion* 59, 3448–3460. doi: 10.1111/trf.15483

Burnouf, T., Strunk, D., Koh, M. B., and Schallmoser, K. (2016). Human platelet lysate: replacing fetal bovine serum as a gold standard for human cell propagation? *Biomaterials* 76, 371–387. doi: 10.1016/j.biomaterials.2015.10.065

Cesarz, Z., Funnell, J. L., Guan, J., and Tamama, K. (2016). Soft elasticity-associated signaling and bone morphogenic protein 2 are key regulators of mesenchymal stem cell spheroidal aggregates. *Stem Cells Dev.* 25, 622–635. doi: 10.1089/scd. 2015.0356

Chen, B., Sun, H. H., Wang, H. G., Kong, H., Chen, F. M., and Yu, Q. (2012). The effects of human platelet lysate on dental pulp stem cells derived from impacted human third molars. *Biomaterials* 33, 5023–5035. doi: 10.1016/j.biomaterials. 2012.03.057

Cuthbert, R. J., Giannoudis, P. V., Wang, X. N., Nicholson, L., Pawson, D., Lubenko, A., et al. (2015). Examining the feasibility of clinical grade CD271+

Shanbhag et al.   Xeno-Free Spheroids of Gingival Progenitor Cells

enrichment of mesenchymal stromal cells for bone regeneration. *PLoS One* 10:e0117855. doi: 10.1371/journal.pone.0117855

Denu, R. A., Nemcek, S., Bloom, D. D., Goodrich, A. D., Kim, J., Mosher, D. F., et al. (2016). Fibroblasts and mesenchymal stromal/stem cells are phenotypically indistinguishable. *Acta Haematol.* 136, 85–97. doi: 10.1159/000445096

Diomede, F., Gugliandolo, A., Scionti, D., Merciaro, I., Cavalcanti, M. F., Mazzon, E., et al. (2018). Biotherapeutic effect of gingival stem cells conditioned medium in bone tissue restoration. *Int. J. Mol. Sci.* 19:39. doi: 10.3390/ijms19020329

Dominici, M., Le Blanc, K., Mueller, I., Slaper-Cortenbach, I., Marini, F., Krause, D., et al. (2006). Minimal criteria for defining multipotent mesenchymal stromal cells. The International Society for Cellular Therapy position statement. *Cytotherapy* 8, 315–317. doi: 10.1080/14653240600855905

Dong, G., Wang, S., Ge, Y., Deng, Q., Cao, Q., Wang, Q., et al. (2019). Serum-free culture system for spontaneous human mesenchymal stem cell spheroid formation. *Stem Cells Int.* 2019:6041816. doi: 10.1155/2019/6041816

Facer, S. R., Zaharias, R. S., Andracki, M. E., Lafoon, J., Hunter, S. K., and Schneider, G. B. (2005). Rotary culture enhances pre-osteoblast aggregation and mineralization. *J. Dent. Res.* 84, 542–547. doi: 10.1177/154405910508400611

Follin, B., Juhl, M., Cohen, S., Pedersen, A. E., Kastrup, J., and Ekblond, A. (2016). Increased paracrine immunomodulatory potential of mesenchymal stromal cells in three-dimensional culture. *Tissue Eng. Part B Rev.* 22, 322–329. doi: 10.1089/ten.TEB.2015.0532

Fournier, B. P., Ferre, F. C., Couty, L., Lataillade, J. J., Gourven, M., Naveau, A., et al. (2010). Multipotent progenitor cells in gingival connective tissue. *Tissue Eng. Part A* 16, 2891–2899. doi: 10.1089/ten.TEA.2009.0796

Friedenstein, A. J., Petrakova, K. V., Kurolesova, A. I., and Frolova, G. P. (1968). Heterotopic of bone marrow. Analysis of precursor cells for osteogenic and hematopoietic tissues. *Transplantation* 6, 230–247.

Ge, S., Mrozik, K. M., Menicanin, D., Gronthos, S., and Bartold, P. M. (2012). Isolation and characterization of mesenchymal stem cell-like cells from healthy and inflamed gingival tissue: potential use for clinical therapy. *Regen. Med.* 7, 819–832. doi: 10.2217/rme.12.61

Ghazanfari, R., Zacharaki, D., Li, H., Ching Lim, H., Soneji, S., and Scheding, S. (2017). Human primary bone marrow mesenchymal stromal cells and their in vitro progenies display distinct transcriptional profile signatures. *Sci. Rep.* 7:10338. doi: 10.1038/s41598-017-09449-x

Go, M. J., Takenaka, C., and Ohgushi, H. (2008). Forced expression of Sox2 or Nanog in human bone marrow derived mesenchymal stem cells maintains their expansion and differentiation capabilities. *Exp. Cell Res.* 314, 1147–1154. doi: 10.1016/j.yexcr.2007.11.021

Gugliandolo, A., Diomede, F., Scionti, D., Bramanti, P., Trubiani, O., and Mazzon, E. (2019). The role of hypoxia on the neuronal differentiation of gingival mesenchymal stem cells: a transcriptional study. *Cell Transplant* 28, 538–552. doi: 10.1177/0963689718814470

Guo, L., Zhou, Y., Wang, S., and Wu, Y. (2014). Epigenetic changes of mesenchymal stem cells in three-dimensional (3D) spheroids. *J. Cell. Mol. Med.* 18, 2009–2019. doi: 10.1111/jcmm.12336

Halfon, S., Abramov, N., Grinblat, B., and Ginis, I. (2011). Markers distinguishing mesenchymal stem cells from fibroblasts are downregulated with passaging. *Stem Cells Dev.* 20, 53–66. doi: 10.1089/scd.2010.0040

Hall, B. K., and Miyake, T. (2000). All for one and one for all: condensations and the initiation of skeletal development. *Bioessays* 22, 138–147. doi: 10.1002/(sici)1521-1878(200002)22:2<138::aid-bies5>3.0.co;2-4

He, S., Nakada, D., and Morrison, S. J. (2009). Mechanisms of stem cell self-renewal. *Annu. Rev. Cell Dev. Biol.* 25, 377–406. doi: 10.1146/annurev.cellbio.042308.113248

Ichim, T. E., O'Heeron, P., and Kesari, S. (2018). Fibroblasts as a practical alternative to mesenchymal stem cells. *J. Transl. Med.* 16:212. doi: 10.1186/s12967-018-1536-1

Isern, J., Martin-Antonio, B., Ghazanfari, R., Martin, A. M., Lopez, J. A., del Toro, R., et al. (2013). Self-renewing human bone marrow mesenspheres promote hematopoietic stem cell expansion. *Cell Rep.* 3, 1714–1724. doi: 10.1016/j.celrep.2013.03.041

Iwasaki, K., Nagata, M., Akazawa, K., Watabe, T., and Morita, I. (2019). Changes in characteristics of periodontal ligament stem cells in spheroid culture. *J. Periodontal Res.* 54, 364–373. doi: 10.1111/jre.12637

Kabiri, M., Kul, B., Lott, W. B., Futrega, K., Ghanavi, P., Upton, Z., et al. (2012). 3D mesenchymal stem/stromal cell osteogenesis and autocrine signalling. *Biochem. Biophys. Res. Commun.* 419, 142–147. doi: 10.1016/j.bbrc.2012.01.017

Kale, S., Biermann, S., Edwards, C., Tarnowski, C., Morris, M., and Long, M. W. (2000). Three-dimensional cellular development is essential for ex vivo formation of human bone. *Nat. Biotechnol.* 18, 954–958. doi: 10.1038/79439

Kaul, H., Hall, B. K., Newby, C., and Ventikos, Y. (2015). Synergistic activity of polarised osteoblasts inside condensations cause their differentiation. *Sci. Rep.* 5:11838. doi: 10.1038/srep11838

Kim, J., and Adachi, T. (2019). Cell condensation triggers the differentiation of osteoblast precursor cells to osteocyte-like cells. *Front. Bioeng. Biotechnol.* 7:288. doi: 10.3389/fbioe.2019.00288

Kolf, C. M., Cho, E., and Tuan, R. S. (2007). Mesenchymal stromal cells. Biology of adult mesenchymal stem cells: regulation of niche, self-renewal and differentiation. *Arthritis Res. Ther.* 9:204. doi: 10.1186/ar2116

Kuroda, Y., Kitada, M., Wakao, S., Nishikawa, K., Tanimura, Y., Makinoshima, H., et al. (2010). Unique multipotent cells in adult human mesenchymal cell populations. *Proc. Natl. Acad. Sci. U.S.A.* 107, 8639–8643. doi: 10.1073/pnas.0911647107

Lee, S. H., Inaba, A., Mohindroo, N., Ganesh, D., Martin, C. E., Chugal, N., et al. (2017). Three-dimensional sphere-forming cells are unique multipotent cell population in dental pulp cells. *J. Endod.* 43, 1302–1308. doi: 10.1016/j.joen.2017.03.016

Liu, T. M., and Lee, E. H. (2013). Transcriptional regulatory cascades in Runx2-dependent bone development. *Tissue Eng. B Rev.* 19, 254–263. doi: 10.1089/ten.TEB.2012.0527

Lo, L. M., Raghunath, M., and Lee, K. K. H. (2019). Growing human dermal fibroblasts as spheroids renders them susceptible for early expression of pluripotency genes. *Adv. Biosyst.* 3:1900094. doi: 10.1002/adbi.201900094

Lv, F. J., Tuan, R. S., Cheung, K. M., and Leung, V. Y. (2014). Concise review: the surface markers and identity of human mesenchymal stem cells. *Stem Cells* 32, 1408–1419. doi: 10.1002/stem.1681

Mareddy, S., Dhaliwal, N., Crawford, R., and Xiao, Y. (2010). Stem cell-related gene expression in clonal populations of mesenchymal stromal cells from bone marrow. *Tissue Eng. A* 16, 749–758. doi: 10.1089/ten.TEA.2009.0307

Miranda, J. P., Camoes, S. P., Gaspar, M. M., Rodrigues, J. S., Carvalheiro, M., Barcia, R. N., et al. (2019). The secretome derived from 3D-cultured umbilical cord tissue MSCs counteracts manifestations typifying rheumatoid arthritis. *Front. Immunol.* 10:18. doi: 10.3389/fimmu.2019.00018

Mitrano, T. I., Grob, M. S., Carrion, F., Nova-Lamperti, E., Luz, P. A., Fierro, F. S., et al. (2010). Culture and characterization of mesenchymal stem cells from human gingival tissue. *J. Periodontol.* 81, 917–925. doi: 10.1902/jop.2010.090566

Mohamed-Ahmed, S., Fristad, I., Lie, S. A., Suliman, S., Mustafa, K., Vindenes, H., et al. (2018). Adipose-derived and bone marrow mesenchymal stem cells: a donor-matched comparison. *Stem Cell. Res. Ther.* 9:168. doi: 10.1186/s13287-018-0914-1

Moritani, Y., Usui, M., Sano, K., Nakazawa, K., Hanatani, T., Nakatomi, M., et al. (2018). Spheroid culture enhances osteogenic potential of periodontal ligament mesenchymal stem cells. *J. Periodontal. Res.* 53, 870–882. doi: 10.1111/jre.12577

Moshaverinia, A., Chen, C., Xu, X., Akiyama, K., Ansari, S., Zadeh, H. H., et al. (2014). Bone regeneration potential of stem cells derived from periodontal ligament or gingival tissue sources encapsulated in RGD-modified alginate scaffold. *Tissue Eng. A* 20, 611–621. doi: 10.1089/ten.TEA.2013.0229

Mostafa, N. Z., Uludağ, H., Varkey, M., Dederich, D. N., Doschak, M. R., and El-Bialy, T. H. (2011). In vitro osteogenic induction of human gingival fibroblasts for bone regeneration. *Open Dent. J.* 5, 139–145. doi: 10.2174/1874210601105010139

Murphy, K. C., Fang, S. Y., and Leach, J. K. (2014). Human mesenchymal stem cell spheroids in fibrin hydrogels exhibit improved cell survival and potential for bone healing. *Cell Tissue Res.* 357, 91–99. doi: 10.1007/s00441-014-1830-z

Naveau, A., Lataillade, J. J., Fournier, B. P., Couty, L., Prat, M., Ferre, F. C., et al. (2011). Phenotypic study of human gingival fibroblasts in a medium enriched with platelet lysate. *J. Periodontol.* 82, 632–641. doi: 10.1902/jop.2010.100179

Nebie, O., Barro, L., Wu, Y. W., Knutson, F., Buee, L., Devos, D., et al. (2020). Heat-treated human platelet pellet lysate modulates microglia activation, favors wound healing and promotes neuronal differentiation in vitro. *Platelets* [Epub ahead of print]. doi: 10.1080/09537104.2020.1732324

Shanbhag et al.   Xeno-Free Spheroids of Gingival Progenitor Cells

Ogasawara, T., Ohba, S., Yano, F., Kawaguchi, H., Chung, U. I., Saito, T., et al. (2013). Nanog promotes osteogenic differentiation of the mouse mesenchymal cell line C3H10T1/2 by modulating bone morphogenetic protein (BMP) signaling. J. Cell Physiol. 228, 163–171. doi: 10.1002/jcp.24116

Petrenko, Y., Sykova, E., and Kubinova, S. (2017). The therapeutic potential of three-dimensional multipotent mesenchymal stromal cell spheroids. Stem Cell Res. Ther. 8:94. doi: 10.1186/s13287-017-0558-6

Phimphilai, M., Zhao, Z., Boules, H., Roca, H., and Franceschi, R. T. (2006). BMP signaling is required for RUNX2-dependent induction of the osteoblast phenotype. J. Bone Miner. Res. 21, 637–646. doi: 10.1359/jbmr.060109

Pittenger, M. F., Discher, D. E., Péault, B. M., Phinney, D. G., Hare, J. M., and Caplan, A. I. (2019). Mesenchymal stem cell perspective: cell biology to clinical progress. NPJ Regen. Med. 4:22. doi: 10.1038/s41536-019-0083-6

Pittenger, M. F., Mackay, A. M., Beck, S. C., Jaiswal, R. K., Douglas, R., Mosca, J. D., et al. (1999). Multilineage potential of adult human mesenchymal stem cells. Science 284, 143–147. doi: 10.1126/science.284.5411.143

Potapova, I. A., Gaudette, G. R., Brink, P. R., Robinson, R. B., Rosen, M. R., Cohen, I. S., et al. (2007). Mesenchymal stem cells support migration, extracellular matrix invasion, proliferation, and survival of endothelial cells in vitro. Stem Cells 25, 1761–1768. doi: 10.1634/stemcells.2007-0022

Qiu, J., Wang, X., Zhou, H., Zhang, C., Wang, Y., Huang, J., et al. (2020). Enhancement of periodontal tissue regeneration by conditioned media from gingiva-derived or periodontal ligament-derived mesenchymal stem cells: a comparative study in rats. Stem Cell Res. Ther. 11:42. doi: 10.1186/s13287-019-1546-9

Samavarchi-Tehrani, P., Golipour, A., David, L., Sung, H. K., Beyer, T. A., Datti, A., et al. (2010). Functional genomics reveals a BMP-driven mesenchymal-to-epithelial transition in the initiation of somatic cell reprogramming. Cell Stem Cell 7, 64–77. doi: 10.1016/j.stem.2010.04.015

Sart, S., Tsai, A. C., Li, Y., and Ma, T. (2014). Three-dimensional aggregates of mesenchymal stem cells: cellular mechanisms, biological properties, and applications. Tissue Eng. B Rev. 20, 365–380. doi: 10.1089/ten.TEB.2013.0537

Shanbhag, S., Stavropoulos, A., Suliman, S., Hervig, T., and Mustafa, K. (2017). Efficacy of humanized mesenchymal stem cell cultures for bone tissue engineering: a systematic review with a focus on platelet derivatives. Tissue Eng. Part B Rev. 23, 552–569. doi: 10.1089/ten.TEB.2017.0093

Sharpe, P. T. (2016). Dental mesenchymal stem cells. Development 143, 2273–2280. doi: 10.1242/dev.134189

Silin, S. (2012). Round-bottomed honeycomb microwells: embryoid body shape correlates with stem cell fate. J. Dev. Biol. Tissue Eng. 4, 12–22. doi: 10.5897/jdbte11.025

Subbarayan, R., Murugan Girija, D., Mukherjee, J., Mamidanna, S. R. R., and Ranga Rao, S. (2017). Comparision of gingival and umbilical cord stem cells based on its modulus and neuronal differentiation. J. Cell. Biochem. 118, 2000–2008. doi: 10.1002/jcb.25918

Subbarayan, R., Murugan Girija, D., and Ranga Rao, S. (2018). Gingival spheroids possess multilineage differentiation potential. J. Cell. Physiol. 233, 1952–1958. doi: 10.1002/jcp.25894

Suenaga, H., Furukawa, K. S., Suzuki, Y., Takato, T., and Ushida, T. (2015). Bone regeneration in calvarial defects in a rat model by implantation of human bone marrow-derived mesenchymal stromal cell spheroids. J. Mater. Sci. Mater. Med. 26:254. doi: 10.1007/s10856-015-5591-3

Sun, Q., Nakata, H., Yamamoto, M., Kasugai, S., and Kuroda, S. (2019). Comparison of gingiva-derived and bone marrow mesenchymal stem cells for osteogenesis. J. Cell. Mol. Med. 23, 7592–7601. doi: 10.1111/jcmm.14632

Tomar, G. B., Srivastava, R. K., Gupta, N., Barhanpurkar, A. P., Pote, S. T., Jhaveri, H. M., et al. (2010). Human gingiva-derived mesenchymal stem cells are superior to bone marrow-derived mesenchymal stem cells for cell therapy in regenerative medicine. Biochem. Biophys. Res. Commun. 393, 377–383. doi: 10.1016/j.bbrc.2010.01.126

van Strien, M. E., Sluijs, J. A., Reynolds, B. A., Steindler, D. A., Aronica, E., and Hol, E. M. (2014). Isolation of neural progenitor cells from the human adult subventricular zone based on expression of the cell surface marker CD271. Stem Cells Transl. Med. 3, 470–480. doi: 10.5966/sctm.2013-0038

Wang, F., Yu, M., Yan, X., Wen, Y., Zeng, Q., Yue, W., et al. (2011). Gingiva-derived mesenchymal stem cell-mediated therapeutic approach for bone tissue regeneration. Stem Cells Dev. 20, 2093–2102. doi: 10.1089/scd.2010.0523

Wilson, A., Hodgson-Garms, M., Frith, J. E., and Genever, P. (2019). Multiplicity of mesenchymal stromal cells: finding the right route to therapy. Front. Immunol. 10:1112. doi: 10.3389/fimmu.2019.01112

Wu, R. X., Yu, Y., Yin, Y., Zhang, X. Y., Gao, L. N., and Chen, F. M. (2017). Platelet lysate supports the in vitro expansion of human periodontal ligament stem cells for cytotherapeutic use. J. Tissue Eng. Regen. Med. 11, 2261–2275. doi: 10.1002/term.2124

Xu, X., Chen, C., Akiyama, K., Chai, Y., Le, A. D., Wang, Z., et al. (2013). Gingivae contain neural-crest- and mesoderm-derived mesenchymal stem cells. J. Dent. Res. 92, 825–832. doi: 10.1177/0022034513497961

Yang, H., Gao, L. N., An, Y., Hu, C. H., Jin, F., Zhou, J., et al. (2013). Comparison of mesenchymal stem cells derived from gingival tissue and periodontal ligament in different incubation conditions. Biomaterials 34, 7033–7047. doi: 10.1016/j.biomaterials.2013.05.025

Yassin, M. A., Mustafa, K., Xing, Z., Sun, Y., Fasmer, K. E., Waag, T., et al. (2017). A copolymer scaffold functionalized with nanodiamond particles enhances osteogenic metabolic activity and bone regeneration. Macromol. Biosci. 17:1600427. doi: 10.1002/mabi.201600427

Ylostalo, J. H., Bazhanov, N., Mohammadipoor, A., and Bartosh, T. J. (2017). Production and administration of therapeutic mesenchymal stem/stromal cell (MSC) spheroids primed in 3-D cultures under xeno-free conditions. J. Vis. Exp. 121:55126. doi: 10.3791/55126

Yue, R., Shen, B., and Morrison, S. J. (2016). Clec11a/osteolectin is an osteogenic growth factor that promotes the maintenance of the adult skeleton. eLife 5:e18782. doi: 10.7554/eLife.18782

Zhang, Q., Nguyen, A. L., Shi, S., Hill, C., Wilder-Smith, P., Krasieva, T. B., et al. (2012). Three-dimensional spheroid culture of human gingiva-derived mesenchymal stem cells enhances mitigation of chemotherapy-induced oral mucositis. Stem Cells Dev. 21, 937–947. doi: 10.1089/scd.2011.0252

Supplementary material

1.   Supplementary methods

1.1.   Production of human platelet lysate (HPL)
The HPL herein (Bergenlys®, Bergen, Norway) was prepared from outdated pooled whole blood-derived platelet concentrates (PCs) at the Department of Immunology and Transfusion Medicine, Haukeland University Hospital, Bergen, Norway. Briefly, unused 7 d-old PCs were used for HPL production via multiple freezing (–80°C) and thawing cycles (+37°C). Pooled PCs were then centrifuged at 3000 x g (4°C, 15 min) to remove platelet fragments and aliquoted as the final HPL product. HPL aliquots were stored at –80°C and thawed overnight at 4°C for subsequent use in experiments. In HPL-supplemented media, 1 IU/mL of heparin was added to prevent gelation and the medium was sterile filtered (0.2 µm) before use.

2.   Supplementary tables and figures

2.1.   Supplementary table 1: Real-time PCR assays

Gene	TaqMan® Assay ID	Amplicon length
Housekeeping gene		
GAPDH	Hs 02758991_g1	93
Adipogenesis-related		
PPARG	Hs01115513_m1	90
LPL	Hs00173425_m1	103
Osteogenesis-related		
RUNX2	Hs01047973_m1	86
BMP2	Hs00154192_m1	60
ALPL	Hs01029144_m1	79
COL1A2	Hs00164099_m1	68
OPN (SPP1)	Hs00959010_m1	84
OCN (BGLAP)	Hs01587814_g1	138
Stemness-related		
SOX2	Hs01053049_s1	91
OCT4 (POU5F1)	Hs00999632_g1	77
NANOG	Hs02387400_g1	109

GAPDH glyceraldehyde 3-phosphate dehydrogenase, PPARG peroxisome proliferator activated receptor gamma, LPL lipoprotein lipase, RUNX2 runt-related transcription factor 2, BMP2 bone morphogenetic protein 2, ALPL alkaline phosphatase, COL1A2 Collagen type 1, OPN/SPP1 Osteopontin, OCN/BGLAP Osteocalcin, SOX2 sex determining region Y-box 2, OCT4/POU5F1 octamer-binding transcription factor 4, NANOG homeobox transcription factor nanog

2.2. Supplementary table 2: Multiplex human cytokine screening panel

| Abbreviation	Cytokine
b-FGF/FGF2	Basic fibroblast growth factor
Eotaxin/CCL11	C-C chemokine 11
G-CSF	Granulocyte colony stimulating factor
GM-CSF	Granulocyte-macrophage colony-stimulating factor
IFN-γ	Interferon-γ
IL-1β	Interleukin-1β
IL-1ra	Interleukin 1 receptor antagonist
IL-1α	Interleukin-1α
IL-2Rα	Interleukin-2 receptor α
IL-3	Interleukin-3
IL-12 (p40)	Interleukin-12 subunit beta
IL-16	Interleukin-16
IL-2	Interleukin-2
IL-4	Interleukin-4
IL-5	Interleukin-5
IL-6	Interleukin-6
IL-7	Interleukin-7
IL-8	Interleukin-8
IL-9	Interleukin-9
GRO-α/CXCL1	Growth-regulated alpha protein/CXC ligand 1
HGF	Hepatocyte growth factor
IFN-α2	Interferon-α2
LIF	Leukemia inhibitory factor
MCP-3/CCL7	Monocyte chemotactic protein-3
IL-10	Interleukin-10
IL-12 (p70)	Interleukin-12
IL-13	Interleukin-13
IL-15	Interleukin-15
IL-17A	Interleukin-17
IL-18	Interleukin-18
IP-10/CXCL10	Interferon gamma-induced protein 10/CXC chemokine 10
MCP-1/CCL2	Monocyte Chemoattractant Protein-1
MIG/CXCL9	Monokine induced by gamma interferon/CXC ligand 9
β-NGF	Nerve growth factor
SCF/KITLG	Stem cell factor/KIT-ligand
SCGF-β	Stem cell growth factor
SDF-1α/CXCL12	Stromal cell-derived factor 1
MIP-1α/CCL3	Macrophage inflammatory protein
MIP-1β/CCL4	Macrophage inflammatory protein
PDGF-BB	Platelet-derived growth factor-BB
RANTES/CCL5	Regulated on activation, normal T cell expressed and secreted
Eotaxin/CCL11	Eotaxin
TNF-α	Tumor necrosis factor-α
TNF-β	Tumor necrosis factor-β
VEGF	Vascular endothelial growth factor
CTACK/CCL27	Cutaneous T-Cell Attracting Chemokine
MIF	Macrophage migration inhibitory factor
TRAIL	TNF-related apoptosis-inducing ligand
M-CSF	Macrophage colony-stimulating factor

Supplementary material

2.3. Supplementary figure 1: Osteogenic differentiation of monolayer GPCs and BMSCs on copolymer scaffolds
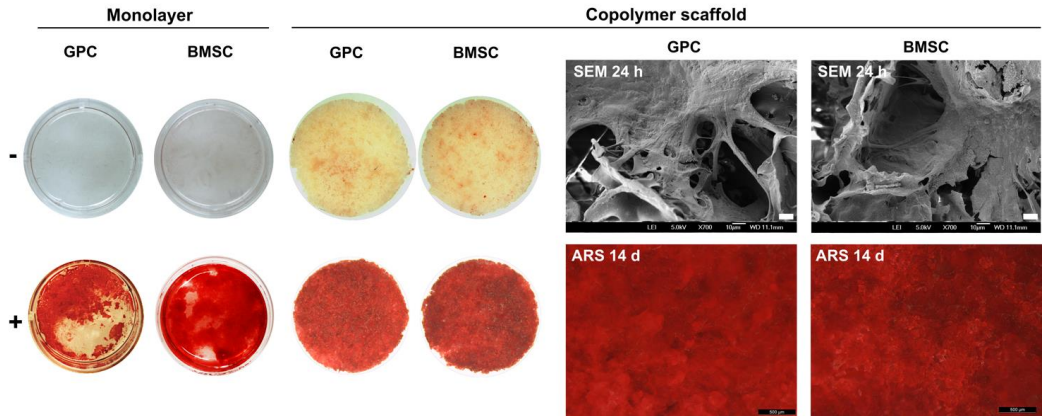
Alizarin red S staining (ARS) reveals osteogenic differentiation of GPCs and BMSCs in monolayer (21 d) and on poly(LLA-co-CL) scaffolds (14 d) under osteogenically induced (+) and non-induced (–) conditions; SEM reveals cell attachment and spreading on the scaffold surface after 24 h; scale bars 10 µm (*top*); magnified view of Alizarin red-stained scaffolds (*bottom*, scale bars 500 µm)

2.4. Supplementary figure 2: Gene expression in 3D spheroids of independent donors.
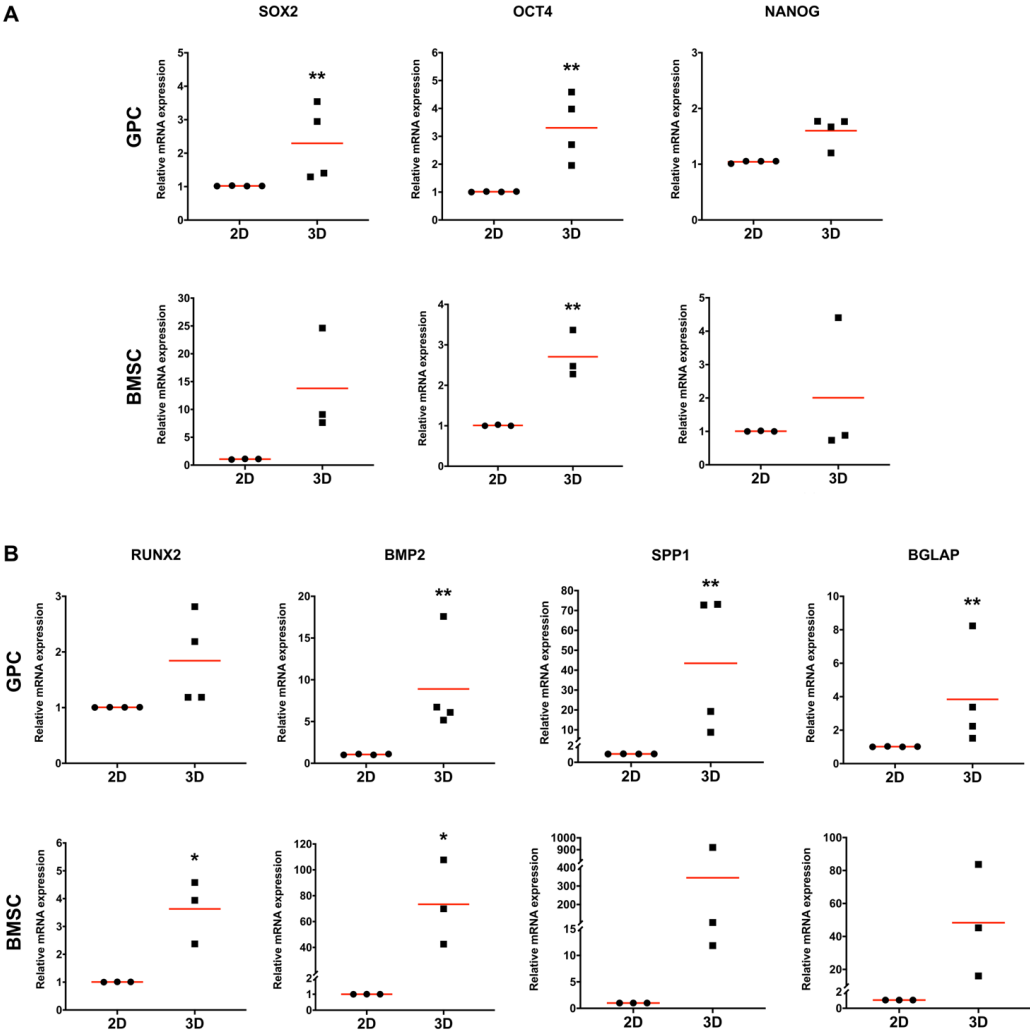
Relative expression (fold changes) of stemness- (A) and osteogenesis-related genes (B) after 7 d in 2D vs. 3D GPCs and BMSCs; data represent means; each symbol represents a single donor (n=>3); statistical analyses are based on delta-Ct values; *$p < 0.05$; **$p < 0.001$.

**Supplementary material**

2.5. Supplementary figure 3: Immunofluorescence staining of 2D GPCs and BMSCs
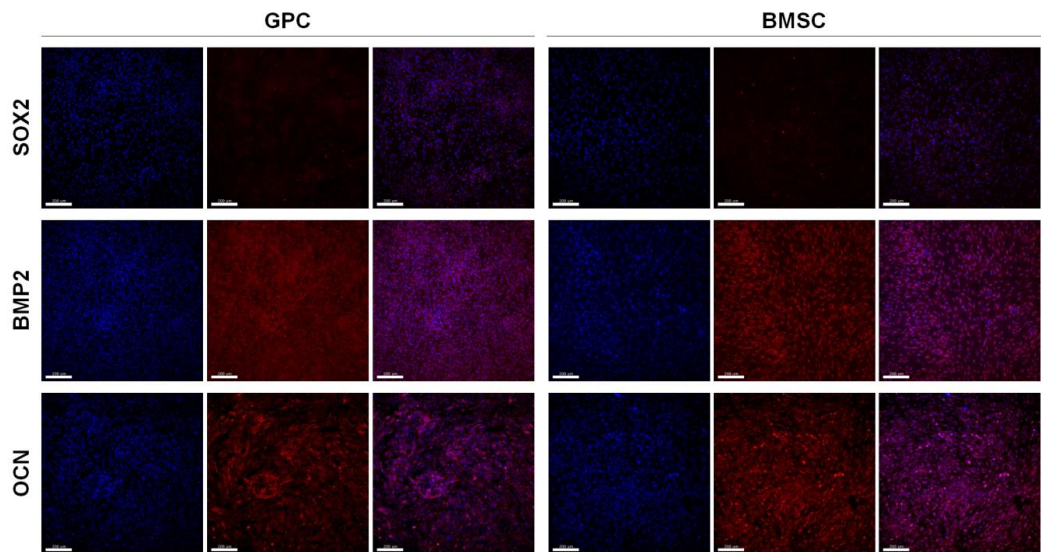
IF staining of 2D monolayer GPCs and BMSCs for stemness (SOX2) and osteogenesis-related markers (BMP2, OCN) after 14 d culture in standard and osteogenic induction media, respectively; scale bars 100 μm. Positive and comparable staining for BMP2 and OCN was observed in GPCs and BMSCs.

Supplementary material

2.6. Supplementary figure 4: Protein estimation of BMP2 via western blotting in 2D and 3D GPCs and BMSCs
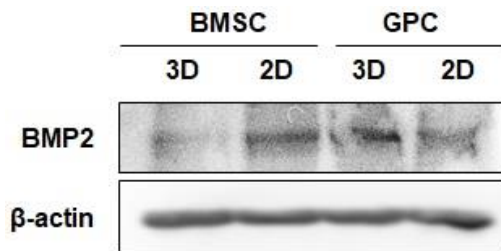
Protein estimation of BMP2 was performed via western blotting via SDS gel electrophoresis and blotting onto polyvinylidene difluoride (PVDF) membranes. The membranes were incubated with the following primary antibodies overnight at 4°C: anti-BMP2 (R&D systems) and anti-β-actin as a reference protein (Invitrogen). After extensive washing, the membranes were further incubated with horseradish peroxidase-conjugated secondary antibodies for 1 h and then developed using an enhanced chemiluminescence detection system (all from Bio-rad).
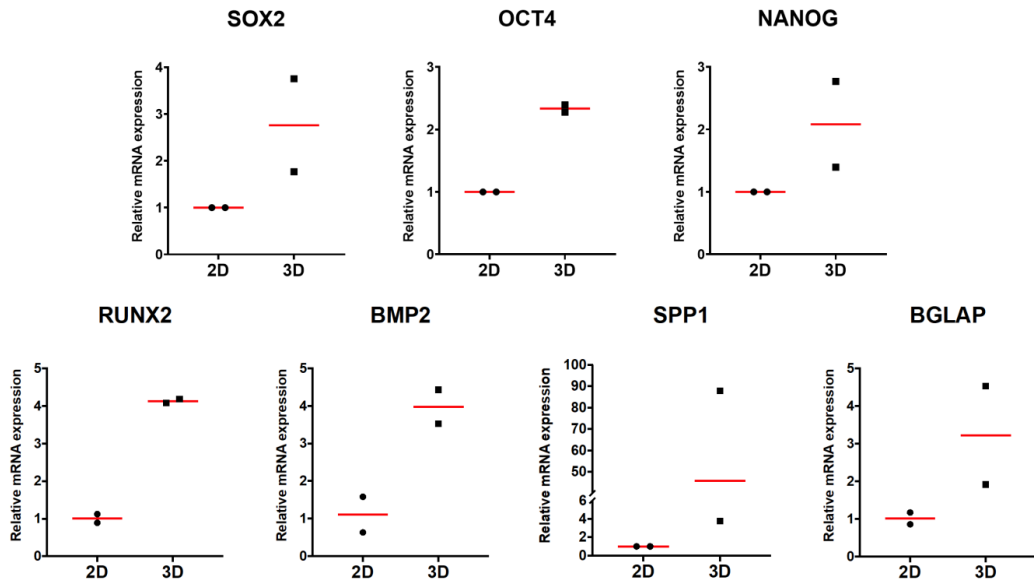
Supplementary material

2.7. Supplementary table 3: Cytokine concentrations in 2D and 3D GPCs and BMSCs.

| | GPC | | | | BMSC | | | |
| | 2D | | 3D | | 2D | | 3D | |
	Mean	SD	Mean	SD	Mean	SD	Mean	SD
Growth factors								
FGF2	0.04012	0.00478	0.18143	0.00197	0.02768	0.00530	0.04271	0.00001
PDGFbb	0.04337	0.01677	0.13879	0.00952	0.03152	0.00506	0.13655	0.00067
HGF	24.24730	0.87560	42.10489	1.40289	1.99578	0.25363	3.77988	0.06782
VEGF	0.72088	0.12111	1.69592	0.04196	3.94904	0.43366	1.69724	0.05659
TGFb1	24.50784	25.92031	53.98704	6.14884	17.95800	1.87240	35.67928	6.78256
SCF	0.04295	0.00382	0.04931	0.00303	0.05008	0.00406	0.01840	0.00024
SCGFb	113.14256	3.54892	95.36207	2.94256	110.21860	8.45354	74.49511	1.97597
GCSF	0.25382	0.03767	0.45470	0.03915	0.16630	0.00391	0.13473	0.00454
GMCSF	0.00281	0.00422	0.00456	0.00021	0.00202	0.00021	0.00082	0.00012
MCSF	0.03043	0.00432	0.02100	0.00062	0.04031	0.00780	0.01267	0.00030
Chemokines								
CCL11	0.16741	0.00556	0.04998	0.00012	0.01049	0.00137	0.00118	0.00003
CXCL10	0.03273	0.00471	0.02468	0.00072	0.00911	0.00330	0.00907	0.00001
CCL2	2.13776	0.13538	2.27424	0.07038	0.93586	0.12059	1.47786	0.02184
CCL3	0.00086	0.00029	0.00129	0.00001	0.00088	0.00023	0.00073	0.00005
CCL4	0.04168	0.01010	0.10332	0.00365	0.03960	0.01123	0.08331	0.00226
CCL5	5.85575	0.20835	7.63716	0.15172	1.44246	0.22004	9.65767	0.20100
CXCL1	3.65130	0.01579	2.06174	0.13972	0.16873	0.03515	6.66148	0.41839
CCL7	0.08885	0.00569	0.15191	0.00706	0.53342	0.06061	0.20476	0.00486
LIF	0.12380	0.02919	0.66383	0.01056	0.07635	0.01774	0.65338	0.00975
MIF	1.30814	0.07396	4.06624	0.26745	0.72819	0.29118	5.04052	0.25619
CXCL12	0.23595	0.02569	0.18201	0.00560	0.21189	0.03144	0.11132	0.00479
Inflammatory cytokines								
IL1a	0.02693	0.00994	0.02109	0.00164	0.02588	0.00858	0.00960	0.00001
IL1b	0.00251	0.00102	0.00247	0.00001	0.00222	0.00067	0.00081	0.00011
IL2	0.00471	0.00280	0.00180	0.00001	0.00324	0.00223	0.00109	0.00032
IL4	0.00353	0.00214	0.00307	0.00019	0.00376	0.00068	0.00194	0.00004
IL5	0.05189	0.05215	0.03438	0.00001	0.03339	0.00435	0.02244	0.00091
IL6	4.37381	0.03748	0.68100	0.06986	0.82140	0.10703	2.16931	0.07043
IL7	0.01789	0.00672	0.02066	0.00310	0.01402	0.00315	0.00608	0.00083
IL8	0.31796	0.06139	0.63340	0.07276	0.07324	0.01182	3.57365	0.03481
IL9	0.06582	0.02222	0.16124	0.00506	0.06258	0.01968	0.12090	0.00044
IL10	0.00854	0.00080	0.00387	0.00001	0.00502	0.00252	0.00256	0.00033
TNFa	0.01963	0.00316	0.02714	0.00001	0.02310	0.00592	0.01133	0.00123
IFNg	0.07505	0.00856	0.03856	0.00394	0.06054	0.00678	0.01762	0.00123

To account for differences in cell numbers between 2D and 3D cultures at the end of the culture period, cytokine concentrations (pg/mL) were normalized to the corresponding total DNA (ng/mL); data represent pg protein/ng DNA.

Supplementary material

2.8.   Supplementary figure 5: Gene expression in 3D spheroids of FBS-cultured GPCs.

Relative expression (fold changes) of stemness- and osteogenesis-related genes after 7 d in 2D vs. 3D GPCs; data represent means; each symbol represents a single donor (n=2).

Supplementary material

2.9. **Supplementary figure 6: Schematic representation of the hypothesized mechanism for self-renewal and lineage commitment in 3D spheroids.**
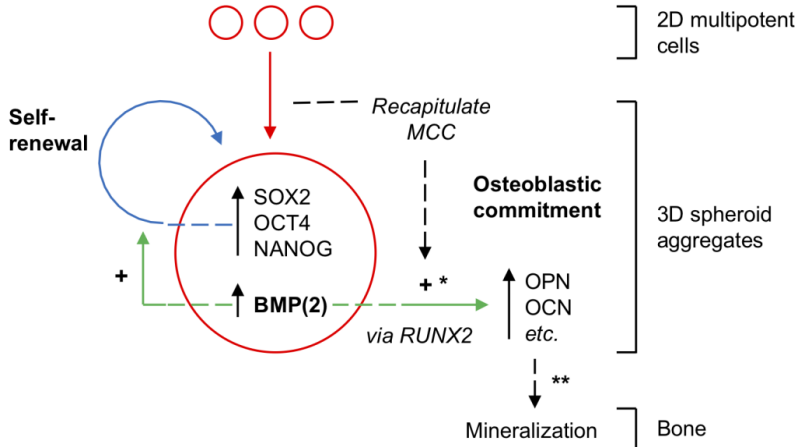
MCC, mesenchymal cell condensations; * independent of osteogenic induction; ** dependent on osteogenic induction.

Paper IV

Xeno-free 3D coculture of human gingiva-derived progenitor cells and endothelial cells to promote angiogenesis.

Shanbhag S, Rashad A, Suliman S, Osman TA, de Lange Davies C, Stavropoulos A, Bolstad AI, Mustafa K.

Manuscript

Paper V

Xeno-free constructs of mesenchymal stromal cells and 3D printed scaffolds for bone tissue engineering.

Shanbhag S, Mohamed-Ahmed S, Suliman S, Kampleitner C, Dongre H, Hassan MN, Yassin MA, Costea DE, Tangl S, Bolstad AI, Mustafa K.

Manuscript

Errata for
Xeno-free 3D culture of mesenchymal stromal cells
for bone tissue engineering

Siddharth Vivek Shanbhag

Thesis for the degree philosophiae doctor (PhD)

at the University of Bergen

27.11.2020

_____   _____

(date and sign. of candidate)   (date and sign. of faculty)

2

Errata

Page 30, Chapter 1.3.4. Typing error: "In the context of MSCs… spontaneously assembled into spheroids *in the lungs of rats* - later studies demonstrated that cell behaviour in *spheroid culture* was very similar to that in vivo" – corrected to "In the context of MSCs… which spontaneously assembled into spheroids when injected *in mice*; later studies demonstrated that cell behaviour in *spheroids* was very similar to that in vivo"

Page 31, Figure 1.5 legend. Typing error: Reference [112] – changed to [113]

Page 82, Acknowledgements. Some names removed – "…Camilo, Katrine…" deleted.

Page 88, Bibliography. Formatting error: Reference [110] "Bartosh, T.J. and J.H. Ylostalo, *Mesenchymal Stem Cell (MSC) Aggregate Formation in vivo.* Bio Protoc, 2014. 4(14)." – changed to "Bartosh, T.J., et al. *Dynamic compaction of human mesenchymal stem/precursor cells into spheres self-activates caspase-dependent IL1 signaling to enhance secretion of modulators of inflammation and immunity (PGE2, TSG6, and STC1).* Stem Cells 2013 **31**: p. 2443-56."

Pages 83-94, Other formatting errors (EndNote) in the Bibliography where page/volume/doi numbers in individual references have been added or corrected:

10.   Sanz-Sánchez, I., et al., Effectiveness of lateral bone augmentation on the alveolar crest dimension: A systematic review and meta--analysis. Journal of Dental Research, 2015. **94**(9). p 128-142

23.   Patterson, T.E., et al., The efficiency of bone marrow aspiration for the harvest of connective tissue progenitors from the human iliac crest. Journal of Bone and Joint Surgery. American Volume, 2017. **99**: p. 1673–1682.

29.   Wilson, A., et al., Multiplicity of mesenchymal stromal cells: finding the right route to therapy. Front. Immunol. 2019. **10**:1112.

30.   Fraser, J.K., et al., The Celution® system: Automated processing of adipose-- derived regenerative cells in a functionally closed system. Advance in Wound Care. (New Rochelle) 2014. **3**(1): p. 38–45.

39.   Mohamed-Ahmed, S., et al., *Comparison of Bone Regenerative Capacity of Donor-matched Human Adipose-Derived and Bone Marrow Mesenchymal Stem Cells.* Cell Tissue Res., 2020. **doi**: 10.1007/s00441-020-03315-5.

56.   Stefanska, K., et al., *Stemness Potency of Human Gingival Cells-Application in Anticancer Therapies and Clinical Trials.* Cells, 2020. **9**(8): p. 1916.

65.   Kandalam, U., et al., *Predifferentiated Gingival Stem Cell-Induced Bone Regeneration in Rat Alveolar Bone Defect Model.* Tissue Eng Part A, 2020. **doi**: 10.1089/ten.TEA.2020.0052.

82.   Wolff, J., et al., *GMP--level adipose stem cells combined with computer--aided manufacturing to reconstruct mandibular ameloblastoma resection defects: Experience with three cases.* Annals of Maxillofacial Surgery, 2013. **3**: p. 114-125.

103.   Ghazanfari, R., et al., *Human primary bone marrow mesenchymal stromal cells and their in vitro progenies display distinct transcriptional profile signatures.* Sci. Rep, 2017. **7**(1): p. 10338.

104.   Petrenko, Y., E. Sykova, and S. Kubinova, *The therapeutic potential of three-dimensional multipotent mesenchymal stromal cell spheroids.* Stem Cell Res Ther. 2017. **8**(1): p. 94.

114.   Hall, B.K. and T. Miyake, *All for one and one for all: condensations and the initiation of skeletal development.* Bioessays, 2000. **22**: p. 138-147.

116.   Facer, S.R., et al., *Rotary culture enhances pre-osteoblast aggregation and mineralization.* J. Dent. Res, 2005. **84**: p. 542-547.

120.   Kolf, C.M., E. Cho, and R.S. Tuan, *Mesenchymal stromal cells. Biology of adult mesenchymal stem cells: regulation of niche, self-renewal and differentiation.* Arthritis Res Ther. 2007. **9**(1): p. 204.

124.   Lo, L.M., M. Raghunath, and K.K.H. Lee, *Growing human dermal fibroblasts as spheroids renders them susceptible for early expression of pluripotency genes.* Adv Biosyst. 2019. **3**: 1900094.

140.   Cesarz, Z., et al., *Soft elasticity-associated signaling and bone morphogenic protein 2 are key regulators of mesenchymal stem cell spheroidal aggregates.* Stem Cells Dev., 2016. **33**(5023–5035): p. 622-635.

141.   Kim, J. and T. Adachi, *Cell condensation triggers the differentiation of osteoblast precursor cells to osteocyte-like cells.* Front. Bioeng. Biotechnol, 2019. **7**: 288.

156.   Kalka, C., et al., *Transplantation of ex vivo expanded endothelial progenitor cells*, in *for therapeutic neovascularization. Proc Natl Acad Sci. USA* 2000. **97**: p. 3422.

175.   Aatonen, M.T., et al., *Isolation and characterization of platelet-derived extracellular vesicles.* J Extracell Vesicles, 2014. **doi:** 10.3402/jev.v3.24692.

187.   Jaquiery, C., et al., *In vitro osteogenic differentiation and in vivo bone-forming capacity of human isogenic jaw periosteal cells and bone marrow stromal cells.* Ann Surg, 2005. **242**(6): p. 859-68

194.   Stute, N., et al., Autologous serum for isolation and expansion of human mesenchymal stem cells for clinical use. Exp Hematol, 2004. **32**: 1212.

195.   Shahdadfar, A., et al., *In vitro expansion of human mesenchymal stem cells: choice of serum is a determinant of cell proliferation, differentiation, gene expression, and transcriptome stability.* Stem Cells, 2005. **23**: 1357.

205.   Widholz, B., et al., *Pooling of Patient-Derived Mesenchymal Stromal Cells Reduces Inter-Individual Confounder-Associated Variation without Negative Impact on Cell Viability, Proliferation and Osteogenic Differentiation.* Cells, 2019. **8**(6): 633.

Paper V (manuscript), Page 7, line 14: Typing error "Ten" changed to "Twelve".

Paper V (manuscript), Page 7, line 17: Missing "per time point added"

uib.no